IMPROVED LIVE LOAD DISTRIBUTION FACTORS FOR USE IN LOAD RATING OF SLAB AND T-BEAM REINFORCED CONCRETE BRIDGES

by

Faezeh Ravazdezh

A Dissertation

Submitted to the Faculty of Purdue University

In Partial Fulfillment of the Requirements for the degree of

Doctor of Philosophy

Lyles School of Civil Engineering

West Lafayette, Indiana

May 2021

THE PURDUE UNIVERSITY GRADUATE SCHOOL
STATEMENT OF COMMITTEE APPROVAL

Dr. Julio Ramirez, Co-Chair

Lyles School of Civil Engineering

Dr. Ghadir Haikal, Co-Chair

Mechanical Engineering Division, Southwest Research Institute

Dr. Christopher Williams

Lyles School of Civil Engineering

Dr. Lesley Sneed

School of Civil, Materials, and Environmental Engineering, University of Illinois at Chicago

Dr. Shirley Dyke

Lyles School of Civil Engineering

Approved by:

Dr. Dulcy M. Abraham

dedicated to my parents who spoiled me with their endless love

ACKNOWLEDGMENTS

I would like to express my sincere gratitude to my advisor Professor Julio Ramirez for the continuous support of my Ph.D. study and related research, for his patience, motivation, and immense knowledge. Besides my advisor, I would like to express my appreciation to Dr. Ghadir Haikal for her dedicated support, guidance, and continuous optimism. I also thank my thesis committee members, Professor Christopher Williams, Professor Lesley Sneed, and Professor Shirley Dyke, for their insightful comments, valuable suggestions, and encouragement, which incented me to widen my research from various perspectives.

This research was made possible by the sponsorship of the Joint Transportation Research Program (JTRP) and the Indiana Department of Transportation (INDOT). I gratefully acknowledge the Study Advisory Committee for their valuable assistance and technical guidance in the course of performing this study.

Finally, my deep and sincere gratitude to my parents for their unconditional love and endless encouragement and my sisters, Fardaneh and Fatima, for their unfailing emotional support. I would like to say a special thank you to Amir, who has supported me throughout this experience and has constantly encouraged me and never let me give up.

TABLE OF CONTENTS

LIST OF TABLES

LIST OF FIGURES

ABSTRACT

This study aimed to investigate potential improvements in load estimation in the standard load rating procedure of reinforced concrete slab and girder bridges. Three-Dimensional (3D) Finite Element (FE) models were used to conduct refined analyses of bridges using full-scale models that account for non-structural elements in superstructure modeling. The rating results obtained from FE analysis for a small sample of bridges indicated that Conventional Load Rating (CLR) methodology could lead to conservative rating factors mainly due to demand overestimation. A parametric study associated with demand assessment showed a substantial impact of geometric features on bridge moment and shear values. The study showed that edge-elements such as railings and end-diaphragms significantly changed the distribution of loads over the bridge width due to the edge-stiffening effect.

Effects from the presence of edge components are not reflected in the methodology outlined in American Association of State Highway and Transportation Officials (AASHTO) specifications and may be a source of overestimation or underestimation of demands on bridges. Potential improvements to current live load Distribution Factor (DF) formulations were identified based on statistical studies where bridge responses subjected to standard truck load configurations obtained from FE analysis were compared to the current procedure’s corresponding results. Modification Factors (MF) to live load DF were proposed to incorporate secondary elements’ effect in demand estimates. Updated DFs could result in more accurate rating factors when used in the CLR of existing slab and T-beam bridges. This would benefit a great population of bridges conservatively rated as structurally deficient. The proposed modifications could prevent unnecessary rerouting, weight posting, bridge closure, and replacement.

EXECUTIVE SUMMARY

As an important component of transportation infrastructure systems, bridges play a critical role within the highway and railway networks. According to the Federal Highway Administration (FHWA) of the U.S. Department of Transportation, there are more than 600,000 bridges providing highway links and connections in the United States, with about 19,000 of them located in the State of Indiana. Reinforced Concrete (RC) bridges include almost 70% of the Indiana bridge population. Bridge construction in Indiana illustrates a significant uptick in reinforced concrete slab and slab-on-girder system designs in the decades of 1950 and 1960, implying that they have exceeded their 50-year design life (FHWA 2019). In Indiana, older RC bridges represent an important component of the existing network inventory still in function and are therefore required to satisfy current load-carrying capacity specifications. This is checked using load rating procedures and if found deficient need to be posted or replaced.

Load rating is a component of the bridge routine inspection process and is a measure of bridge live load capacity. Bridge engineers apply this procedure to assess structural strength and determine safe traffic load-bearing capacity a bridge can handle under its current structural condition. In this procedure, demand assessment is one of the key aspects which estimates bridge response under standard vehicular live load applications. American Association of State Highway and Transportation Officials (AASHTO) manual (AASHTO 2017) outlines the use of a simple and practical method for rapid demand estimates in evaluation process of slab and girder bridges. In this method, bridge superstructure is divided into individual beams, separately analyzed to obtain bending moment and shear forces. This simplified procedure reduces the two-way bending problem's complexity to a one-way bending problem, which is based on a Two-Dimensional (2D) beam theory. Then, the continuity of the beams in the transverse direction is indirectly accounted for by lateral load Distribution Factors (DF).

The distribution factor reflects the lateral effect of live loads across the bridge width and assigns the share of a vehicle load to each individual beam. Therefore, it is a key parameter in the design and evaluation of new and existing bridges. AASHTO Load and Resistance Factor Design (LRFD) specification provides approximate DF formulations for moment and shear calculations of a bridge subjected to standard truck loads. Distribution factor provisions are applicable to girders and 1-ft beam strips in T-beams and slab bridges, respectively. DFs are a function of geometrical features such as span length and deck width in slab bridges and span, deck, and girder dimensions in T-beam bridges. Moreover, LRFD specifies skew correction factors to adjust the longitudinal moment and shear responses in bridges with skewed decks. However, the effect of non-structural members has not been included in the development of current DF formulations.

The non-structural members, also known as secondary elements, such as railings, parapets, curbs, sidewalks, and end-diaphragms are critical components in slab and girder bridges contributing to the overall structural mechanism. The typical superstructure of RC bridges features reinforced concrete beams, integrated with the slab, located at deck edges. Moreover, concrete diaphragms are built at span ends of the T-beam bridges restraining girders at the abutment interfaces. These edge components change regional stiffness and hence, lateral distribution of the forces throughout a bridge when monolithically constructed with the slab. According to available literature, bridges possess significant reserve strength that is not predicted by conventional analytical methods and neglecting the effect of the edge-elements on live load distribution is one of the main sources of discrepancies observed between results obtained from field tests and code-specified DF formulations. The edge-stiffening effect changes load distribution patterns across the bridge width by attracting more loads to exterior sections of the deck, which results in a decreased share of load to interior sections. Neglecting this effect could result in an overestimated demand and consequently, conservative rating factors for interior sections of the bridge superstructure. This calls for a modification for more accurate demand estimates in bridge evaluations.

Modern computational tools empower engineers to efficiently carry out accurate and comprehensive structural analyses. Finite Element (FE) methods gained popularity in bridge studies to explore whole-system behavior compared to conventional member-by-member analysis. Three-Dimensional (3D) models are suitable for detailed representation of bridge superstructures that include non-structural components that are neglected in current specifications and reflect their effects on bridge structural mechanisms. Therefore, their contribution in moment and shear responses can be simulated.

This research aimed to investigate potential improvements in demand evaluation methodology for slab and T-beam bridges in Indiana using FE analysis tools. To this end, a case study of Indiana bridges was assessed using Conventional Load Rating (CLR) methodology, and the load rating results were compared to those obtained using FE methods. This comparison indicated that CLR leads to a conservative evaluation of the RFs for the studied ten sample bridges.

It was observed that distribution factor formulations did not properly estimated bridge bending moment and one-way shear demand mainly due to a simplified representation of structural members and lack of consideration of the participation of non-structural elements. Findings from this analysis were the basis to perform an extensive parametric study using 3D finite elements to model the response of several archetypical bridges to investigate the bending moment and shear demand from the application of vehicular loads in slab and T-beam bridges.

The parametric study was designed to explore the participation of superstructure geometrical characteristics in the estimation of moment and shear due to vehicular loads. Dimensions of secondary elements such as edge-elements, including railing height and end-diaphragm width, were the main variables included in the parametric study. The study was conducted using skewed and non-skewed bridges of both structural types, single-span and continuous. The National Bridge Inventory (NBI) was surveyed to define reference (archetype) bridges with average geometrical properties. Using 3D modeling, parameters were varied one at a time in the reference bridge model, and live load (truck loading) responses were obtained and compared to those obtained based on current LRFD distribution factors. The findings confirmed the sensitivity of demand estimation to inclusion of the previously described superstructure secondary elements. The edge barriers were found to substantially affect the bending moment and shear demand estimates. With the increase of railing height, moment and shear demands increased in exterior sections of both bridge types and consequently, demand reduction was observed in interior parts. The same effect was observed with the addition of diaphragms in T-beam bridges, resulting in reduced moment and shear responses in interior girders.

To address the limitations of the current procedure, Modification Factors (MF) to live load DF formulations seemed a potential solution that could incorporate the effect of non-structural elements in demand estimation while maintaining the current load rating procedures. Therefore, statistical analysis was performed to numerically assess parametric study results, and regression models were used to define a proper mathematical formulation for MFs as a function of non-structural element dimensions, i.e., railing height and diaphragm width. Statistical tests such as analysis of residuals, the goodness of fit, and t-statistics were performed to evaluate performance of regression models. Moreover, the proposed MFs were assessed using a sample of twenty Indiana slab and T-beam RC bridges randomly selected from the NBI dataset with geometrical properties different from those of reference slab and T-beam bridges considered in the parametric study. An acceptable discrepancy was observed between the results obtained from MF formulations (prediction) and 3D models (actual) based on analysis of calculated errors (bellow 10% in all cases).

The findings from this thesis may be used to update the demand evaluation process by the Indiana Department of Transportation for rating and design practices. As of 2013 (FHWA 2019), about 200 bridges were either posted or closed for not meeting rating requirements in the State of Indiana. 21% of the bridge population is identified as structurally deficient or functionally obsolete, and about 15% of the RC bridges in Indiana are more than 75 years old and are closely monitored for rating requirements. From the comparison with 3D FE ratings, the proposed modifications would benefit a great population of Indiana bridges. This could prevent unnecessary rerouting, weight limits, bridge closure, and replacement. In particular, those bridges that show no signs of structural deficiency and with proper maintenance could be expected to serve well into the future.

1. INTRODUCTION

1.1 Motivation

Bridges are one of the most important components in transportation infrastructure systems and play a critical role within the highway and railway networks. Federal Highway Administration (FHWA) of the U.S. Department of Transportation provides design, construction, and maintenance dataset of the nation's highway bridges (FHWA 2019). According to FHWA, there are over 610,000 bridges providing highway links and connections in the United States. A major proportion of the current bridges was built during the late 1950s through the early 1970s, and many are still in use. There are more than 19,000 bridges located in the State of Indiana. About 50% of the reinforced concrete bridges in service in Indiana were constructed before 1970, implying that they have exceeded their 50-year design life. Figure 1-1 shows the construction year distribution of reinforced concrete bridge populations in the U.S and Indiana as of 2013 and 2019, respectively.

Bridge construction in Indiana in the 1950s and 1960s favored reinforced concrete slab design, using either a flat-slab or variable-depth ribbed (T-beams) systems. Examples of these structural systems are shown in Figure 1-2. Based on the FHWA database, there are about 3000 slab and 700 T-beam bridges in Indiana. These bridges represent an important component of the existing network inventory still in function and are therefore required to satisfy current load-carrying capacity specifications. The load rating is a standard procedure specified by the American Association of State Highway and Transportation Officials (AASHTO). It is used to evaluate the load-carrying capacity of existing bridges routinely. Load rating results are presented as Rating Factor (RF). This factor determines whether a bridge is safe to accommodate current traffic or repair, posting, or replacement strategies are needed. Therefore, the accuracy of the rating procedure is crucial in both safety and financial aspects.

Demand assessment is one of the key aspects of the load rating procedure where the bridge deck is subjected to standard vehicular live loads and analyzed using a girder-by-girder approach, which is based on a Two-Dimensional (2D) beam theory. In this simple and rapid approach, the share of loads for each beam is accounted for by using the Distribution Factor (DF). This factor reflects the transverse effect of live loads across the bridge width. Despite the favorability of this methodology due to its simplicity, it has been reported that it could lead to an overestimation of members' load share and consequent underestimation of the bridge rating factor. Results of field tests (Eom and Nowak 2001; Bell et al. 2013) and analytical studies (Jauregui and Barr 2004; Eamon and Nowak 2004; Hasancebi and Dumlupinar 2013; Sanayie et al. 2016) conducted on existing bridges has indicated that such conservative evaluation could be attributed to ignoring Three-Dimensional (3D) behavior of bridge superstructure, simplifying the representation of members, and neglecting the effect of non-structural components such as curbs, barriers, sidewalks, and end-diaphragms. In particular, it was found that exclusion of secondary members in the structural analysis was the main source of overestimation in the development of distribution factor formulation (Amer et al. 1999; Eamon and Nowak 2002; Conner and Huo 2006; Cai et al. 2007).

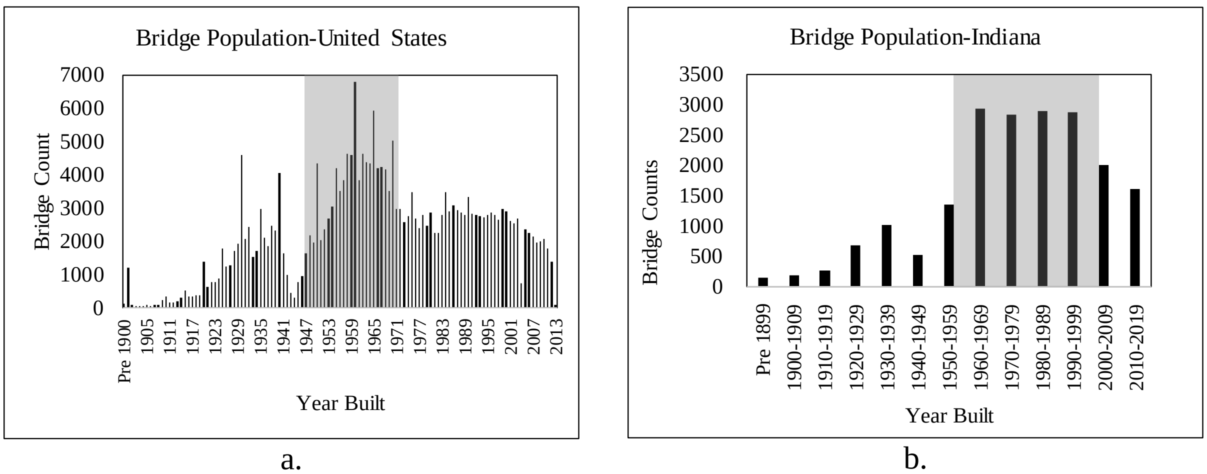

Figure 1-1 Bridge Population; a. United States, b. Indiana

The current load rating procedure is the basis for the Indiana Department of Transportation (INDOT) program for the load rating of bridges, AASHTOWare Bridge Rating (BrR). This method may underestimate the capacity of slab and T-beam bridges. Therefore, it is important to revisit the assumptions and principles of the method to identify potential areas of improvement for a more accurate bridge strength and load distribution assessments.

Available computational tools facilitated full-scale bridge superstructure modeling to perform three-dimensional structural analysis. 3D modeling is an efficient alternative to experimental tests with the relatively low cost associated with numerical analysis compared to the prohibitive cost of field studies. Finite Element (FE) methods gained popularity in bridge studies to explore the advantage of whole-system behavior compared to conventional member-by-member analysis. 3D finite element models enable large-scale parametric studies of the factors influencing structural capacity. These models are capable of including bridge components that are neglected in current specifications and reflect their impacts on bridge structural mechanisms. Therefore, their contribution in moment and shear responses can be simulated. More importantly, with 3D models, the load distribution in the transverse direction of the deck can be explicitly represented. Therefore, it has become possible to revisit the assumptions of 2D beam theory to investigate the effect of lateral load distribution on the load rating of bridges.

a.

b.

Figure 1-2 Structural Bridge Systems; a. Slab-Texas, b. T-beam-Virginia

FE modeling might be considered as a tool for an accurate and thorough assessment of bridges; however, it could become impractical for larger populations and everyday engineering practices. This study aimed to examine the limits and investigate potential improvements in demand evaluation methodology for slab and T-beam reinforced concrete bridges in Indiana using FE analysis. A parametric study was conducted on samples of the two bridge types, focusing on the inclusion of secondary elements in the 3D models. Distribution factors obtained from FE analysis were compared with those of the AASHTO procedure. While maintaining the current procedure, DFs were updated using modification factors proposed to include the favorable effect of secondary elements neglected in the development of distribution factors.

As reported by FHWA as of 2013, reinforced concrete bridges include almost 70% of the Indiana bridge population, which 84% of them have slab and T-beam structural systems (see Figure 1-3). Among them, about 200 bridges were either posted or closed for not meeting rating requirements. Also, 15% of reinforced concrete bridges in Indiana age more than 75 years and are closely monitored for rating requirements. For bridges designed under older versions of the specifications, given differences in loading and design standards, it is important not to excessively underestimate their load-carrying capacity, which can have serious implications for rehabilitation and maintenance or unnecessary rerouting and weight posting.

Therefore, an accurate estimation of load-carrying capacity could potentially relieve a large financial burden on the state and further extend bridges life span. Especially since many existing bridges show no signs of structural deficiency and, with proper maintenance, could be expected to serve well in the future. The findings of this study could be used to update the demand evaluation process for rating and design practices. The modified methodology could benefit a great population of Indiana bridges (21%) that might be conservatively identified as structurally deficient or functionally obsolete.

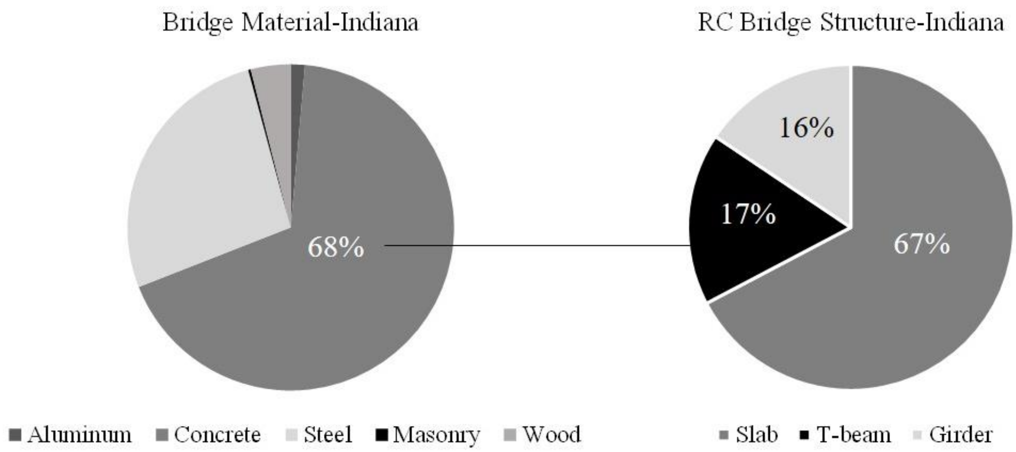

Figure 1-3 Distribution of Indiana Bridges by Material and Structural System

1.2 Literature Review

Live load distribution factor is designed to facilitate the computation of live load distribution over the bridge deck in bridge demand estimates. The use of this factor simplifies the complex three-dimensional analysis of a bridge superstructure to a two-dimensional problem. With this method, the bridge deck is divided into individual beams, and DF allocates the share of the live load in the transverse direction to each girder and beam strip in T-beam and slab bridges, respectively.

This concept has been implemented in T-beam bridges since the 1930s using empirical DFs (Newmark 1948), known to be in S/D format, where S is girder spacing and D the bridge type. S/D provisions were specified in AASHTO Load and Factor Design Standard specifications (LFD) until its last edition in 2002 (AASHTO 2002). These formulations were simple but accurate only within a specific range of geometrical parameters, i.e., girder spacing near 6 ft and span length about 60 ft (Hays et al. 1986). Hays et al. study was focused on the effect of span length on the distribution of loads, which was neglected in the S/D formulation. For simple-span concrete girder bridges investigated in this study, the effect of span length was found to be considerable. It was shown that LFD distribution factors could be conservative and unconservative for long and short span bridges, respectively.

Researchers argued that this form of formulation could lead to unrealistic results as some bridge characteristics influencing the distribution of loads were ignored (Kuzmanovic and Sanchez 1986; Bakht and Moses 1988). Bakht and Moses investigated the effect of span length, number of traffic lanes, and edge-stiffening on the distribution of loads on girder bridges using refined analysis methods. The results indicated that LFD formulations could lead to overly conservative designs due to the neglect of bridge aspects that influence its demand characteristics.

Moreover, the S/D equations, which form the basis of the distribution factor formulas, were only applicable to simply-supported non-skewed bridges and lost accuracy for continuous and skewed decks (Chen et al. 1957; Marx et al. 1986). One hundred twelve (112) continuous concrete girder bridges with skew angle varying between 0 to 60 degree were analyzed employing FE methods in Khaleel and Itani study. It was shown that deck skew could decrease the moment demand in interior girders and increase it in exterior ones (Khaleel and Itani 1990). In another study, Decastro et al. evaluated the accuracy of load distribution provisions for one hundred twenty (120) simply-supported concrete girder bridges using the finite element approach and proposed skew correction factors to include deck skewness effect in demand calculations (Decastro et al. 1979).

Empirical DFs in standard specifications were used only with minor changes until 1994 when experimental tests and mathematical analyses were conducted on lateral live load distribution to investigate the accuracy of DFs (Zokaie et al. 1991; Tarhini and Frederick 1992;

Bishara et al. 1993). Later, the DFs were revised based on a comprehensive study conducted on wheel loads distribution on highway bridges in the National Cooperative Highway Research Program, NCHRP 12-26 project, where the effect of the different bridge features such as span length, slab thickness, girder dimensions/spacing, and the skew angle was investigated (Zokaie et al. 1991). It was reported that revised DF formulas provided higher accuracy compared to empirical equations by including additional bridge geometrical characteristics with a wider range of applicability (Mabsout et al. 1997a; Zokaie 2000). These formulas were adopted by AASHTO Load and Resistance Factor Design standard specifications (LRFD) as the guide specifications for distribution of live loads on highway bridges since 1994 (AASHTO 1994).

The above NCHRP 12-26 project focused on the response of the bridge superstructures under a defined set of trucks specified by standard codes (HS trucks). The main objective of this project was to update provisions for DFs using refined analysis and propose simplified methods for routine design and rating of bridges. The research was focused on more commonly used bridge types, including slab and slab-on-girder bridges. To study the range of applicability and common values of bridge parameters, a database of actual bridges was compiled, including three hundred sixty-five (365) girder bridges (steel and prestressed/reinforced concrete). Span length/width, skew angle, number of girders, girder spacing, girder dimensions, slab thickness, and over-hang were considered variables in the parametric study performed in this project.

A hypothetical average bridge was obtained with average properties. Using finite element analysis, parameters were varied one at a time in the average bridge model, and live load distribution factors were obtained for both shear and moment. Using statistical analysis, simplified formulas were developed to capture DF variation with each parameter for single and multiple lane loadings. In the Zokaie et al. parametric study, it was assumed that the different parameters are independent of each other. DFs were developed for simple-span non-skewed interior girders, and correction factors proposed to consider continuity, skewness, and girder-exteriority effects. The contribution of non-structural components, such as edge-elements were neglected in this study.

Recent field tests and analytical studies have shown that the Zokaie et al. proposed modifications can be improved (Chen 1999; Hou et al. 2004; Yousif and Hindi 2007). Shahawy and Huang performed an extensive parametric study on prestressed concrete girder bridges with different span length/width and girder spacing (Shahawy and Huang 2001). Comparison of test and FE results with code-specified distribution factors showed that LRFD formulations are greatly conservative. It has been observed that neglecting the effect of diaphragms (Green et al. 2002), parapet/railings (Mabsout et al. 1997b), deck skewness (Barr et al. 2001; Khaloo and Mirzabozorg 2003), and spans continuity (Mabsout et al. 1998; Barr et al. 2001) could result in conservative estimates of loads assigned to each girder when using the LRFD distribution factor provisions.

Test results of six (6) prestressed concrete bridges with diaphragms were presented in the study of Cai et al., where measured distribution factors were compared to those obtained using LRFD provisions (Cai et al. 2002). It was shown that the neglecting effect of diaphragms could lead to an overestimated demand in girders. Cai and Shahawy showed in another study that distribution and rating factors of six (6) concrete girder bridges approached test measurements when factors such as diaphragms and parapets were included in their 3D modeling (Cai and Shahawy 2004).

Barker conducted field testing on a continuous girder bridge with substantial curbs and railings. The test results showed that the experimental lateral distribution of load is significantly lower than the code-specified one. Consequently, measured rating factors were higher than those calculated using the LRFD procedure. It was stated that the unaccounted system stiffness due to the presence of curbs and railings provided additional capacity since these components contributed to the load-carrying capacity of the bridge (Barker 2001).

In an analytical study, the effect of barriers and sidewalks on bridge ultimate capacity and load distribution was investigated by Eamon and Nowak for simple-span prestressed girder bridges (Eamon and Nowak 2002). The finite element results showed that secondary elements could significantly reduce girder distribution factors depending on the stiffness and geometry of these elements.

Similarly, Conner and Hou performed a parametric study on I-girder continuous concrete bridges to explore the extent of beneficial effects of parapets on distribution factors of such bridges (Conner and Hou 2006). The presence of parapets was shown to reduce distribution factors obtained from FE analysis compared with those from LRFD methods. In another similar study, rating factor results of ten (10) single-span T-beam concrete bridges were presented in Hasancebi and Dumlupinar work using 3D modeling (Hasancebi and Dumlupinar 2013). The results indicated that including parapets and end-diaphragms in superstructure modeling decreased demand and, consequently, improved rating factors of analyzed bridges compared to values obtained from the LRFD approach.

In flat-slab reinforced concrete bridges, the equivalent strip width (E), defined as the transverse distance over which a wheel line is distributed, plays the role of distribution factor to allocate a portion of the live load to each 1-ft wide beam strip. This concept has been used since the 1940s using an empirical formulation based on research by Westergaard (1930), Newmark (1938), and Jensen (1938). Earlier provisions of E were the only function of span length and did not include other geometrical features such as bridge width/thickness and deck skew. Empirical formulations were the basis of distribution factors (E) for slab bridges in standard LFD procedures until 2002. Like in girder bridges, it was claimed that empirical DF formulations for this type of bridge were not accurate before provisions of NCHRP 12-26 (Azizinamini et al. 1994b).

A continuous reinforced concrete slab concrete bridge was tested to failure by Jorgenson and Larson and it was reported that the measured load-carrying capacity of the bridge was larger than that calculated according to LFD procedure (Jorgenson and Larson 1976). Six (6) slab bridges were tested under service loads in an experimental study conducted by Azizinamini et al. to evaluate the accuracy of load distribution predictions based on LFD specifications (Azizinamini et al. 1994a). Bridges were selected with single and multiple spans and different skew angles to identify parameters other than span length, affecting the results. The comparison between experimental and analytical results indicated that the load-carrying capacity of slab bridges was underestimated when the standard LFD procedure was followed.

Frederick and Tarhini compared moment responses obtained from finite element analysis, model testing, and application of LFD design procedures for single-span slab bridges with different length and width dimensions (Frederick and Tarhini 2000). It was shown that code-predicted bending moments were not accurate when compared to FE analysis results. The results revealed under/overestimation depending on the span length of bridges.

Mabsout et al. performed a parametric study on single-span slab bridges. The finite element method was used to investigate the effect of span length, slab width, and wheel load configurations on longitudinal bending moments. It was observed that LFD moment predictions could be under/overestimated compared to refined analysis results (Mabsout et al. 2004).

In another parametric study, Mabsout et al. investigated the effect of deck skew on moment response of single-span slab bridges (Mabsout et al. 2002). It was shown that increasing the skew angle of the bridge deck could decrease the distribution of loads and neglecting this parameter could result in a conservative demand estimate. Similarly, Menassa et al. studied the influence of skew angle on the response of single-span concrete slab bridges. Bending moments were obtained for bridges with different span lengths/widths when the skew angle was increased from 0 to 50 degrees. Reduced demand was observed for skewed bridges indicating that LFD predictions were overestimated since the skew effect was neglected in the development of distribution factor formulation (Menassa et al. 2007).

In the NCHRP project (Zokaie et al. 1991), span length, deck width, skew angle, number of lanes, and slab thickness of one hundred and thirty (130) actual slab bridges were considered to obtain a common range of geometrical features of this bridge type. The DF formulation was developed following the same assumptions and procedure as in girder bridges. It must be noted that in the NCHRP 12-26 report, for the first time, bridge width, slab thickness, and skew were geometrical parameters considered in the formulation of E. Similar to T-beam bridges, the E formulation proposed in this report was adopted in LRFD provisions. A limited number of studies were conducted to explore the accuracy and range of application for slab DFs.

Mabsout et al. analyzed one hundred and twelve (112) non-skewed slab bridges with different geometrical features using FE methods (Mabsout et al. 2004). It was reported that moment responses obtained from the LRFD procedure was overestimated compared to finite element results.

Menassa et al. evaluated the accuracy of the skew reduction factor specified in LRFD for slab bridges with six district skew values. This study indicated that the LRFD skew reduction factor is conservative, especially for large skew values. It was shown that the discrepancy between code and FE results increases for larger skew angles (more than 20 degrees).

Similar to T-beam bridges, the effect of non-structural elements is not considered in the E provisions for slab reinforced concrete bridges. Neglecting the relatively high flexural stiffness of the barrier compared with the relatively low stiffness of the reinforced concrete slab impacts the demand distribution over exterior and interior beam strips. Previous studies (Amer et al. 1999; Feredrick and Tarhini 2000; Mabsout et al. 2004; Menassa et al. 2007) have shown that ignoring this effect might overestimate the live load share of the equivalent interior beam strips and underestimate it on the exterior strips.

In an analytical research by Jensen, longitudinal moments were calculated for single-span slabs with stiffened edges under dead and live load applications (Jensen 1939). Moment values for slab and edge-beams were provided graphically for different edge stiffness values. The aspect ratio of the slab and stiffness of the edge-beam were two factors that influenced the moment developments. Although they may have been placed from safety and architectural viewpoints, it was also concluded that curbs and handrails have a structural function to perform if properly designed.

In an earlier mentioned experimental study conducted by Azizinamini et al., in addition to instrumenting the slabs, strain gages were installed to curbs to explore the effect of edge-beams on load distribution of the six (6) studied slab bridges. Strain distribution obtained from field measurements revealed that curbs behaved in a composite manner with the slab. Reduced slab responses in the vicinity of curbs were attributed to this composite action between structural (slab) and non-structural (curb) components of the bridge superstructure.

Amer et al. performed a small-scale parametric study on twenty-seven (27) single-span non-skewed slab bridges to evaluate the accuracy of current distribution factor formulation, focusing on edge-stiffening effect (Amer et al. 1999). Span length, bridge width, slab thickness, and edge-beam dimensions were the main parameters considered in this study. It was shown that LRFD gives a conservative estimate of the distribution factor. Including edges in superstructure analysis decreased the distribution factor for interior portions of the bridge deck. It was found that edge-beam depth is the main parameter affecting the demand distribution in the transverse direction.

1.3 Problem Statement and Original Contribution

The original contribution of this research is to update current DFs with proposed modification factors that reflect the effect of non-structural elements in load estimate process.

In AASHTO Load and Factor Design (LFD) specifications (AASHTO 2002), empirical distribution factors were only related to girder spacing in T-beam bridges and span length in slab bridges. The effect of angle of skew and continuity of bridge spans on the distribution of loads was not incorporated. Subsequently, and based on the NCHRP 12-26 project findings, more geometrical features were included in the DF formulations such as bridge length, deck thickness, and girder dimensions in T-beam bridges and bridge width in slab bridges. Skew correction factors were proposed to adjust the longitudinal moment and shear responses. DFs proposed in the NCHRP 12-26 report were implemented in AASHTO Load and Resistance Factor Design (LRFD) specifications (AASHTO 2017) with minor changes.

Table 1-1 and Table 1-2 summarize the evolution of DF formulations. In Table 1-1, for slab bridges, E, L, W, and N_l are equivalent strip width, span length, edge-to-edge bridge width, and number of lanes, respectively. For T-beam bridges (Table 1-2), S, L, $K_g = n(I + Ae^2)$, and t_s are respectively girder spacing, span length, longitudinal stiffness, and slab thickness. d_e is horizontal distance from the centerline of the exterior web of exterior beam at deck level to the interior edge of curb or traffic barrier. In K_g formula, n is the modular ratio between beam and slab materials, I is girder stiffness, A is girder area, and e is the eccentricity between centroids of girder and slab.

To date, the effect of secondary members has been neglected in the DFs. In this thesis, the sensitivity of demand estimate to non-structural elements was assessed in a small sample of bridges in Indiana. Then, in a parametric study, non-structural elements were included in 3D modeling of the slab and T-beam bridge superstructure. Their effect on the distribution of loads across the interior sections of the bridge deck was evaluated. In both bridge types, skewed and continuous superstructures combined with secondary elements were modeled to investigate the possible interaction between these parameters and assess the reliability of available skew correction factors. Afterward, a statistical study was applied to the parametric study results to formulate the effect of secondary elements on moment and shear responses of studied bridges.

1.4 Document Overview

This document involves five chapters. Chapter 1 includes the motivation of the study, research background in the form of literature review, and problem statements followed by research objectives and its original contribution. In Chapter 2[1], research methods are explained in analysis of a case study including ten samples of slab and T-beam reinforced concrete bridges in Indiana. Procedures of bridge sample selection, 2D and 3D methods of analysis for bridge evaluation are

[1] F. Ravazdezh, S. Seok, G. Haikal, and J. A. Ramirez (2021). “Effect of Nonstructural Elements on Lateral Load Distribution and Rating of Slab and T-Beam Bridges.” *Journal of Bridge Engineering*. Under review. S. Seok, F. Ravazdezh, G. Haikal, and J. A. Ramirez (2019). “Strength Assessment of Older Continuous Slab and T-beam Reinforced Concrete Bridges.” *Joint Transportation Research Program Publication*, Purdue University, IN.

elaborated in this chapter. In Chapter 3[2], approaches followed in the parametric study are provided followed by a thorough discussion on findings of effect of studied parameters in demand evaluation of slab and T-beam bridges. In Chapter 4[3], conducted statistical analysis, regression modeling, and the framework for developing modification factors to update current load estimate procedures are discussed in detail. Lastly, Chapter 5 includes summary of the key results of the study, presents potential improvements to the load estimate procedure of slab and T-beam bridges, and provides recommendations for future research.

Table 1-1 Equivalent Strip Width (E) for Slab Bridges

Bridge	Flat-Slab	
Effect	Moment and Shear	
Traffic	Single-Lane	Multiple-Lane
AASHTO (LFD) 1970-2002	$4 + 0.06L \leq 7$	
NCHRP (12-26) 1991	$0.5 + 0.25\sqrt{LW}$	$3.5 + 0.06\sqrt{LW}$
AASHTO (LRFD) 1994-present	$0.4 + 0.21\sqrt{LW}$	$3.5 + 0.06\sqrt{LW} \leq \frac{W}{N_L}$

[2] F. Ravazdezh, J. A. Ramirez, and G. Haikal (2021). "Modification Factors for Live Load Distribution Factors of Slab and T-Beam Reinforced Concrete Bridges." *Journal of Bridge Engineering*. Under Preparation.

[3] F. Ravazdezh, J. A. Ramirez, and G. Haikal (2021). "Improved Live Load Distribution Factors for Use in Load Rating of Slab and T-Beam Reinforced Concrete Bridges." *Joint Transportation Research Program Publication*, Purdue University, IN.

Table 1-2 Distribution Factors for T-beam Bridges

Moment				
Girder	Interior		Exterior	
Traffic	Single Lane	Multiple Lane (g_m)	Single Lane	Multiple Lane
AASHTO (LFD)* 1970-2002	$\frac{S}{6.5}$ Lever Rule if $S > 6$	$\frac{S}{6}$ Lever Rule if $S > 10$	Lever Rule	
NCHRP (12-26) 1991	$0.1 + \left(\frac{S}{4}\right)^{0.4} \left(\frac{S}{L}\right)^{0.3} \left(\frac{K_g}{12Lt_s{}^3}\right)^{0.1}$	$0.15 + \left(\frac{S}{3}\right)^{0.6} \left(\frac{S}{L}\right)^{0.2} \left(\frac{K_g}{12Lt_s{}^3}\right)^{0.1}$	Lever Rule	$g_{Mm} \left(0.77 + \frac{d_e}{9.1}\right)$
AASHTO (LRFD)** 1994-present	$0.06 + \left(\frac{S}{14}\right)^{0.4} \left(\frac{S}{L}\right)^{0.3} \left(\frac{K_g}{12Lt_s{}^3}\right)^{0.1}$	$0.075 + \left(\frac{S}{9.5}\right)^{0.6} \left(\frac{S}{L}\right)^{0.2} \left(\frac{K_g}{12Lt_s{}^3}\right)^{0.1}$	Lever Rule	$g_{Mm} \left(0.77 + \frac{d_e}{9.1}\right)$
Shear				
AASHTO (LFD)* 1970-2002	-			
NCHRP (12-26) 1991	$0.6 + \frac{S}{15}$	$0.4 + \frac{S}{6} - \left(\frac{S}{25}\right)^2$	Lever Rule	$g_{Vm} \left(0.6 + \frac{d_e}{10}\right)$
AASHTO (LRFD)** 1994-present	$0.36 + \frac{S}{25}$	$0.2 + \frac{S}{12} - \left(\frac{S}{35}\right)^2$	Lever Rule	$g_{Vm} \left(0.6 + \frac{d_e}{10}\right)$

* Distribution factor per truck wheel
** Distribution factor per truck lane

2. STRENGTH ASSESSMENT OF REINFORCED CONCRTE BRIDGES EXPLORATORY CASE STUDY: INDIANA BRIDGE SAMPLES

2.1 Introduction

Bridge construction in the 1950s and 1960s favored Reinforced Concrete (RC) flat-slab and T-beam structural systems for overpasses or bridges across water streams and roads. These bridges represent an important component of the existing network inventory with 2834 slab bridges and 766 T-beam bridges in Indiana. They are therefore required to satisfy existing specifications when checked for load-carrying capacity. Bridge capacity is evaluated using the standard load rating procedure specified by the American Association of State Highway and Transportation Officials (AASHTO). The load rating procedure is used for bridge evaluation under current and future traffic and overload permit vehicles. Based on load rating results, a bridge falls in safe, posted, and closed categories.

According to the Federal Highway Administration (FHWA), almost 21% of RC slab and T-beam bridges in Indiana were identified as structurally deficient or functionally obsolete based on load rating results as of 2013 (FHWA 2019). Among them, about 200 of these bridges were either closed or posted. Also, around 40% of existing slab bridges and about 90% of T-beam ones in Indiana have exceeded their 50-year design life, and their load-carrying capacity is being monitored closely. Therefore, the accurate and reliable evaluation of bridge live load-carrying capacity is critical to state and local government agencies from safety and financial points of view.

Indiana Department of Transportation (INDOT) applies a Conventional Load Rating approach (CLR) for bridge strength assessment, which relies on a two-dimensional (2D) analysis, based on beam theory, to establish bridge demand in moments and shears. The bridge is modeled using centerline dimensions, and live load Distribution Factors (DF) are used to account for load distribution in the transverse direction. This method has been implemented in the BrR software used by INDOT for bridge load rating and overload permitting assessments. Recent findings, however, have indicated that the CLR may underestimate bridge capacity. Since the actual behavior of a bridge structure is three-dimensional (3D) in nature, a 3D computational model is better suited to estimate bridge carrying capacity for load rating. Using 3D models, it is also possible to explicitly account for transverse load distribution and include non-structural components such as curbs, railings, parapets, sidewalks, and end-diaphragms that impact bridge structural behavior.

This chapter presents investigation on an improved rating methodology for slab and T-beam bridges using the tools of 3D Finite Element analysis (FE). The effect of simplifying assumptions used in CLR on rating results of ten bridge samples was identified. Bridge load rating results obtained following CLR and 3D methods were compared, and effective factors were identified. Findings of case study analysis were served as a basis to perform an extensive parametric study using 3D finite element models for a thorough investigation of the evaluation of slab and T-beam bridges presented in Chapter 3.

2.2 Case Study Details

Two reinforced concrete bridge types, solid slab and T-beam, were assessed employing conventional 2D and 3D FE linear-elastic analyses. Dead and live loads responses in terms of bending moments and shear forces were determined. The structural capacity of the bridge superstructure was calculated and used to evaluate the Rating Factors (RF) of the analyzed bridges. Results of FE methods were compared to those obtained using 2D analysis. The effect of reinforced concrete secondary elements (guardrails, sidewalks, and diaphragms) on the structural behavior of bridges was fully studied in both response and capacity aspects. Sample bridge selection procedure, two-dimensional analysis, and three-dimensional method are discussed in the following subsections.

2.2.1 Sample of Representative Bridges

A sample of ten reinforced concrete bridges was selected based on a statistical study on the National Bridge Inventory (NBI) database for Indiana. The dataset consists of 3500 reinforced concrete bridges with 2834 flat-slab and 766 T-beam systems. Bridge age, span length, number of spans, roadway width, number of traffic lanes, skew angle, and deck/girders thickness were considered to determine relative frequencies and common variety ranges of geometrical parameters. The final sample group, represented in Table 2-1 contains five slab and five T-beam bridges with geometrical characteristics falling within the range of highest relative frequencies.

Figure 2-1.a and Figure 2-1.b illustrate a cross-section sketch of a typical reinforced concrete slab and T-beam bridge, respectively.

As illustrated in Figure 2-2, about 50% of the reinforced concrete bridges in service in Indiana have exceeded their 50-year design life. Additionally, slab bridges have been favored over recent decades. Maximum span lengths for most bridges of the type considered in this study fall within the range between 20 ft and 50 ft. Among the bridges considered, three-span bridges predominate, accounting for 66% of the total sample. Single-span bridges are the second largest population, with 24% of the total. For both bridge types, two-lane bridges are predominant, accounting for almost 90% of the total. The roadway width of nearly half of the database's bridges lies within the range from 20 ft to 30 ft. Almost 50% of the bridges have a skew angle less than 15 degrees.

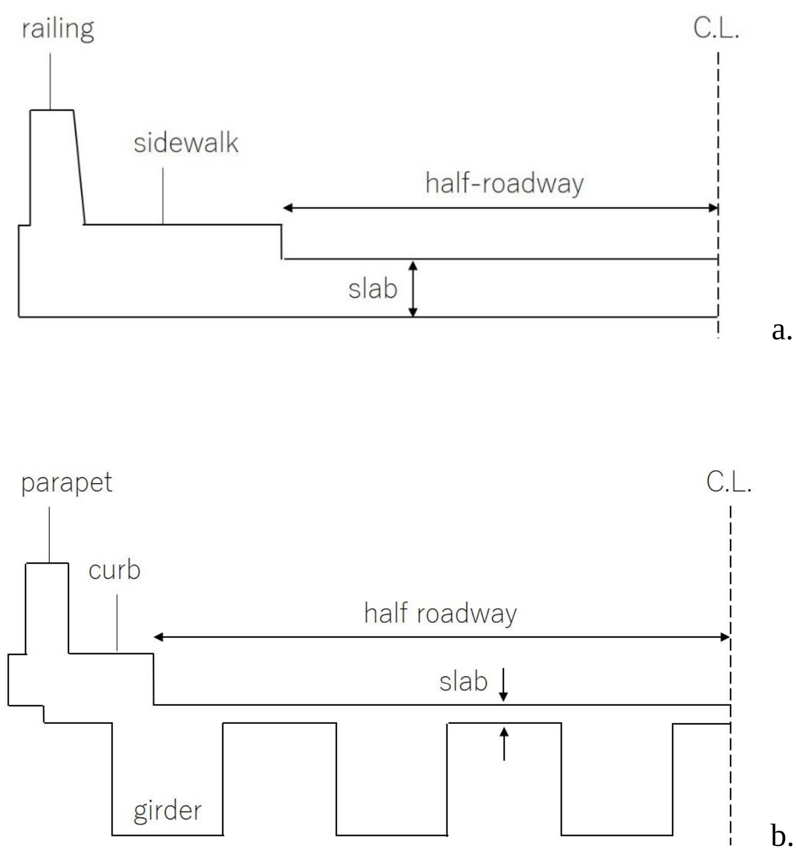

Figure 2-1 Typical Cross-Section Configuration; a. Slab, b. T-beam

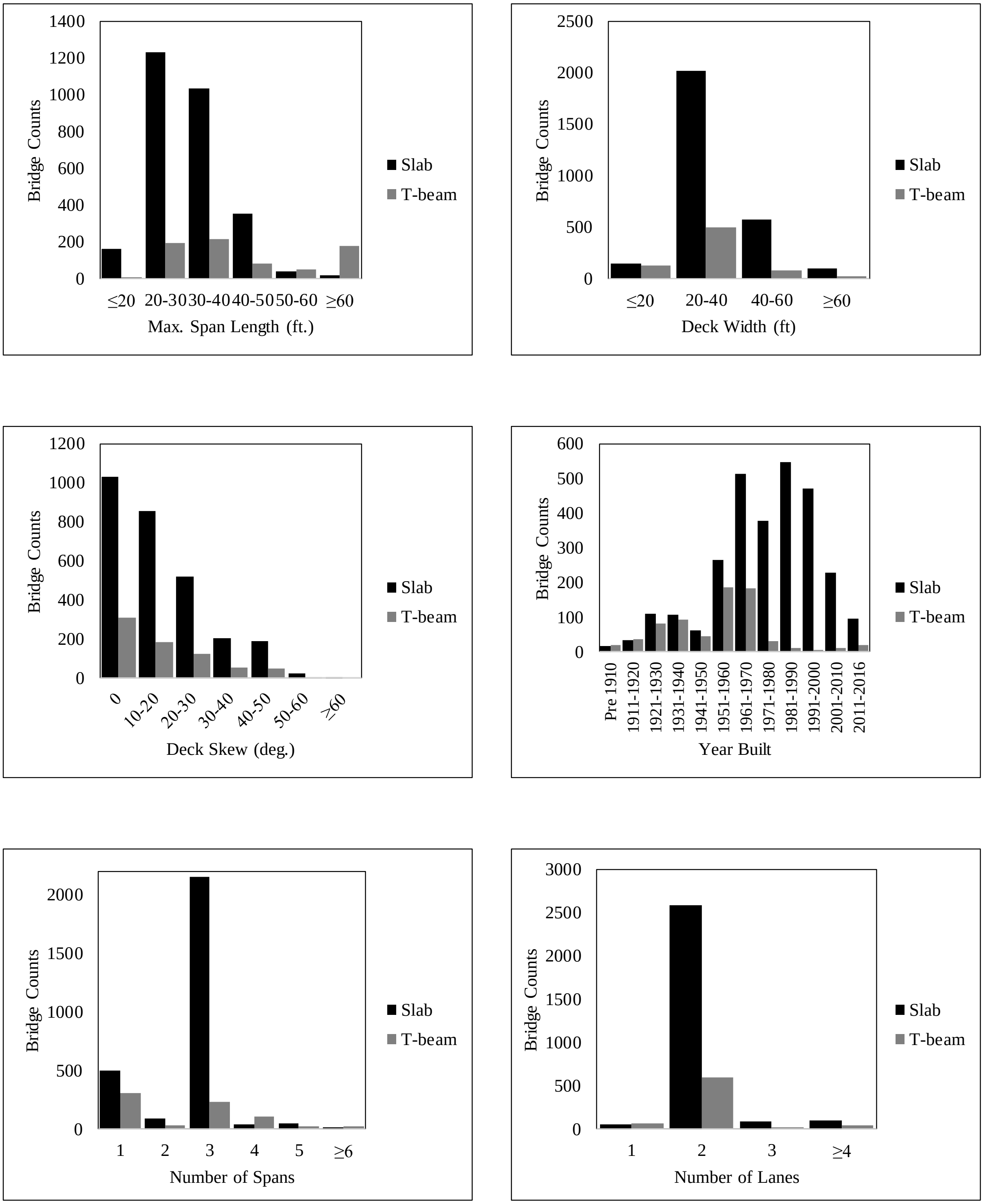

Figure 2-2 Statistical Distribution of Bridge Characteristics

Table 2-1 Representative Sample Bridges

Sample No.	Bridge Type	Year of Built	No. of Spans	Span Length (ft)	Width (ft)	Slab Thickness (in.)	Skew Angle (deg.)	Girder Height-Width (in.)	Girder Spacing (ft)	Number of Girders
1	Flat Slab	1968	3	18-25-18	39.8	14.0	35	-		
2	Flat Slab	1964	1	50	39.4	28.0	20	-		
3	Flat Slab	1970	3	30-42-30	36.5	22.5*	7	-		
4	Flat Slab	1962	3	21-28-21	44.0	14.0	45	-		
5	Flat Slab	1982	3	32-42.5-32	46.5	21.0	20	-		
6	T-Beam	1951	1	36	41.0	7.5	30	33.2-20.9	7.9	6
7	T-Beam	1924	1	38	41.0	7.2	30	31.7-24.0	7.9	6
8	T-Beam	1957	3	40	28.0	6.0	0	24.0-24.0	6.9	5
9	T-Beam	1960	1	28	40.0	6.5	15	27.0-17.5	7.5	6
10	T-Beam	1938	1	28	28.0	7.7	30	20.7-18.1	6.9	5

* Average value of the variable thicknesses along the bridge length (15 in. to 30 in.)

2.2.2 Two-Dimensional (2D) Analysis

Selected bridges were analyzed based on the 7th edition of AASHTO Load and Resistance Factor Design Specifications (AASHTO 2017) and the 2nd edition of Manual for Bridge Evaluation (AASHTO 2011). Based on the MBE, only permanent loads and vehicular loads are considered to be of importance in the load rating process, and environmental loads such as wind, ice, temperature, streamflow, and earthquake are usually ignored in this procedure. In the 2D approach, each bridge's superstructure was simplified as a simply-supported continuous beam with span length measured between center-to-center of the columns. The deck was divided into beam strips for slab bridges, and for T-beam bridges, it was divided into interior and exterior girders. Beams in slab bridges were measured in 1-ft width and height equal to the thickness of the slab. In T-beam bridges, the effective flange widths of T-section beams were computed in accordance with the specifications of Article 4.6.2.6 in LRFD. Figure 2-3 shows cross-section of beams used for 2D analysis.

2.2.2.1 Load Applications

The dead loads were computed based on dimensions obtained from the bridge plans. Unit weights of materials were selected following LRFD Table 3.5.1-1. According to this Table, unit weights of 0.150 kcf, 0.145 kcf, and 0.045 kcf were selected for structural reinforced concrete, plain surface concrete, and asphalt overlays, respectively. The values of structural loads (DC) and surface-wearing load (DW) for sample bridges are summarized in Table 2-2 and Table 2-3.

The live load was applied using vehicular HL-93 truck plus standard lane-load configuration as specified by AASHTO standards. Truck HL-93 consists of three axle loads of 8, 32, and 32 kips spaced 14 ft from each other, and the wheels are 6 ft apart. Lane-load configuration includes a uniform distributed load of 0.64 kips per ft. Vehicular loadings have been applied in the longitudinal direction transversely occupying 10-ft width as specified in LRFD specifications. A Matlab code was developed to obtain moment and shear envelopes under moving vehicular load applications. To validate the code, obtained responses for one case (Sample 1) were compared to those obtained using SAP-2000 software. The software features a moving-load function for 2D structural analysis. Figure 2-4 illustrates reliability of the developed script with good agreement between the results obtained from the two approaches.

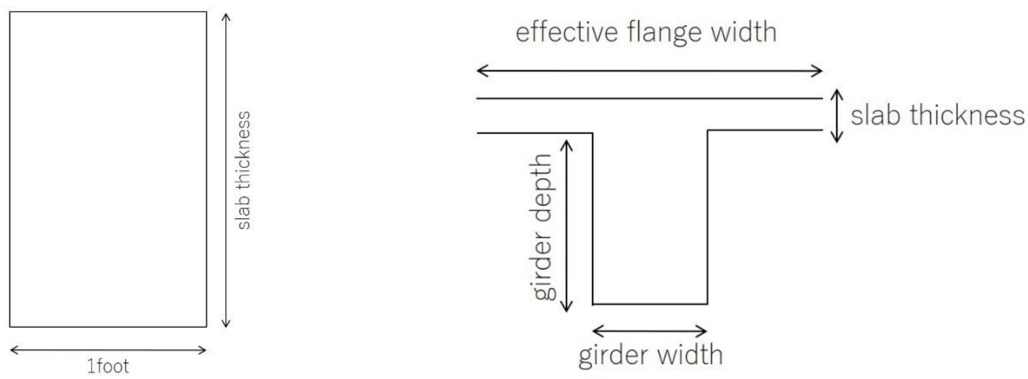

a. b.

Figure 2-3 Beam Cross-Sections; a. Slab, b. T-beam

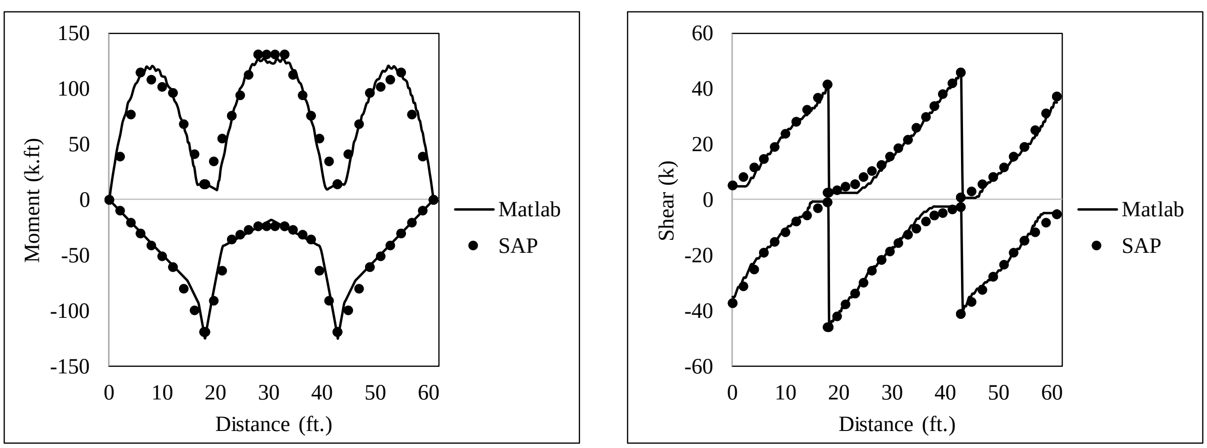

a. b.

Figure 2-4 SAP and Matlab Results Comparison; a. Moment Envelope, b. Shear Envelope

2.2.2.2 Load Distribution Factor

For 2D analysis, the live load distribution factor determines the portion of the live load assigned to a 1 ft beam-strip in slab type bridges and interior/exterior girders in T-beam type bridges. In slab bridges, DF is defined as equivalent strip width (E), a function of length and width of the bridge, and specified separately for single and multiple-lane loading according to Article 4.6.2.3 in LRFD. To compute DFs for interior and exterior girders in T-beam bridges, equations provided in Tables 4.6.2.2.2b-1, 4.6.2.2.2d-1, 4.6.2.2.3a-1, 4.6.2.2.3b-1 of LRFD specifications were used. Table 2-4 summarizes current DF formulations used for demand estimate in sample bridges.

In Table 2-4, for T-beam bridges, S, L, $K_g = n(I + Ae^2)$, and t_s are respectively girder spacing, span length, longitudinal stiffness, and slab thickness. d_e is horizontal distance from the centerline of the exterior web of exterior beam at deck level to the interior edge of curb or traffic barrier. In the K_g formula, n is the modular ratio between beam and slab materials, I is girder stiffness, A is girder area, and e is the eccentricity between centroids of girder and slab. For slab bridges, E, L, W, and N_l are equivalent strip width, span length, edge-to-edge bridge width, and number of lanes, respectively.

Table 2-2 Dead Loads on 1 ft Slab Strip of Slab Bridges

Sample No.	DC (k/ft)/1ft	DW (k/ft)/1ft
1	0.208	0.012
2	0.390	0.119
3	0.311	0.012
4	0.225	0.030
5	0.288	0.018

Table 2-3 Dead Loads on Interior and Exterior Girders of T-beam Bridges

Sample No.	DC (k/ft)		DW (k/ft)	
	Interior Girder	Exterior Girder	Interior Girder	Exterior Girder
6	1.388	1.558	0.024	0.015
7	1.510	1.750	0.024	0.015
8	1.110	1.450	0.210	0.140
9	1.090	1.490	0.023	0.018
10	1.080	1.640	0.043	0.038

It should be noted that multiple presence factors from Table 3.6.1.1.2-1 of LRFD were applied to consider the effect of the number of loaded traffic lanes. Also, skew correction factors are defined in LRFD specifications to adjust the moment and shear responses of skewed bridges. Skew factors reported in Table 2-5 were calculated under provisions of Tables 4.6.2.2.2e-1 and 4.6.2.2.3c-1 (T-beam bridges) and Equation 4.6.2.3-3 (slab bridges) in LRFD.

Table 2-4 Live Load Distribution Factors

Effect		Moment	Shear
T-beam Bridge			
Interior Girder	Single Lane	$0.06+\left(\frac{S}{14}\right)^{0.4}\left(\frac{S}{L}\right)^{0.3}\left(\frac{K_g}{12Lt_s{}^3}\right)^{0.1}$	$0.36+\frac{S}{25}$
	Multiple Lane	$0.075+\left(\frac{S}{9.5}\right)^{0.6}\left(\frac{S}{L}\right)^{0.2}\left(\frac{K_g}{12Lt_s{}^3}\right)^{0.1}$	$0.2+\frac{S}{12}-\left(\frac{S}{35}\right)^{2}$
Exterior Girder	Single Lane	Lever Rule	Lever Rule
	Multiple Lane	$\left(0.075+\left(\frac{S}{9.5}\right)^{0.6}\left(\frac{S}{L}\right)^{0.2}\left(\frac{K_g}{12Lt_s{}^3}\right)^{0.1}\right)*\left(0.77+\frac{d_e}{9.1}\right)$	$\left(0.2+\frac{S}{12}-\left(\frac{S}{35}\right)^{2}\right)\left(0.6+\frac{d_e}{10}\right)$
Flat-Slab Bridge			
Single-Lane		$E=10+5\sqrt{LW}$	
Multiple-Lane		$E=84+1.44\sqrt{LW}\leq\frac{12W}{N_l}$	

2.2.2.3 Rating Factor Procedure

Rating Factor (RF), as a measure of bridge rating assessment, was calculated following Equation 2-1. In this Equation, R_n is member resistance and DC, DW, and L are dead load effect of structural and nonstructural components, dead load effect of wearing surfaces and utilities, and live load effect, respectively. Dynamic load allowance factor, IM, was selected as 33%. System factor, ϕ_s, and condition factor, ϕ_c, were selected for both slab and T-beam type bridges according to Tables 6A.4.2.4-1 and 6A.4.2.3-1 of MBE. The bridge condition was assumed to be “good” for all bridges. The resistance factor, ϕ , was chosen for both moment and shear effects in accordance with Article 5.5.4.2 of LRFD specifications. From MBE, values provided in Table 6A.4.2.2-1 were selected for dead load factors, γ_{DC} and γ_{DW}, and the live load factor, γ_{LL}. All assumed values for the factors are reported in Table 2-6.

$$RF = \frac{\phi_s \phi_c \phi R_n - \gamma_{DC} * DC - \gamma_{DW} * DW}{\gamma_{LL} * L(1 + IM)} \tag{2-1}$$

Table 2-5 Skew Correction Factors

Sample No.	Skew Angle (deg.)	Skew Correction Factor	
		Moment	Shear
1	35°	0.875	
2	20°	0.959	
3	7°	1.000	
4	45°	0.800	
5	20°	0.959	
6	30°	0.944	1.103
7	30°	0.942	1.094
8	0°	1.000	1.000
9	15°	1.000	1.059
10	30°	0.951	1.124

Table 2-6 Values Considered for Factors in Equation 2-1

ϕ_s	ϕ_c	ϕ	γ_{DC}	γ_{DW}	γ_{LL}	IM
1	1	0.9	1.25	1.5	1.35	33%

To calculate members capacity (R_n), LRFD provisions in Articles 5.7 and 5.8 were followed to evaluate the flexural and shear strengths, respectively. The capacity of rectangular (slab bridges) and T-section (T-beam bridges) beams was computed according to longitudinal and transverse steel reinforcements arrangements provided in bridge structural plans. Concrete compressive strength and steel reinforcement yield strength were obtained from information provided in bridge drawings. When no material information was available, the values provided in Tables 6A.5.2.1-1 and 6A.5.2.2-1 of MBE were used for compressive and yield strength, respectively, based on the year of bridge construction. Rectangular stress block was assumed for compressive stress distribution. For all T-beam bridges, since the compression flange thickness was equal to or greater than the depth of the equivalent rectangular stress block, the section has been considered a rectangular cross-section.

The load rating procedure was performed for all sample bridges. It should be noted that for each bridge, different load rating factors according to different scenarios were calculated, including truck/lane loading, moment/shear effects, single/multiple-lane loading, and interior/exterior sections. Then, minimum RF values were reported as critical ones.

Load rating factors were calculated in a section-by-section approach for each bridge superstructure. A Matlab code was developed to compute capacity, demand estimate, and rating factor at each section along the bridge length. Using this code, vehicular loads were defined as moving loads, and moment/shear envelopes were obtained. To evaluate the reliability of the implemented code, results were compared with BrR outputs for one sample of each bridge type (Sample 5 and Sample 8). Figure 2-5 and Figure 2-6 show the consistency of results obtained from the two approaches for capacity, demand, and rating factor values evaluated at every selected section along the slab and T-beam bridge lengths, respectively.

As observed from the graphs, the results are in good agreement for capacity, demand, and RF estimates for both bridge samples. However, some mismatches exist for flexure rating factors at some locations for the slab sample bridge. These locations are not critical ones and do not affect the final results. Since the capacity and the demand were matched perfectly for this case, the inconsistency might be attributed to the fact that results provided from BrR software are not necessarily at the critical sections, and they depend on how the user has defined the sectional evaluation points.

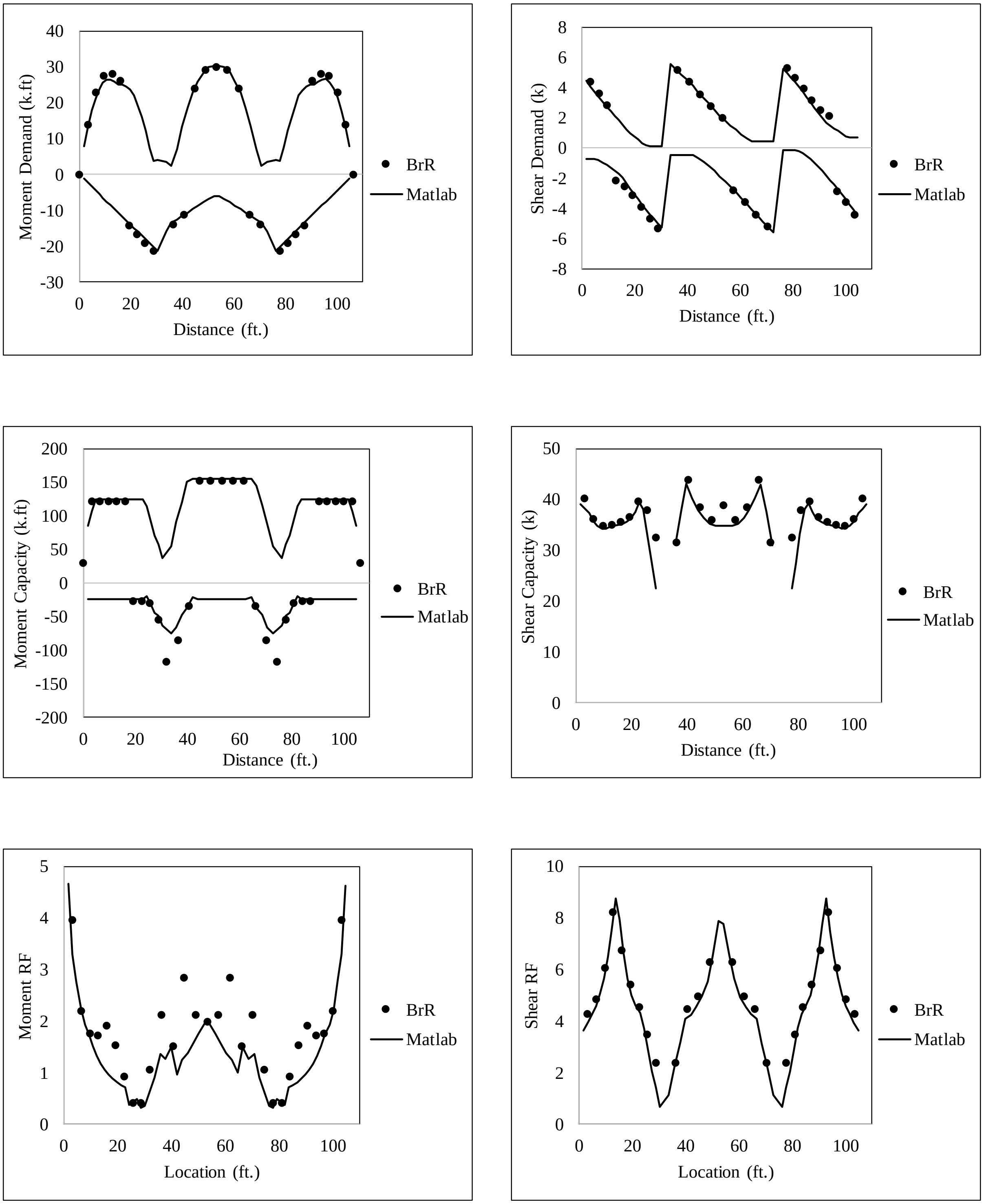

Figure 2-5 Matlab and BrR Results Comparison; Slab Sample 5

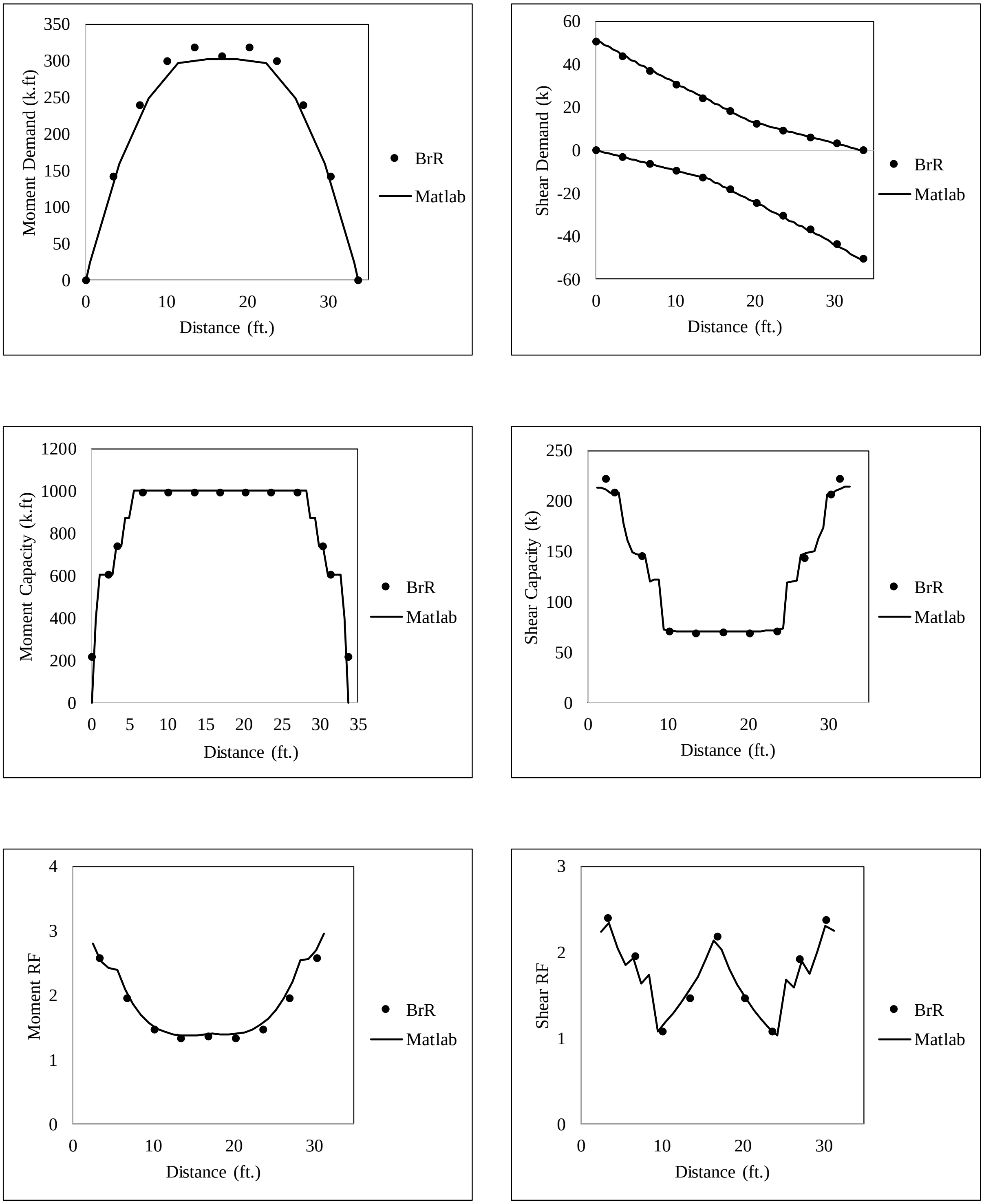

Figure 2-6 Matlab and BrR Results Comparison; T-beam Sample 8

2.2.3 Three-Dimensional (3D) Analysis

3D finite element models for bridge superstructures were analyzed using Abaqus 6.14-2 software. Superstructure features such as skewed deck, girders, curbs, railings, sidewalks, diaphragms, and variable dimensions, along with actual loading configurations were explicitly represented in the models. Influential modeling factors such as element type, mesh size, support modeling, and moving load application were studied based on AASHTO suggestions and recommendations from the available literature. A summary of modeling assumptions, load applications, and load rating procedures adopted for 3D modeling of sample bridges are presented in the following.

2.2.3.1 3D Modeling Assumptions

A solid element type (C3D8R) with three degrees of freedom at each node was selected to model slab and T-beam bridges deck to investigate the superstructure's 3D behavior. Solid elements are suitable to perform complex geometry modeling. They allow full compatibility between the deck and edge components such as railings and end-diaphragms with an integral action between them since the edges could be modeled continuously with slab part to ensure their participation in longitudinal stiffening. Particularly for the T-beam bridge model with solid elements, full composite action could be imposed between slab and girders to prevent any slip and displacement between them.

Steel reinforcement was modeled using 3D truss elements with six degrees of freedom at each node to account for the effect of reinforcement on the 3D distribution of stress in the cross-section. These elements transfer only axial forces and do not transmit bending moments. The truss elements were fully embedded in concrete elements to reflect a perfect bond between steel and concrete (see Figure 2-7).

Material properties such as concrete compressive strength (f_c), steel yield stress (f_y), and corresponding young modulus (E_c, E_s) were extracted from design data if available; otherwise, values suggested by the MBE were selected based on the year of construction. It was assumed that both materials are in the elastic range in FE analysis. A value of 0.2 was selected for the Poisson ratio of both materials. Supports were modeled assuming simple pin constraints at one end and roller one at the other end of the bridge span. For continuous bridges, middle supports were restrained using rollers. The supports were positioned on the bottom of the deck (slab bridges) and girders/diaphragms (T-beam bridges) to represent them sitting on columns/abutments.

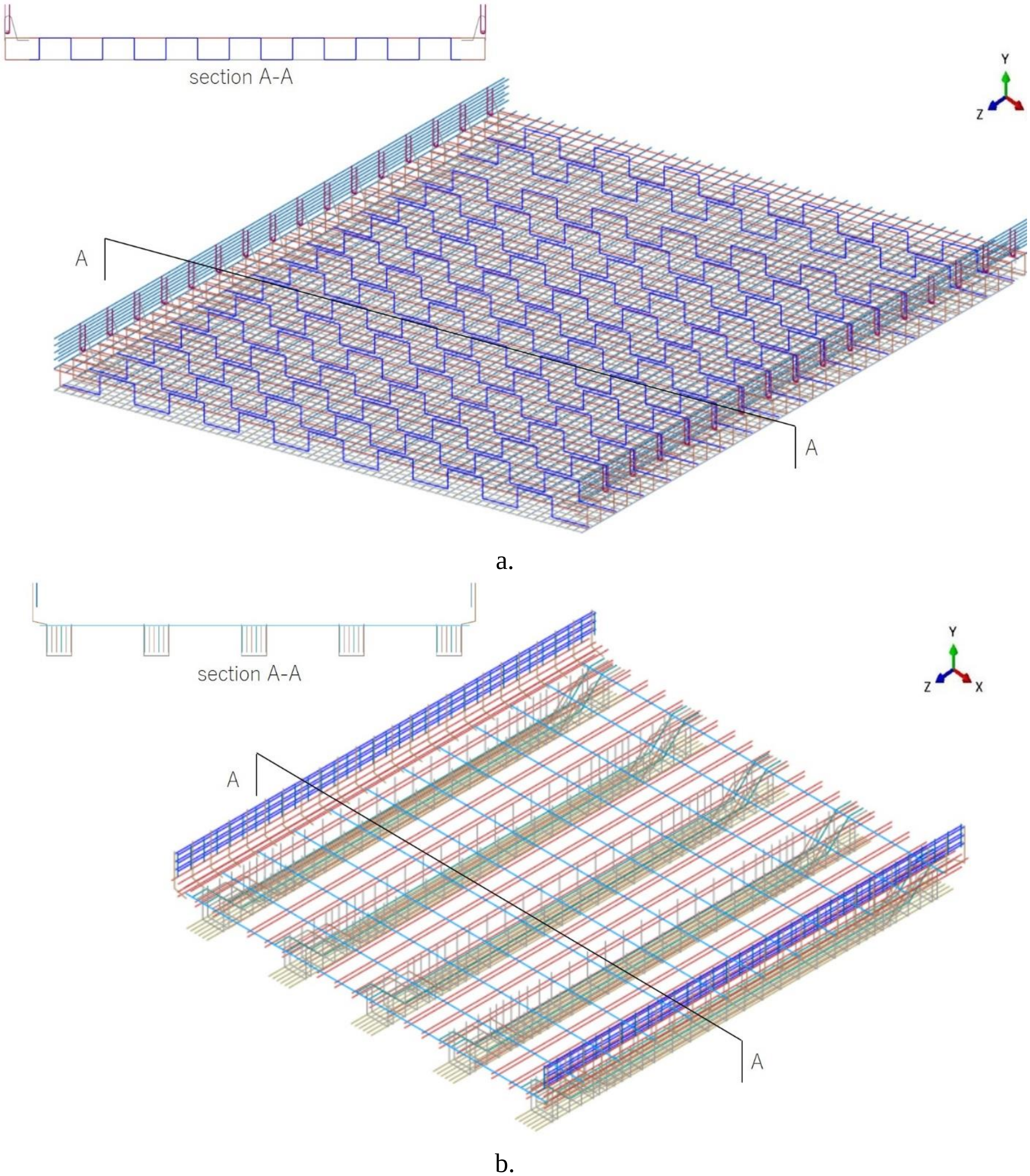

b.

Figure 2-7 Steel Reinforcement Modeling; a. Slab Sample 2, b. T-beam Sample 8

A convergence study was carried out with variable mesh sizes to find an appropriate element size that achieves a good balance between accuracy and computational time. The convergence study was performed on one sample of each bridge type, comparing the maximum moment values for each refinement level. Figure 2-8 illustrates the moment responses for a slab bridge (Sample 2) and a T-beam bridge (Sample 8) subjected to a single HL-93 truck moving close to the left curb using 2 in., 3 in., 6 in., and 10 in. mesh sizes. It is shown that the results did not change significantly beyond the 3 in. size, suggesting that this element size is suitable for the purpose of this study. However, taking computational cost/time (illustrated in Figure 2-8 for slab type bridge) into consideration, element sizes of 6 in. were selected for the FE discretization of slab bridges with an average error of 6%. Mesh refinements are shown in Figure 2-9 on an interior girder/strip of the mentioned sample bridges.

In the 2D approach, the bridge is analyzed and designed in a girder-by-girder approach. Following a similar procedure, bridge superstructures were discretized with interior/exterior beam-strips and girders in the 3D models such that the moment and shear responses would be comparable with results obtained from the 2D analysis. 1 ft interior strips comprise interior sections of the bridge slab, while railing and sidewalk components are included in exterior strips as illustrated in Figure 2-10.a. Figure 2-10.b shows the interior and exterior girders partitioning approach for T-beam bridges with exterior girders including the curb and parapet.

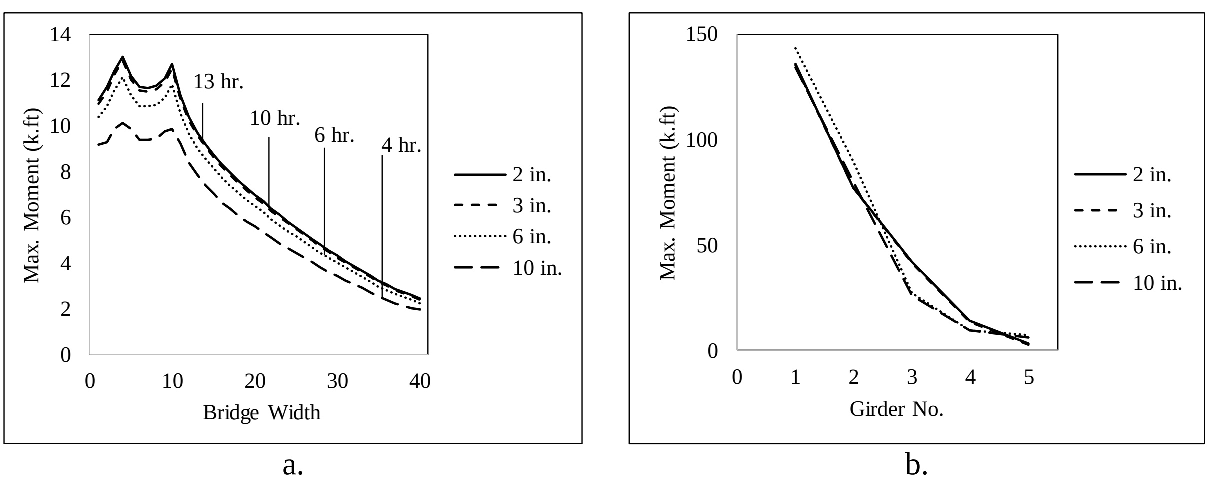

Figure 2-8 Convergence Study; a. Slab Sample 2, b. T-beam Sample 8

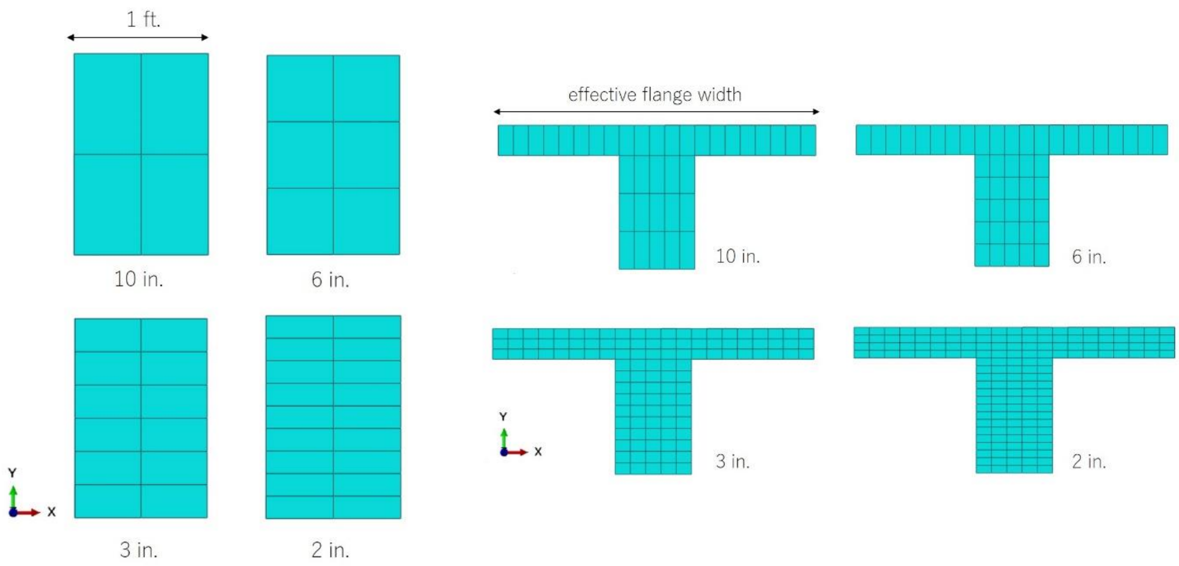

a. b.

Figure 2-9 Mesh Refinement on Typical Interior Beams; a. Slab, b. T-beam

2.2.3.2 Load Applications

To set up the vehicular load application in 3D modeling, beam-scale models were studied as verification models compared to corresponding 2D results. A Python code was developed to calculate moment and shear responses from Abaqus stress outputs and obtain section-by-section results comparable with those obtained from the 2D procedure. Figure 2-11 shows normal and shear stress distributions over FE discretization used in code implementation. Stresses were integrated over each section's elements using Equation 2-2 and Equation 2-3 to obtain moment and shear responses, respectively. In the Equations, $d\sigma$, $d\tau$, dA, and y represent normal stress, shear stress, element area, and element distance from neutral axis, respectively.

To apply a moving load in 3D beam models, a cylinder-shaped rigid body was placed on the beam model and moved forward step-by-step, as shown in Figure 2-12. The Python code was then used to obtain the final moment envelope at each section. As demonstrated in Figure 2-12, the moment response obtained for each loading step and the final moment envelope obtained using the Python code matched the results obtained from 2D analysis using equilibrium principles. After verification of beam models, the same methodology was applied to the full-scale bridge models.

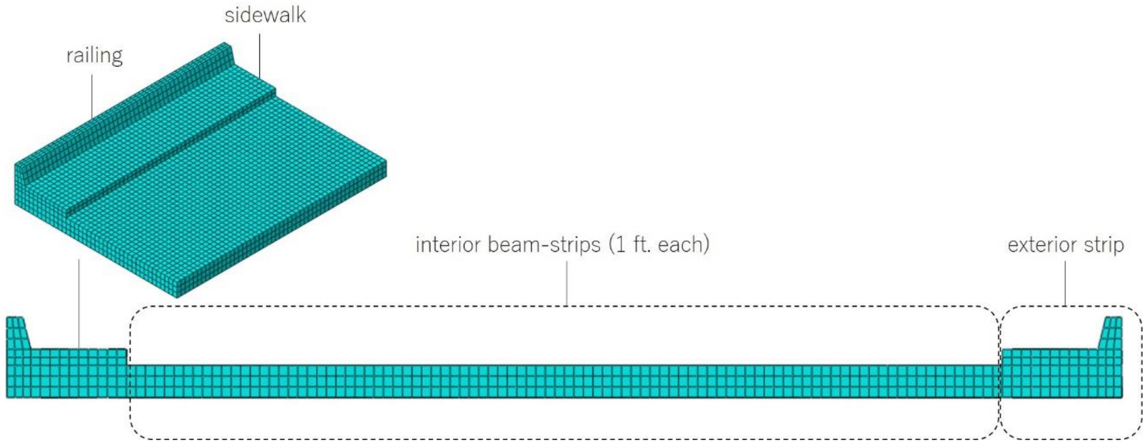

a.

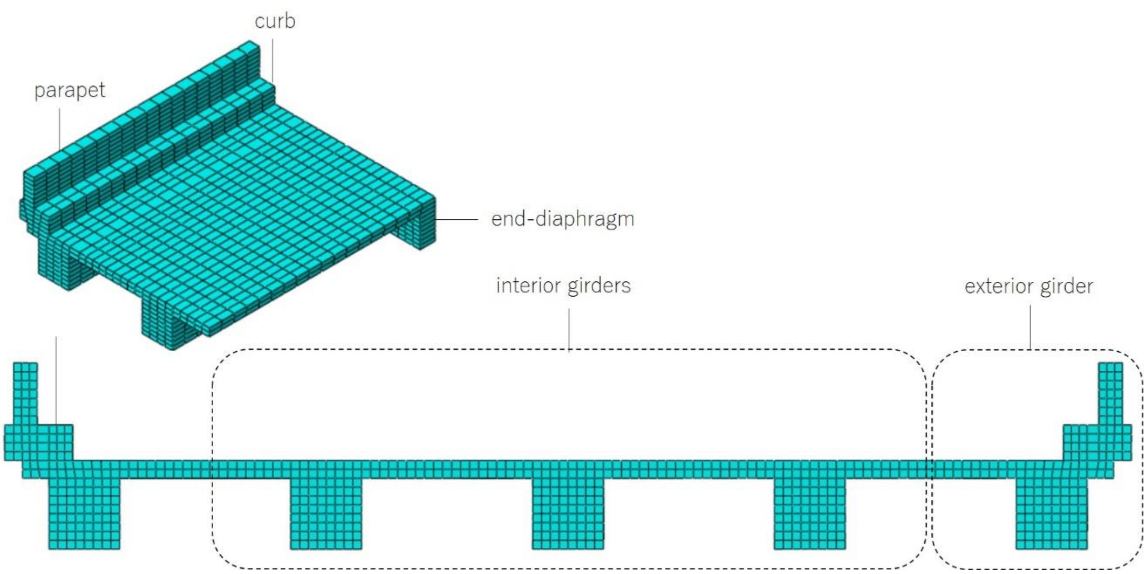

b.

Figure 2-10 Partitioning Approach; a. Slab, b. T-beam

$$M = \int d\sigma . y . dA \tag{2-2}$$

$$V = \int d\tau .\ dA \tag{2-3}$$

Following the same approach, the HL-93 truck was applied to full-scale bridge models. For truck modeling, based on LRFD recommendations, the wheel loads were applied using a rigid patch measured in 20 in. length and 10 in. width with equivalent pressure uniformly distributed over the contact surface instead of point loads to avoid stress concentration and convergence problems. Single and multiple trucks were moved in the longitudinal direction to obtain maximum moment/shear response and positioned transversely in different locations across the bridge width to investigate the effect of lateral load distribution. Moreover, approach slabs were modeled to accommodate trucks moving beyond the bridge deck to explore the effect of partial loading on moment and shear responses. Also, trucks were moved in parallel and opposite directions in multiple lane loading cases. The loading was applied considering a 2 ft distance between the first axle and the curb and a minimum 4 ft distance between trucks for multiple truck loading cases.

Figure 2-13 illustrates a case of multiple-lane loading with trucks positioned close to curbs and moving in the opposite direction on a single-span slab bridge (Sample 2) with two traffic lanes. To check the reliability of the Python code in bridge scale, moment and shear results were compared to corresponding envelopes obtained from the 2D analysis. Figure 2-14 shows that the results are consistent for an arbitrary three-span bridge (85 ft) subjected to one moving HL-93 truck. This bridge was modeled for validation purposes; secondary elements and deck skew angle were not considered in this model.

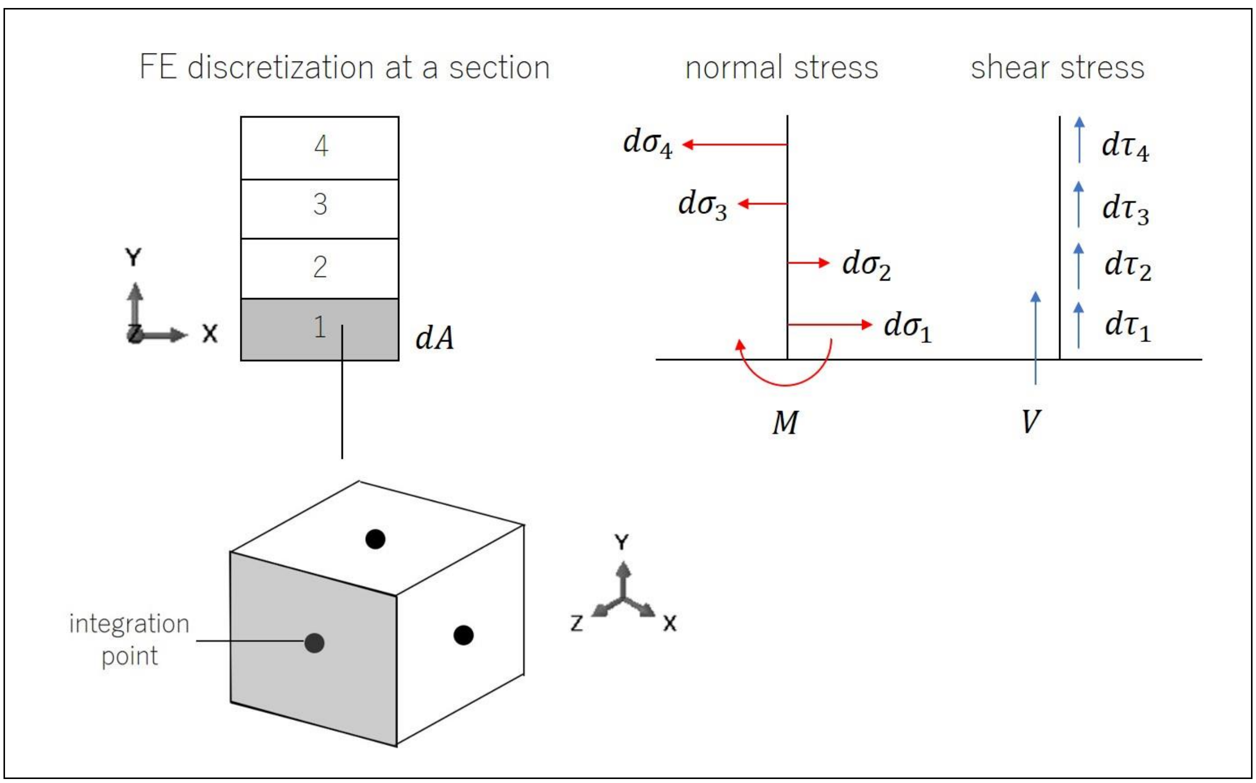

Figure 2-11 Normal and Shear Stress Distribution over FE Discretization

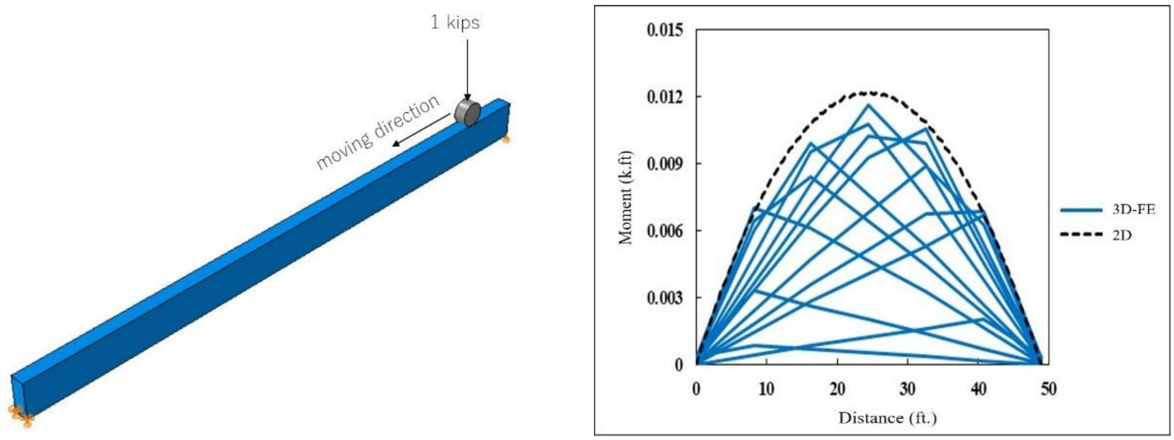

Figure 2-12 Moment Response under Moving Load Application; Beam Scale

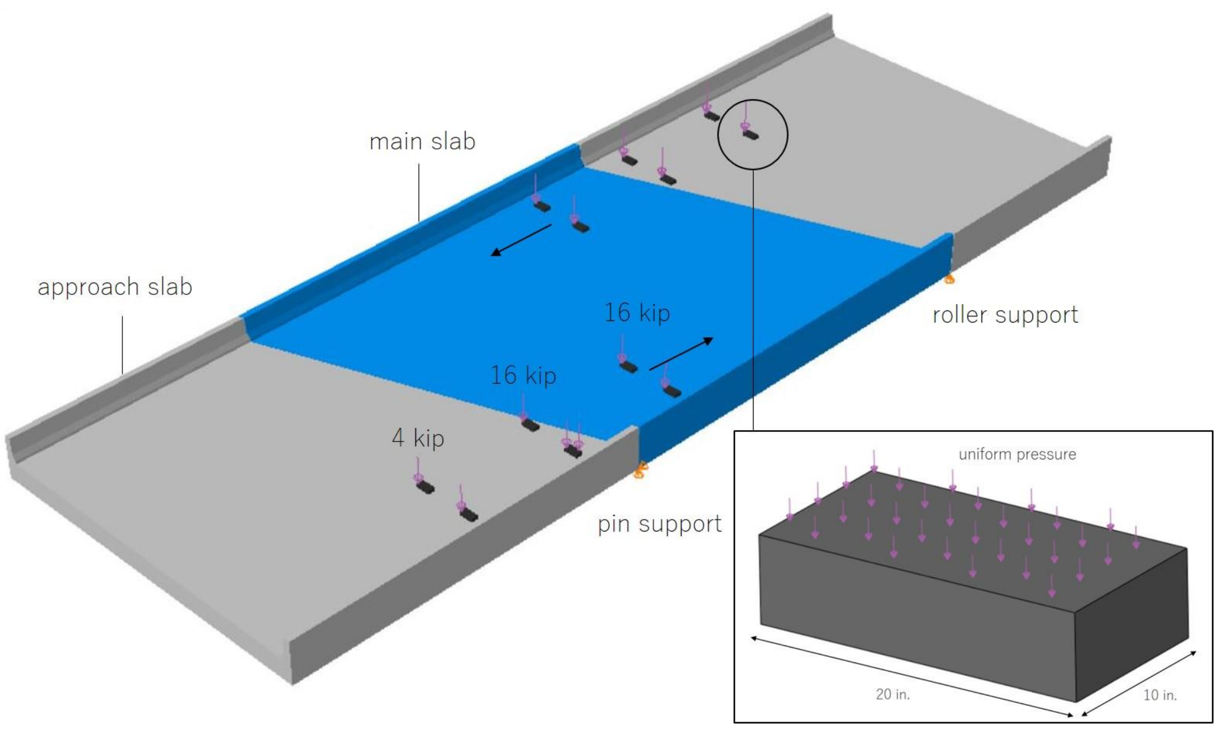

Figure 2-13 HL-93 Truck Modeling (Sample 2)

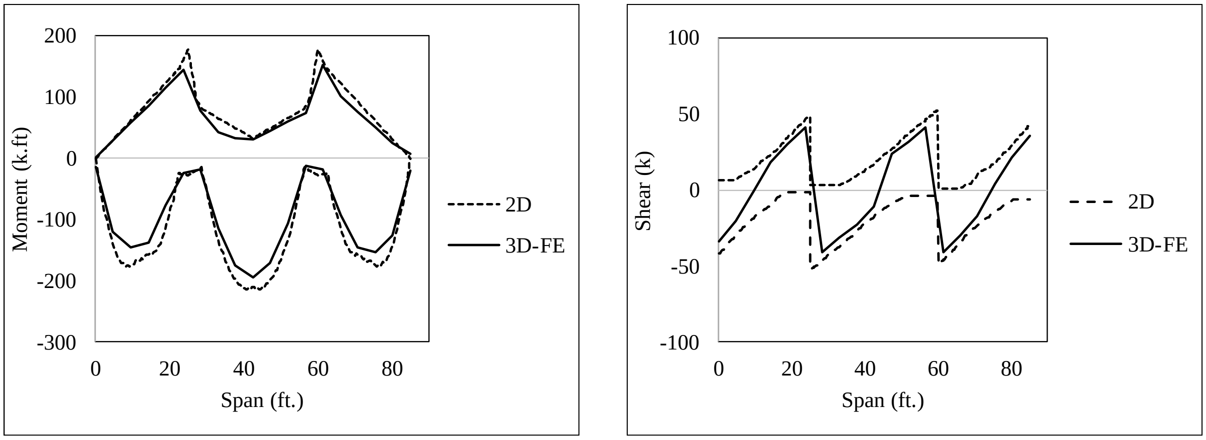

a. b.

Figure 2-14 Bridge Scale 2D and 3D Response Comparison; a. Moment, b. Shear

2.2.3.3 Load Rating Procedure

For each interior/exterior beam-strip in slab bridge models and girder in T-beam ones, moment and shear envelopes were obtained under different loading scenarios, and the maximum effect was used to calculate the 3D distribution factor. As expressed in Equation 2-4, the 3D live load Distribution Factor ($3D\ DF$) was defined as the ratio of maximum moment/shear effect obtained from the FE method to those from the 2D analysis of a simply-supported beam.

$$3D\ DF = \frac{maximum\ moment/shear\ effect\ from\ FE\ (3D)}{maximum\ response\ of\ a\ 2D\ beam} \tag{2-4}$$

Moment and shear capacities were calculated separately for interior and exterior strips/girders. For interior ones, sections used in capacity calculations for the 3D approach are similar to those used in 2D rating procedure. Figure 2-15.a and Figure 2-15.b illustrate sections considered for capacity calculation in the 3D approach for exterior strips and girders, respectively. For slab bridges, the railing section was considered contributing to moment and shear capacity for exterior strips, while for T-beam bridges, observed normal and shear strain patterns suggest that railings mainly add to moment capacity.

As displayed in Figure 2-16, the strain distribution in one exterior girder section shows normal strain developed on railing and girder parts. In contrast, shear strain is mainly developed in the girder web (no contribution from the railing in shear). Since several layers of reinforcement were provided in the railing sections, the location of the neutral axis was calculated via a trial and error procedure using a flowchart shown in Figure 2-17.After determining the neutral axis location, rebars above and below the axis were considered active in compression and tension, respectively.

For each bridge sample, the critical loading scenario was determined based on the 3D analysis results. Section-by-section demand and capacity were calculated for interior and exterior strips/girders. For exterior strips/girders, the railing contribution was also included in capacity calculations. The load rating factor was calculated following the same equation provided in the 2D approach (Equation 2-1). It should be noted that for 3D rating factor calculations, DF was not applied to live load responses.

2.3 Results and Discussion

The results obtained from 2D and 3D analysis methods were compared for the sample of bridges considered in this study. In the evaluation of obtained rating factors, the focus was on differences between the CLR and FE approaches regarding the distribution of dead and live loads as well as capacity calculations.

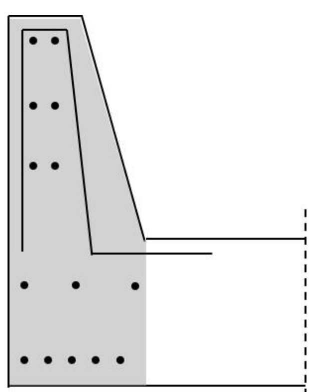

a.

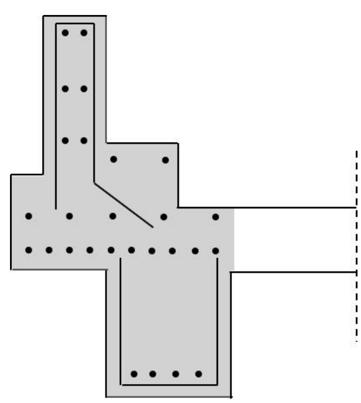

b.

Figure 2-15 Exterior Sections Considered for Capacity Calculation; a. Slab, b. T-beam

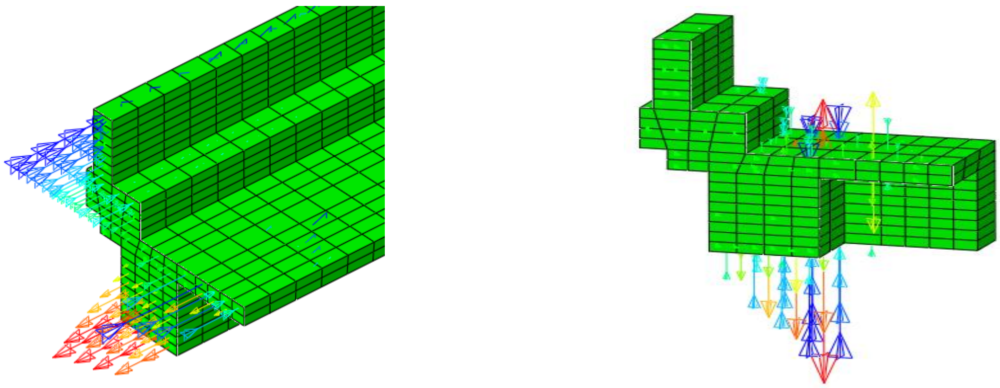

a. b.

Figure 2-16 Strain Distribution; a. Normal, b. Shear

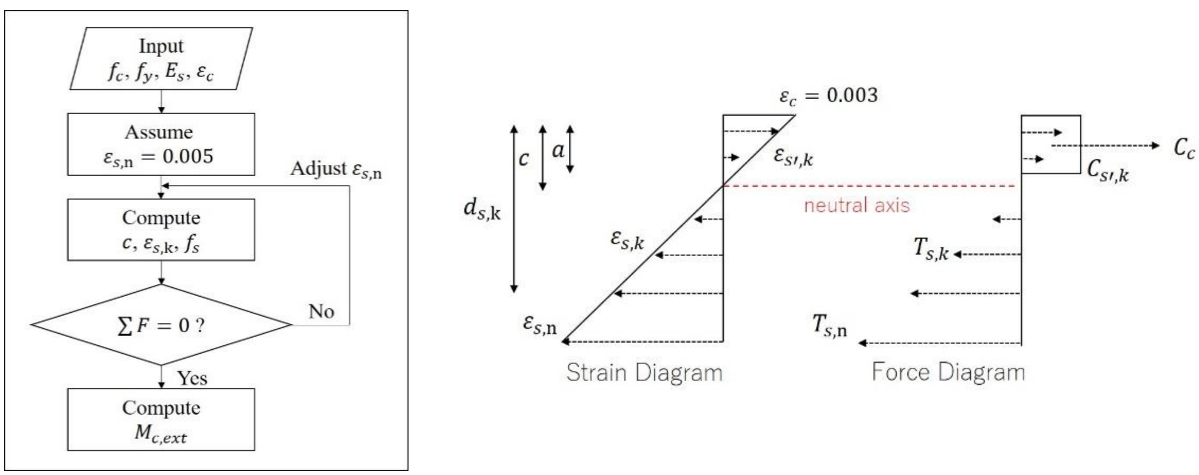

Figure 2-17 Moment Capacity Calculation Procedure for Exterior sections

2.3.1 Dead-Load Demand

This study's findings indicated that bridge responses under dead load application differ in 2D and 3D approaches. In the 2D approach, the dead load was calculated according to the total weight of the superstructure and then evenly distributed over beam-strips (slab bridges) and girders (T-beam). In the 3D approach, the superstructure weight was calculated based on the density of the materials (concrete and steel) and applied as a gravity load on using dead load function in Abaqus. Figure 2-18 illustrates the difference between moment responses obtained from the two approaches for Sample 1 (slab) and Sample 7 (T-beam). The results indicated that the dead load

(DC) response might be overestimated in 2D analysis for interior strips/girders. This finding suggests that distributing the weight of non-structural components, usually located on the edges, evenly over the bridge width could exaggerate the share of interior deck portions, resulting in higher values for DC. In Figure 2-18, the colored graphs indicate interior strip/girder moment envelopes from 3D analysis compared to the 2D envelope shown with a black dashed line.

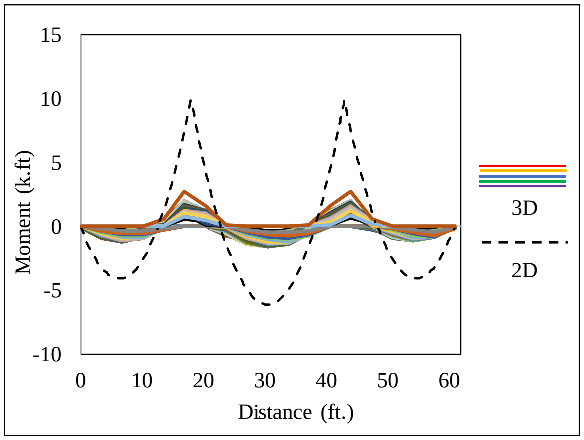

a.

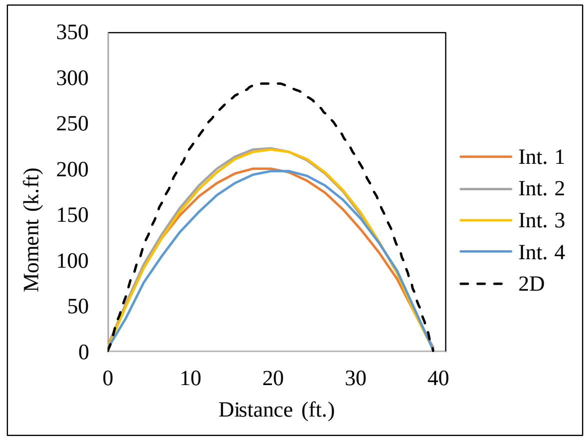

b.

Figure 2-18 2D and 3D Dead Load Response Comparison for Interior Strips/Girders; a. Sample 1, b. Sample 7

2.3.2 Live-Load Demand

Distribution factor is the key component in demand evaluation, which determines the share of moment and shear responses over different sections of a bridge superstructure. The values of DF obtained from 2D and 3D analysis methods for the sample of bridges considered in this study are compared in Table 2-7 for slab bridges and Table 2-8 for T-beam ones. The 2D distribution factors were calculated according to approximate formulations suggested in AASHTO specifications, while the 3D DFs were calculated using Equation 2-4 as explained in Section 2.2. DFs are presented for moment and shear responses in interior and exterior strip/girder per truck lane.

In general, distribution factors obtained from FE analysis were smaller than corresponding 2D ones in both bridge types. For slab bridges, 3D DFs of interior strips decreased by an average of about 37% and 18% in moment and shear, respectively compared to 2D results. In AASHTO, distribution factors are only provided for interior strips however, distribution factors for exterior strips were obtained from FE results for comparison purposes. Substantially large values were observed for exterior strips with an average of 0.45 for moment and 0.30 for shear demands. This finding emphasized the effect of edge-elements included in 3D FE modeling of exterior sections. Increased edge stiffness (on average about 4 times larger than the typical interior one) drew more normal and shear stresses to exterior sections. The difference in stiffness of interior and exterior portions changed load distribution patterns over bridge width. More share of loads was allocated to exterior strips, and consequently, less remained for typical strips in the deck's interior.

According to values provided in Table 2-7,among slab cases, DF reduction for Sample 3 was less than other samples since this bridge had an aluminum guardrail while all other slab bridges had reinforced concrete railings. For this case, the edge-stiffening effect was limited to the presence of a small concrete curb. Also, the relatively large DF of the exterior strip in Sample 4 could be attributed to the presence of a 5 ft sidewalk in addition to railings for this bridge sample. This observation showed that the edge-element's size plays an important role in the withdrawal of loads to the bridge deck's exterior sections.

For T-beam bridges, FE analysis results showed smaller 3D DFs for both interior and exterior girders than code-predicted values for all samples. An average reduction of about 43% and 37% in interior girders and 11% and 19% in exterior girders were observed respectively in moment and shear DFs in T-beam samples. One exception was moment DF of exterior girder in Sample 10, which had a relatively larger barrier (45 in. by 20 in.) compared to other T-beam samples. In total, a larger reduction was observed for interior girders DFs compared to those of exterior ones due to the edge effect discussed above.

The comparison of DF results reported in Table 2-7 and Table 2-8 suggested that the edge impact on the distribution of loads was more dominant for moment responses than for shear in both bridge types. This can be attributed to the fact that in edge-elements, flexural stiffness increased more than shear stiffness with respect to railing height since this factor has an order of three in the former and an order of one in the latter as expressed in Equation 2-2 and Equation 2-3, respectively.

Table 2-7 Distribution Factor Results; Slab Samples

Bridge Number	2D (AASHTO)	3D (FE)			
		Moment		Shear	
		Int.*	Ext.**	Int.	Ext.
1	0.097	0.059	0.807	0.070	0.259
2	0.080	0.036	0.241	0.068	0.362
3	0.084	0.080	0.312	0.074	0.185
4	0.090	0.065	1.667	0.074	0.382
5	0.086	0.036	0.452	0.072	0.317

* Interior beam-strip
** Exterior beam-strip

Table 2-8 Distribution Factor Results; T-beam Samples

Bridge Number	2D (AASHTO)				3D (FE)			
	Moment		Shear		Moment		Shear	
	Int. *	Ext. **	Int.	Ext.	Int.	Ext.	Int.	Ext.
6	0.720	0.634	0.899	0.662	0.409	0.526	0.527	0.456
7	0.723	0.636	0.882	0.649	0.375	0.513	0.535	0.459
8	0.693	0.557	0.729	0.485	0.504	0.516	0.483	0.475
9	0.731	0.619	0.847	0.568	0.342	0.472	0.540	0.452
10	0.646	0.498	0.836	0.501	0.374	0.561	0.555	0.442

* Interior girder
** Exterior girder

2.3.3 Rating Factor Results

As explained before, for each bridge sample, rating factor was calculated using Equation 2-1 in both 2D and 3D approaches. However, in the 3D load rating procedure, DF was not applied to live load responses, dead load effect was implied using gravity function available in Abaqus, and edge contribution was included in capacity calculations of exterior strips/girders. Rating factors obtained from the two approaches are reported in Table 2-9 and Table 2-10 for slab and T-beam bridges, respectively.

Comparing rating factor values obtained from 2D and 3D analyses, a noticeable improvement can be observed for both slab and T-beam bridges, with all bridges except one (Sample 2) showing rating factors above the critical value of 1. Bridge samples that exhibited critical rating factors in the 2D analysis have satisfactory load results when analyzed in 3D.

In slab bridges, average rating factors obtained from 3D analysis for moment were 3.7 and 2.7 times larger than the corresponding 2D values for interior and exterior strips, respectively. These ratios were 1.2 and 6.2 for shear. Similarly, in T-beam bridge samples, the ratio between 3D and 2D moment rating factors were 2.2 and 3.5 for interior and exterior girders, respectively. The corresponding value for shear was 1.5 for both girder types. In general, comparison of the rating values provided in Table 2-9 and Table 2-10 indicates that for interior strips of slab bridges and interior/exterior girders of T-beam ones, moment ratings show higher improvements than shear ratings.

For interior strips and girders, the increase in rating factor results could be attributed to reduced live load and dead load demands due to the edge effect discussed previously. Reduction in DFs of interior components of the bridge resulted in increased RF values obtained from FE analysis. Despite the increase in demand for exterior strips and girders, an increase in capacity from the contribution of edge-elements led to an increase in rating factors. With edge components included in exterior strip/girder, increased lever arm resulted in improved flexural capacity. Moreover, an enlarged cross-section along with the contribution of vertical steel reinforcement provided in the railings, parapets, curbs, and sidewalks resulted in improved shear capacity (refer to Figure 2-15).

In total, the comparison of rating factors obtained from CLR and 3D FE analysis indicated that the methodology outlined in AASHTO specifications results in conservative load rating factor in RC slab and T-beam bridges. The main differences between the two approaches were related to the distribution of live and dead loads and capacity calculations, which are crucial parts of the RF equation. These differences were mainly attributed to the geometrical features that are neglected in the 2D analysis. The evaluation of ten sample bridges showed that 3D models with explicit representation of structural and non-structural features could be effectively used for accurate demand estimates of bridge superstructures. In particular, 3D models could capture the effect of secondary elements such as railings, curbs, and sidewalks that could produce the most drastic change in moment and shear demands of bridges.

Table 2-9 Rating Factor Results; Slab Samples

Bridge Number	2D (AASHTO)		3D (FE)			
	Moment	Shear	Moment		Shear	
			Int.*	Ext.**	Int.	Ext.
1	1.6	2.6	6.0	3.9	3.1	14.0
2	0.7	2.6	4.4	0.9	3.3	6.9
3	1.2	1.6	2.2	1.6	1.5	11.8
4	1.0	2.2	3.9	5.5	2.9	23.1
5	0.5	1.7	1.2	1.3	1.8	7.9

* Interior beam-strip
** Exterior beam-strip

Table 2-10 Rating Factor Results; T-beam Samples

Bridge Number	2D (AASHTO)				3D (FE)			
	Moment		Shear		Moment		Shear	
	Int.*	Ext.**	Int.	Ext.	Int.	Ext.	Int.	Ext.
6	1.13	1.19	1.60	1.90	2.50	4.34	2.57	3.62
7	1.32	1.42	1.35	1.61	3.10	4.67	2.16	2.49
8	1.15	1.31	0.97	1.31	2.58	3.98	1.49	1.84
9	1.58	1.75	1.80	2.27	3.40	6.73	2.32	3.01
10	1.82	1.58	1.72	1.67	3.93	5.65	2.39	2.02

* Interior girder
** Exterior girder

2.4 Summary of Findings

In this chapter, the implementation of three-dimensional finite element modeling was investigated to seek an improved methodology for bridge rating evaluations. For this purpose, a small group of slab and T-beam reinforced concrete bridges were selected as a representative sample of bridges located in Indiana. For a sample of ten RC bridges (five of each type), 3D models were used for accurate estimates of moment and shear responses under live and dead load applications. The results were compared with those obtained using current rating procedures as per AASHTO based on two-dimensional analysis and lateral load distribution factors. The comparison of the CLR and FE results were reported in the present chapter.

Comparison of rating factors obtained using the two approaches revealed that the current procedure outlined in AASHTO could overestimate the bending moment and shear forces and result in a conservative estimate of bridge load rating. Effect of edge components was reflected in structural behavior of bridge superstructure using 3D modeling tools. The presence of secondary elements altered both load share and resistance of different sections of the deck. Reduced load distribution factors obtained from 3D FE analysis improved overall bridge ratings. For interior strips of slab bridges, DFs decreased by an average of about 37% and 18% for moment and shear, respectively. These values were about 43% and 37% for interior and 11% and 19% for exterior girders in T-beam samples. Moreover, the contribution of edge-elements such as railings, curbs, and sidewalks increased capacity and consequently RF of edge sections.

The findings of this study showed that the rating factors of existing RC slab and T-beam bridges could improve when using 3D FE models. Insufficient detailing in the modeling of structural members and supports, lack of consideration of the contribution to the strength of exterior members, and inaccuracies in the sharing of transverse load using DF were the main sources of the inconsistencies between the two methods applied in this study. In particular, a significant impact was observed on rating results due to the change in distribution of loads. Edge barriers had a substantial influence on stress distribution, causing higher stress concentrations in exterior strips and reduced stresses in interior ones. This observation was consistent for both dead and live load applications. This effect is neglected in current load estimate procedures.

In conclusion, given the observed improvement in load rating estimates using 3D FE analysis, it is recommended that bridges that exhibit border-line load rating results be analyzed using the refined analysis. At the same time, the CLR may continue to be used for a conservative estimate of bridge rating. To incorporate the favorable effects of secondary parameters in the load rating procedure, modifications to the current DF formula is necessary. This is feasible by introducing modification factors to current DF to include the impact of non-structural members neglected in available procedures. In the next chapter, a parametric study was performed to identify influential parameters affecting demand calculations, explore potential improvements to current demand estimates, and support the development of a modified live load distribution factor.

3. PARAMETRIC STUDY

3.1 Introduction

With advances in modern computing resources, Three-Dimensional (3D) Finite Element (FE) analysis can be efficiently used to obtain reliable estimates of transverse load distribution in bridges, and systematically investigate possible improvements in bridge response estimates (Hasancebi and Dumlupinar 2013; Sanayei et al. 2016). The research presented in this chapter aimed to investigate longitudinal shear and moment demand across the bridge superstructure using 3D finite element analysis and explore the possible refinement of live load distribution factors in T-beam and slab Reinforced Concrete (RC) bridges.

In Chapter 2, 3D finite element analysis was effectively used to model the bridge superstructure system when subjected to moving vehicles. 3D models were used to predict a more accurate lateral distribution of such live loads on bridge longitudinal girders/strips in a limited sample of representative RC bridges (five T-beam and five slabs). Using the finite element discretization, the effect of simplifying assumptions used in Conventional Load Rating (CLR) on rating results was identified. It was noted that edge-elements such as railings, parapets, curbs, sidewalks, and end-diaphragms significantly influenced the bending moment and shear force distribution across the bridge structure in studied bridges. This study's findings suggested the need for an updated live load distribution factor used the current rating procedure.

In the present chapter, bridge superstructures were modeled in 3D and analyzed using the finite element methods. Superstructure features, along with actual loading configurations, were explicitly represented in the 3D models. In particular, the contributions of barriers and diaphragms were specifically considered. A parametric study was performed to investigate their influence on demand calculations. Critical values of moment and shear responses were obtained on different sections (interior and exterior) of the bridge superstructures. The obtained results were used to investigate the effectivity of studied parameters on bridge demand. A summary of assumptions, verification procedures, and results related to the parametric study are presented in the subsequent sections.

3.2 Parametric Study Details

A parametric study was conducted to evaluate effect of selected parameters noted to influence the bending moment and shear force distribution across the bridge structures studied in Chapter 2. The focus of the parametric study was to investigate the potential effect of secondary elements such as railings and parapets, barriers, curbs, and end-diaphragms on demand evaluation in the rating of reinforced concrete slab and T-beam bridges using 3D finite element analysis. The parametric study was concentrated on demand estimate in load rating procedure aiming to improve the current lateral load distribution factor by addressing the limitations resulting from Two-Dimensional (2D) analysis and ignoring the contribution of nonstructural components.

3.2.1 Identification of the Key Parameters

3.2.1.1 Statistical Distribution of Bridge Parameters

A total of 3550 reinforced concrete slab and T-beam bridges compiled in the National Bridge Inventory (NBI) database for the state of Indiana were surveyed to establish the typical bridge configurations considered in the parametric study. Common ranges of geometrical characteristics such as number of spans, maximum span length, number of traffic lanes, curb-to-curb width, and deck skew angle were compiled using the data in the NBI. Figure 3-1 and Figure 3-2 represent histograms with the relative frequency of mentioned variables for slab and T-beam bridges, respectively.

Among the bridges considered, single and three-span bridges dominated in both bridge types. About 18% and 76% of slab bridge population are single-span and three-span, respectively. These values are 43% and 32% in T-beam bridges. Maximum span lengths for most bridges of the type considered in this study fell within the range between 20 ft and 50 ft, with an average of 31 ft and 34 ft for slab and T-beam bridges, respectively. Roadway width for most of the bridges (70% slab and 60% T-beam) was within 20 ft to 40 ft. The average roadway widths were 33 ft for slab, and 31 ft for T-beam bridges. For both bridge types, two-lane bridges were predominant (about 91% in slabs and 84% in T-beams). About 40% of the bridges were right-angle (non-skewed) in both bridge types considered. Maximum skew angles of 65 and 55 degree were observed for slab and T-beam bridges, respectively.

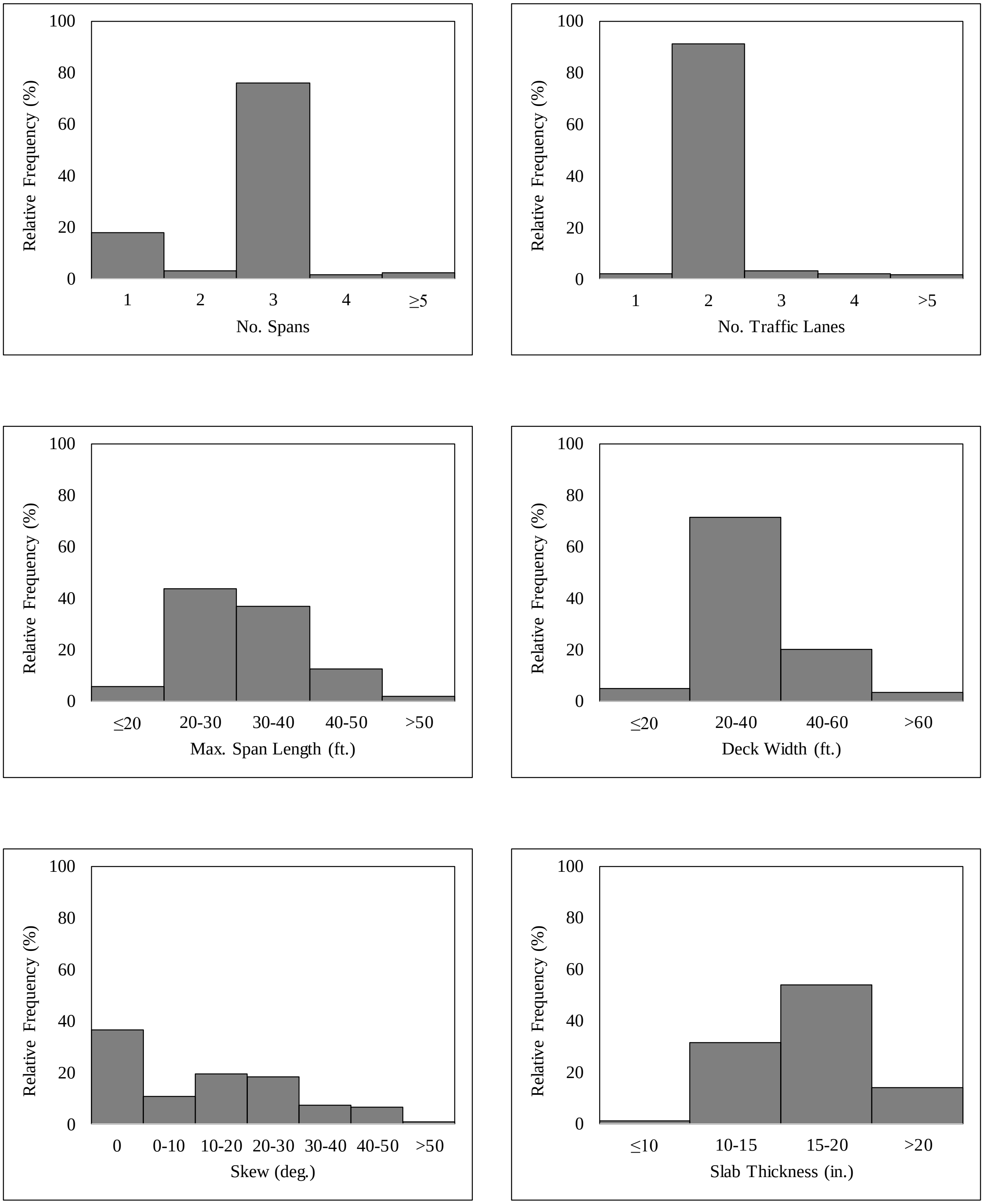

Figure 3-1 Distribution of Geometrical Parameters; Slab Bridges

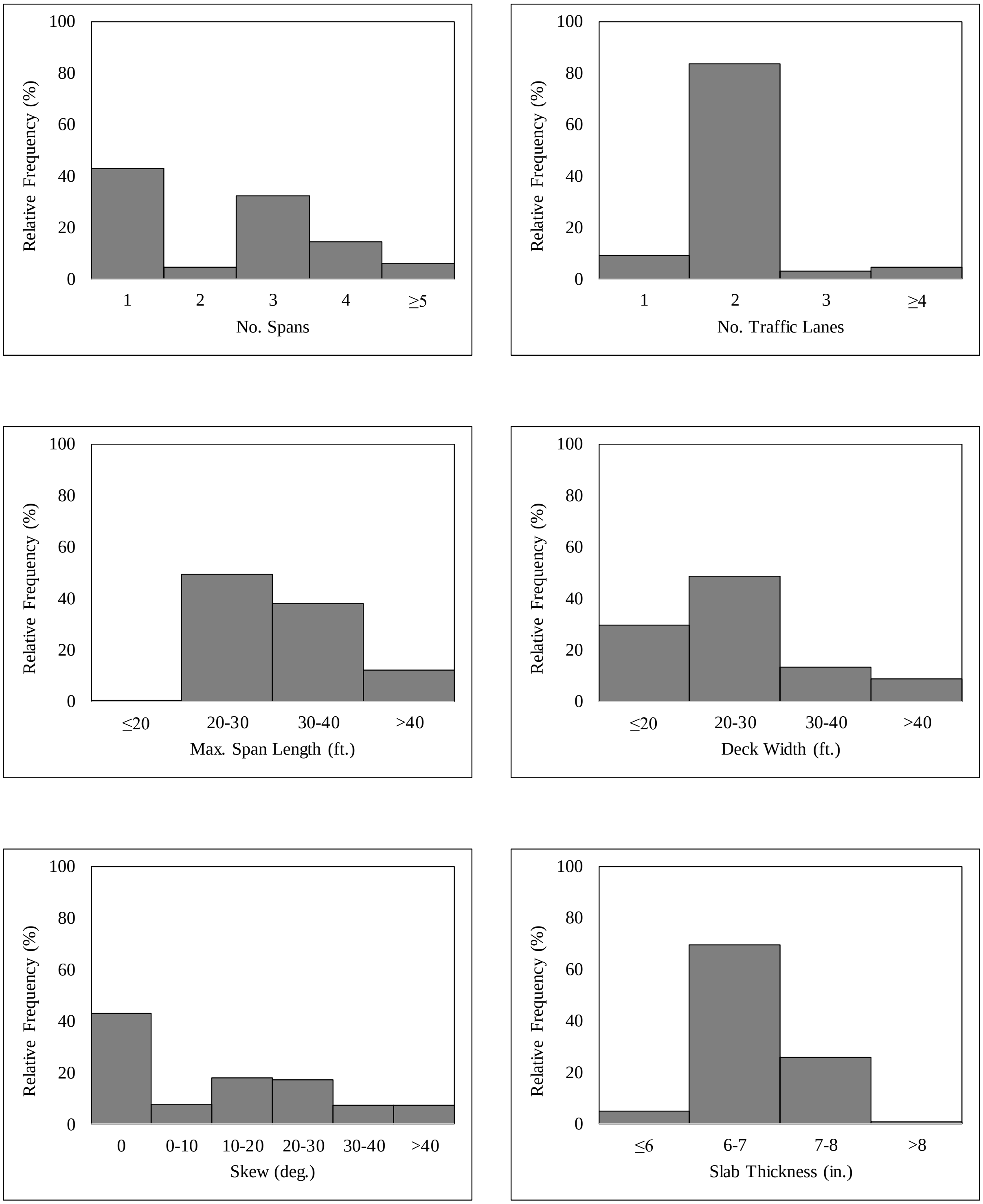

Figure 3-2 Distribution of Geometrical Parameters; T-beam Bridges

In addition to the NBI database, bridge drawings provided by the Indiana Department of Transportation (INDOT) for 35 slab and 210 T-beam Indiana bridges were reviewed to identify possible geometrical features not shown in the dataset such as slab thickness, girder numbers/dimensions/spacing for T-beam bridges, railings and diaphragm dimensions, and concrete compressive strength. Figure 3-3.a and Figure 3-3.b illustrate the geometrical features obtained from bridge drawings of slab and T-beam bridge cross-sections, respectively. Ranges of variation and average values of these parameters are summarized in Table 3-1.

3.2.1.2 Representative Sample Bridges

The number of bridge samples for 3D modeling was determined using the parameters included in current DF formulations such as span length, deck width, slab thickness, and girder spacing/dimensions (for T-beams) as fixed parameters. Parameters identified in the literature review as not included in the development of DFs, such as railing height and width of end-diaphragms, were identified as variable parameters. In addition, despite the inclusion of skew and continuity factors in the DFs in current specifications, number of spans and deck skew were considered as variable parameters since it has been reported that these factors could change the effectiveness of secondary elements on lateral load distribution (Conner and Hou 2006; Seok et al. 2019). Finally, although deck thickness in slab bridges is not included in the current DF formulation, in this study it is considered as a fixed parameter since the findings of previous studies suggested that there was no impact on the distribution of loads from changing the deck thickness (Zokaie et al. 1991; Amer et al. 1999).

Based on the statistical distribution of bridge parameters observed in the NBI dataset and review of bridge drawings, average values were obtained for fixed parameters, and the common range of variation was determined for variable ones. Fixed and variable parameters and their corresponding values are summarized in Table 3-2 and Table 3-3 for slab and T-beam bridge models, respectively. In total, 120 slab bridges and 320 T-beam bridges were modeled in 3D to investigate the effect of variable parameters on load distribution and propose modifications to DF formulations.

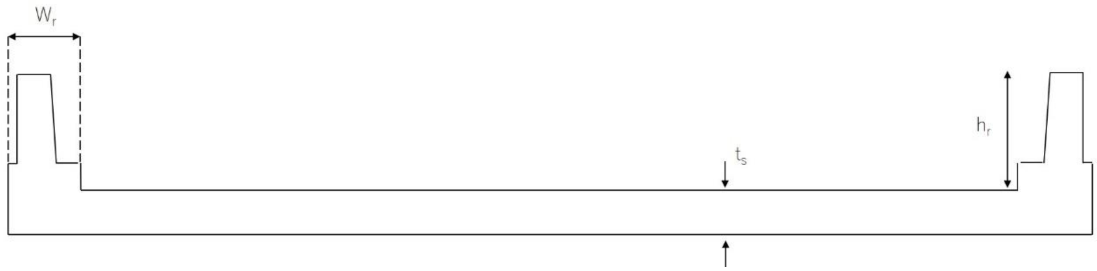

a.

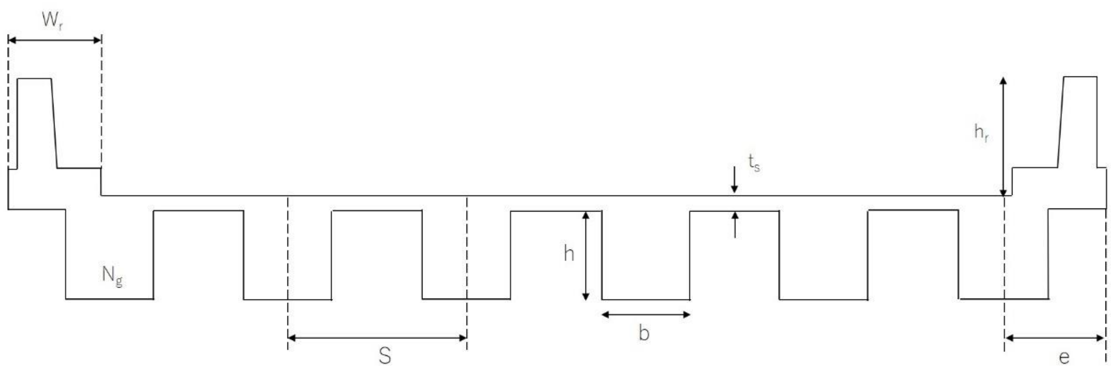

b.

Figure 3-3 Geometrical Parameters Obtained from Bridge Drawings; a. Slab, b. T-Beam

Table 3-1 Range of Cross-Sectional Parameters

Bridge Type	Parameter	Range	Mean
Slab	slab thickness (t_s)	8" - 29"	17"
	railing width (w_r)	1' - 5.5'	1.5'
T-beam	slab thickness (t_s)	6" -10"	7"
	number of girders (N_g)	4 - 9	5
	girders spacing (S)	5' - 9'	7'
	beam height (h)	15" - 63"	32"
	beam width (b)	13" - 32"	20"
	eccentricity (e)	1' - 3'	2'
	railing width (w_r)	8" - 80"	28"

', ", and ° represent foot, inch, and degree, respectively.

3.2.1.3 Reference Models

Two archetypical reference models, one solid slab and one T-beam, were defined to serve as benchmarks for comparison purposes. Reference models had decks with no skew and did not include secondary elements such as barriers and end-diaphragms (in the case of T-beam models). For each bridge type (slab and T-beam), one reference model was simple-span bridge whereas the other one was considered as three-span to investigate effect of continuity. In three-span models, equal length was considered for two exterior spans. Interior span length measured larger than the other two since this pattern was observed in bridge drawings. Average values of 1.25 and 1.4 were obtained for $\frac{L_{\text{interior}}}{L_{\text{exterior}}}$ in slab and T-beam bridges, respectively. Slab reference model consisted of twenty-eight interior and two exterior strips while the T-beam one included three interior and two exterior girders. Dimensions of reference models were selected based on average values reported in Table 3-2 and Table 3-3. Figure 3-4 shows the cross-section dimensions of the reference bridge models.

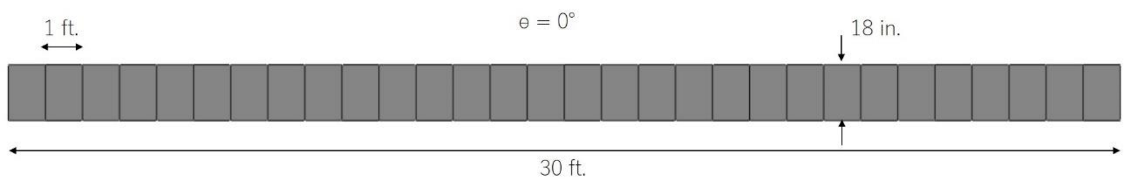

a.

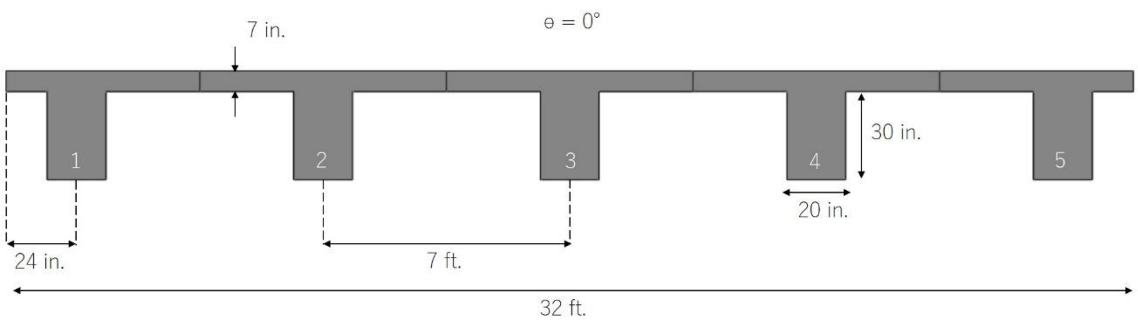

b.

Figure 3-4 Reference Models Cross-Sections; a. Slab, b. T-beam

Table 3-2 Parameters Values Considered for Slab Reference Models

Fixed Parameters	deck width (W)	30'
	slab thickness (t_s)	18"
	span length (L)	29'
	number of lanes (N_L)	2
	railing width (w_r)	12"
Variable Parameters	number of spans (N_s)	1 - 3
	railing height (h_r)	0" - 10" - 20" - 30" - 40" - 50"
	skew angle (ɵ)	0° - 10° - 20° - 30° - 40°

', ", and ° represent foot, inch, and degree, respectively

Table 3-3 Parameters Values Considered for T-beam Reference Models

Fixed Parameters	deck width (W)	32'
	slab thickness (t_s)	7"
	span length (L)	35'
	number of lanes (N_L)	2
	girders (N_g, b, h, S)	5 (20" x 30") @ 7'
	railing width (W_r)	10"
Variable Parameters	number of spans (N_s)	1 - 3
	railing height (h_r)	0" - 15" - 30" - 45"
	skew angle (ɵ)	0° - 15° - 30° - 45°
	end-diaphragm width (W_d)	0" - 5" - 10" - 15"

', ", and ° represent foot, inch, and degree, respectively

3.2.2 Analysis Program

As discussed in Section 2.2, 3D finite element analysis was performed using Abaqus software to model the bridge superstructure system subjected to moving vehicles. The same approach was followed in the parametric study to predict a more accurate response estimate of such loads on longitudinal beam girders/strips and systematically investigate possible improvements in load distribution of bridge types studied in this research.

3.2.2.1 3D Modeling Assumptions

A solid element type (C3D8R) was selected to model the bridge deck to investigate the superstructure’s 3D behavior. Element size was measured 3 in. in height and width and 6 in. in length. A compressive strength (f_c') of 3000 psi was assigned to concrete elements since this value was reported in bridge drawings for more than 87% of cases. Material properties were defined assuming the behavior remains in the elastic range, and nonlinear behavior, including damage and plasticity, was not considered in this study. Steel reinforcement was not included in the 3D modeling performed in the parametric study. Configuration and position of the supports were assumed similar to that explained in Section 2.2.3.

Following the same partitioning approach explained previously, deck width was divided into 1 ft beam strips and interior/exterior girders in slab and T-beam models, respectively, such that the results obtained from 3D models would be comparable with those obtained from the 2D analysis. As illustrated in Figure 3-5.a, 1 ft strips comprised the interior sections of the bridge slab, while the railing component was included in exterior ones. This partitioning approach facilitated demand estimate and DF calculation individually for interior/exterior sections across the bridge deck. Figure 3-5.b shows the interior and exterior girders partitioning method for T-beam bridges. In each girder, the flange width was equal to girder spacing plus girder width. Like the slab case, the exterior girder in the T-beam model included the railing. The end-diaphragms were included in the girder partitioning however, they are not shown in Figure 3-5.b.

Vehicular live loads (truck HL-93) consist of three axle loads of 8, 32, and 32 kips spaced 14 ft from each other, and the wheels are 6 ft apart. AASHTO requires the spacing between the two 32 kips axles to be varied from 14 ft to 30 ft however, axle spacing was not varied in this study since, according to findings of the NCHRP 12-26 project, axles configuration do not produce a significant change in the load distribution patterns (Zokaie et al. 1991). Trucks were moved step-by-step in the longitudinal direction (approximately every 6 in.) to produce maximum moment and shear responses, and for each transverse position across the bridge width to investigate the effect of lateral load distribution. The truck was positioned considering a 2 ft distance between the first axle and the railing curb and a minimum of 4 ft distance between trucks for two-truck loading cases. Moreover, trucks were moved on approach slabs (on each end of the bridge span) to explore the effect of partial loading on live load responses (refer to Figure 2-13).

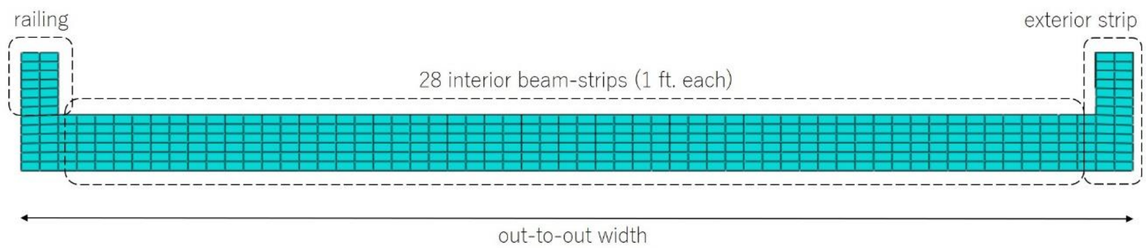

a.

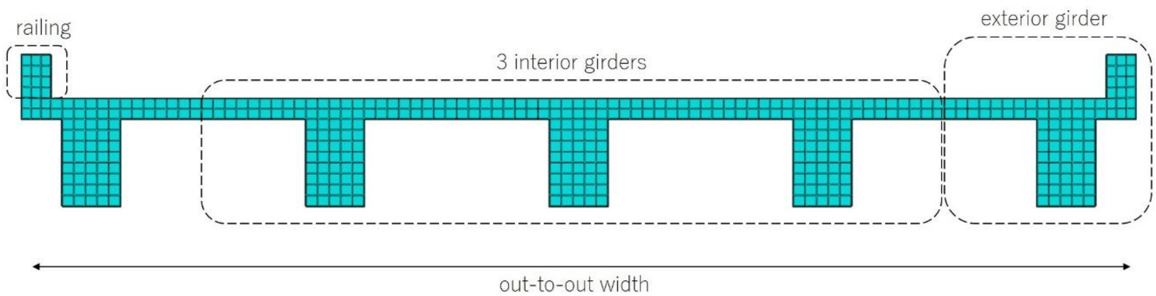

b.

Figure 3-5 Partitioning Approach for 3D Bridge Modeling; a. Slab, b. T-beam

3.2.2.2 Model Validation

To investigate the reliability of the 3D modeling methodology adopted in this study, results obtained using FE analysis were compared to bridge test measurements (Cai et al. 2002). Strain measurements from a prestressed concrete bridge tested in Florida were compared with corresponding values obtained from 3D finite element analyses. This three-lane bridge is located on I-95 over Glades Road in St. Lucie County, Florida. It consists of six simply-supported spans. The tested span has a 125 ft length and consists of nine AASHTO Type V prestressed concrete girders spaced at 6.5 ft. The deck is skewed at a 45-degree angle. Strain gages were installed on the bottom of the girders at 59 ft from the left support. Two standard FDOT trucks' rear axles were positioned at mid-span on the right and middle traffic lanes. Figure 3-6 shows the bridge dimensions and test/truck configurations.

Figure 3-7 illustrates a comparison of strain values obtained from the test and the 3D model. There is an acceptable agreement between the two sets of results. In the analysis of the 3D model, interior diaphragms, elastic bearings, among other field parameters, were not included in the analysis. Strain values obtained from FE analysis were matched relatively well to the results of a similar study conducted by Cai and Shahawy (plotted in Figure 3-7). They found that with detailed modeling of the intermediate diaphragms and elastic bearings, the discrepancy between the model and test results decreased. However, it was concluded that the original model could capture the pattern of strain distribution well and was sufficient for distribution factor estimates (Cai and Shahawy 2004).

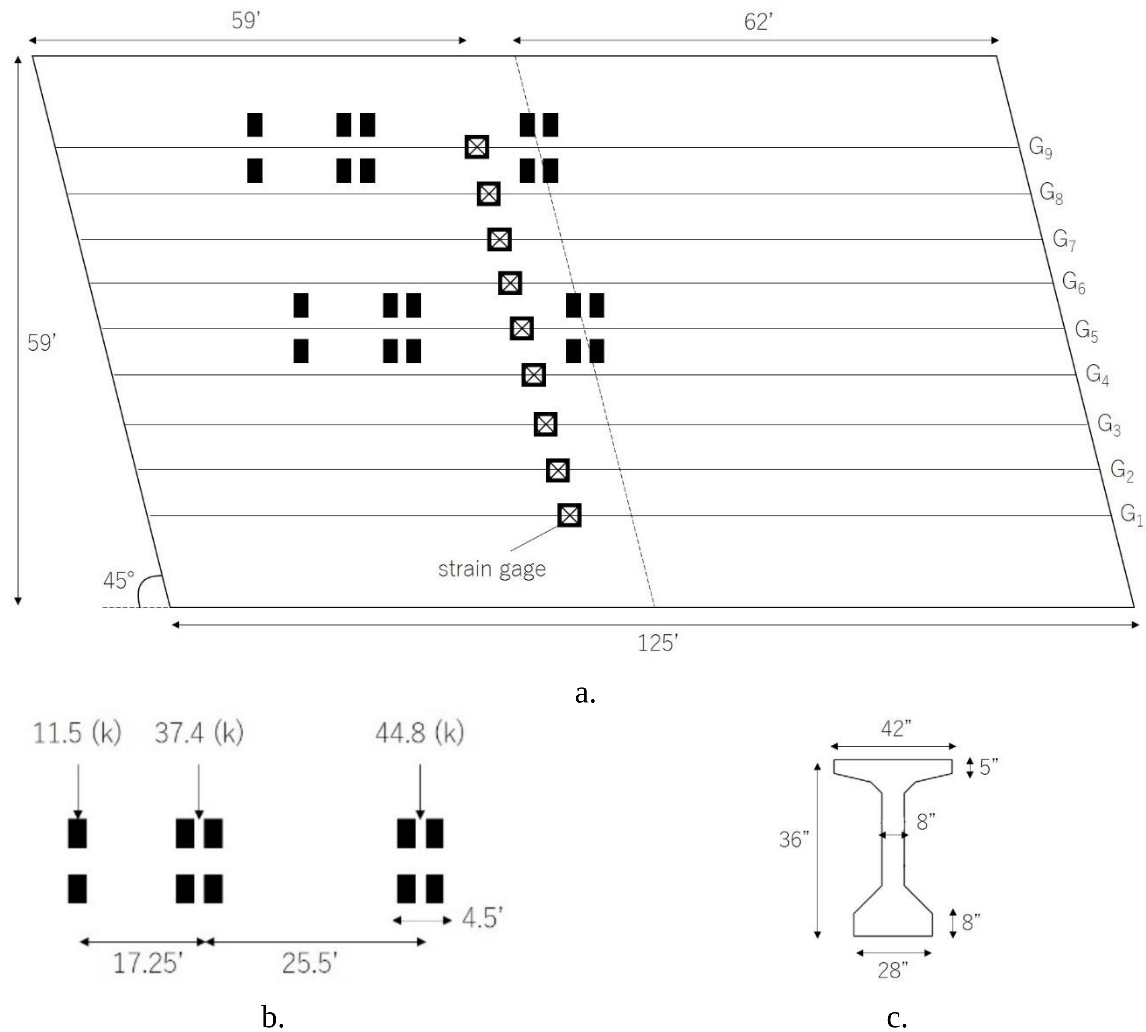

Figure 3-6 Test Details; a. Bridge Configuration, b. Truck Load, c. Girder Dimensions

3.2.2.3 Truck Transverse Positioning

The HL-93 truck configuration was applied in single and multiple traffic-lanes over bridge width. In the case of multiple-lane loading, two trucks were positioned on the bridge superstructure since, according to the NBI database, more than 80% of bridges (slab and T-beam) accommodate two traffic lanes (see Figure 3-1 and Figure 3-2). To identify the critical loading position, trucks were moved along the span length on different transverse positions. In the case of slab bridges, trucks were moved every 2 ft in transverse direction over the bridge width (Figure 3-8.a), while for T-beam bridges, trucks were positioned over each girder, once placing one set of wheels on girder centerline and once placing the girder between two wheels (Figure 3-8.b). This approach resulted in five loading configurations for single-lane and four loading configurations for multiple-lane loadings. It should be noted that loading configurations were applied on one-half of superstructure width, taking advantage of symmetry.

One case of each bridge type was subjected to all loading configurations, and maximum values of moment and shear responses were obtained. These results were used to determine critical loading scenarios. According to results plotted in Figure 3-9, loading configurations 1-1 and 2-1 were the most critical ones for the exterior strip/girder. In these loading positions, trucks were located closest to the edge, resulting in higher stress concentration for the edge components. For slab bridges, the same loading configurations were critical for interior strips. However, in T-beam bridges, loading positions of 1-2, 1-4, and 2-3 resulted in larger demand and, therefore, were selected as critical configurations for interior girders (girders 2 and 3). Narrowing down the loading cases to two (slabs) and five (T-beam) critical ones optimized the analysis effort by decreasing the total number of 3D models.

3.2.3 Parametric Study Procedure

Values of the key parameters identified in Section 3.2.1 were varied in the reference models within the observed ranges reported in Table 3-4 and Table 3-5 for slab and T-beam models, respectively. To study the effect of each variable, values of the parameters were changed one at a time while other variables remained constant similar to the approach followed in the NCHRP 12-26 study. Then, to investigate the combined effect of variables on demand estimates, models were created with combination pairs of parameters.

For each model, sectional normal and shear stresses were obtained for interior and exterior strips/girders under critical truck load configurations. Using the Python code moment and shear envelopes along the strip/girder length were calculated. One more script was developed using Matlab to obtain peak moment and shear values for all strips/girders. Using these results, the strip/girder with the maximum value among the others was identified as a critical one (see flowchart shown in Figure 3-10). Maximum values of shear and bending moment in the critical strip/girder (interior and exterior) were used for comparisons to reference model's results.

To examine the effect of studied variables, maximum demands of critical strip/girder were compared for models with and without (reference) parameters. Changes with respect to each variable were represented using normalized demand value. This normalized value was calculated by dividing the demand for a different independent variable by the demand in the reference bridge (see Equation 3-1). Thus, the demand ratio for the reference models is always 1, and the trend with increasing variable amounts can be easily observed.

$$demand\ ratio = \frac{max.demand\ for\ model\ with\ diff.\ variable}{max.demand\ in\ ref.\ model} \tag{3-1}$$

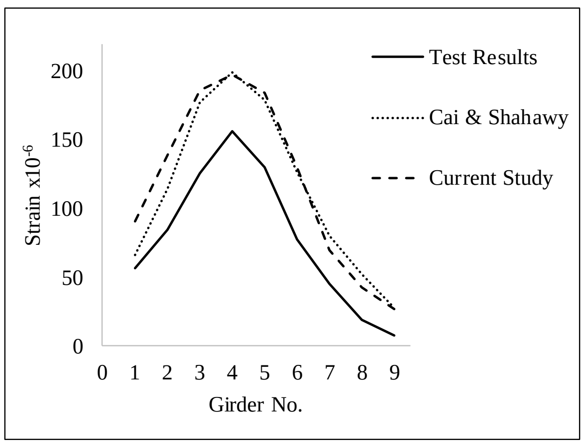

Figure 3-7 FE and Test Results Comparison

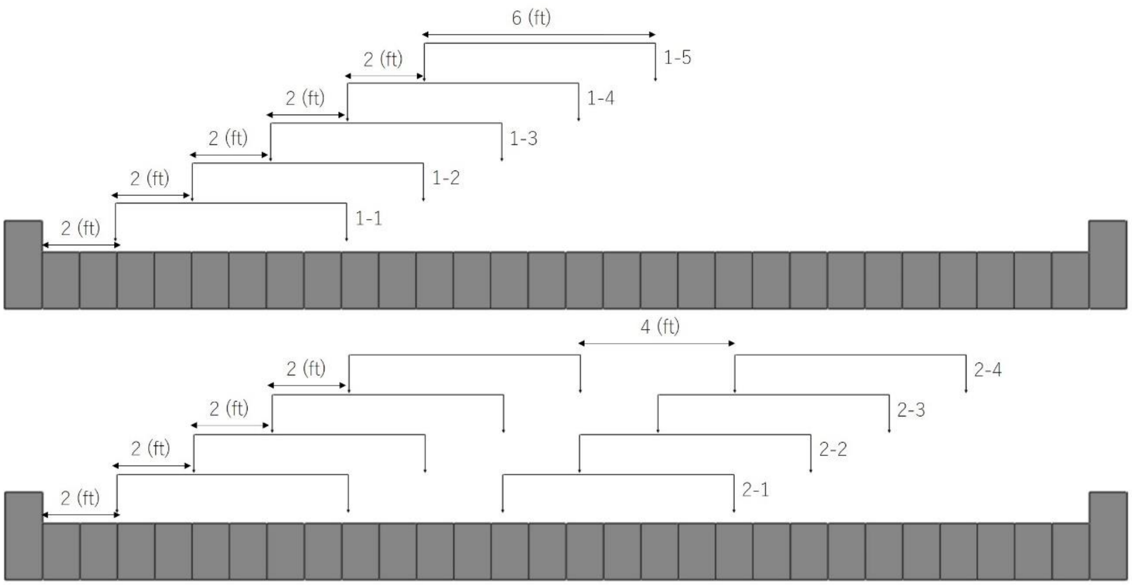

a.

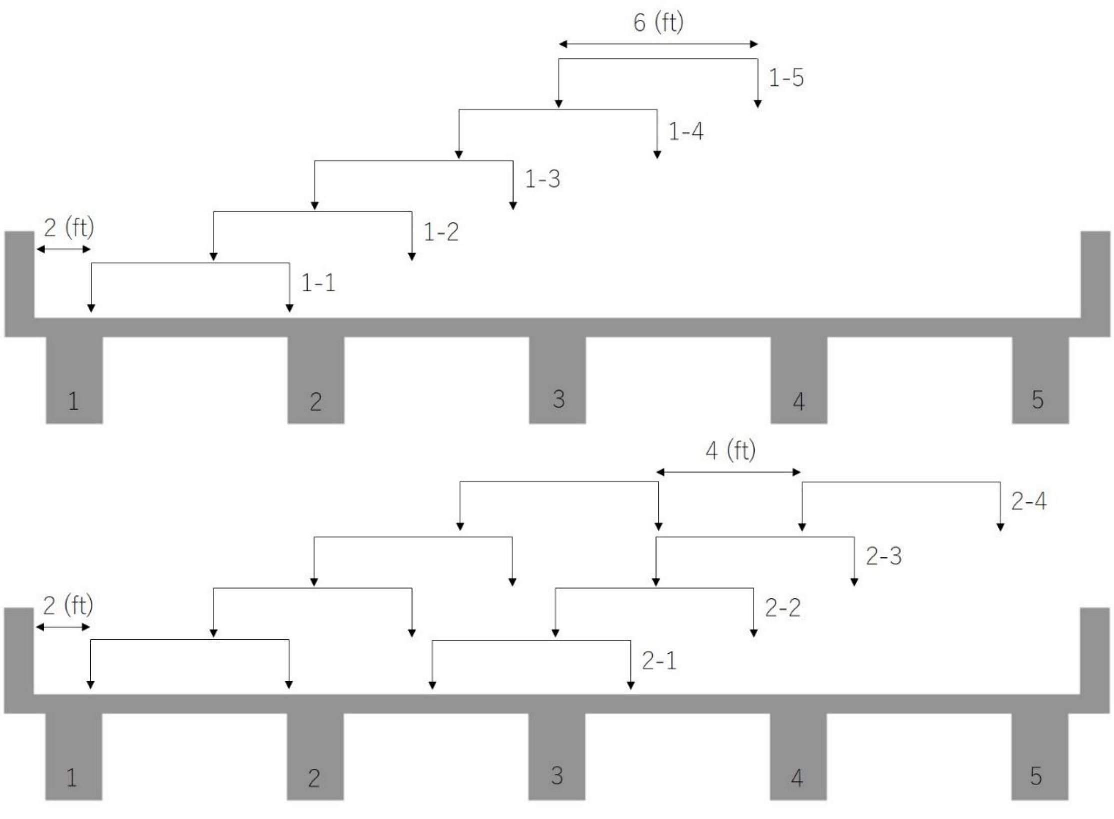

b.

Figure 3-8 Truck Loading Configurations; a. Slab, b. T-beam

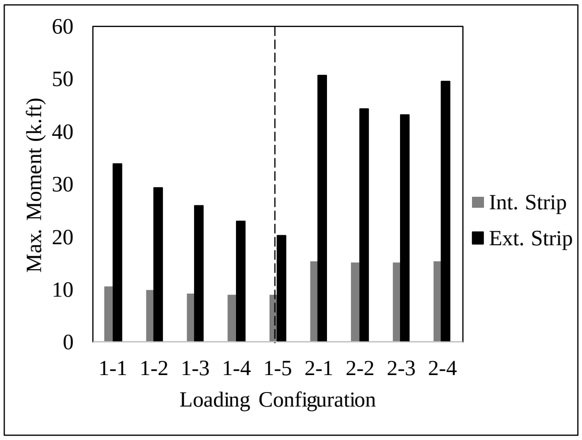

a.

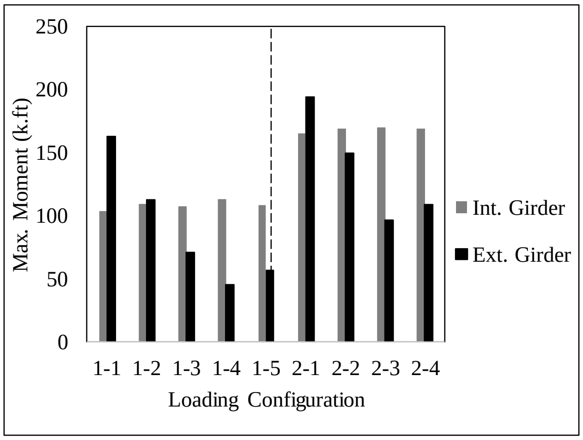

b.

Figure 3-9 Maximum Moment Responses for Different Truck Configurations; a. Slab, b. T-beam

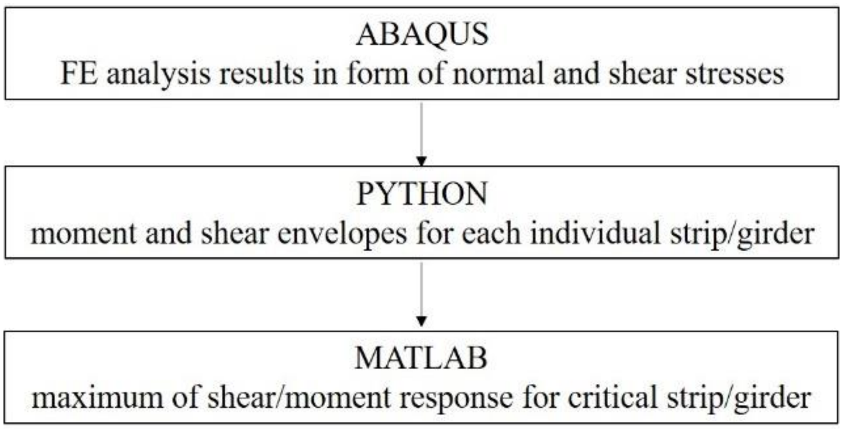

Figure 3-10 Procedure Used to Obtain FE Results in Parametric Study

Table 3-4 Range of Parameter Values in the Analysis Slab Models

Parameters and Range of Variation					
Skew(deg.)	0°	10°	20°	30°	40°
Railing Height (h_r) (in.)	0				
	10				
	20				
	30				
	40				
	50				

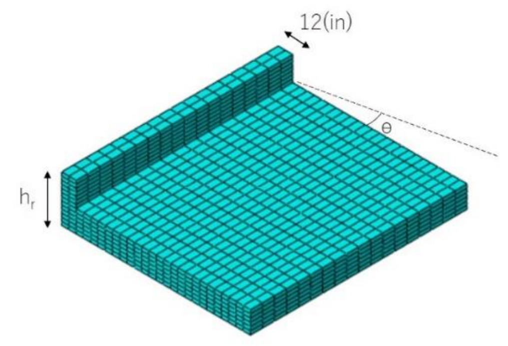

Table 3-5 Range of Parameter Values in the Analysis of T-beam Models

Parameters and Range of Variation					
Skew (deg.)	0°	15°	30°	45°	Diaphragm (W_d) (in.)
Railing Height (h_r) (in.)	0				0
	15				
	30				
	45				
	0				5
	15				
	30				
	45				
	0				10
	15				
	30				
	45				
	0				15
	15				
	30				
	45				

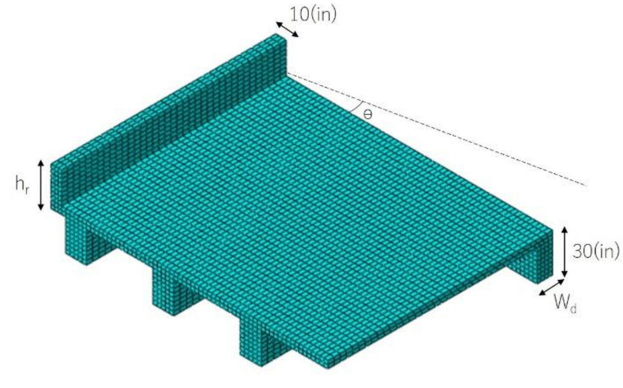

3.3 Results and Discussion

The following analysis results are presented to evaluate the effect of the various variables on load distribution over bridge deck. Herein, the individual effect of each variable is discussed and results on the combined effect of variables are presented in Chapter 4 where statistical studies are discussed.

3.3.1 Edge-Stiffening Effect

The secondary structural elements, such as end-diaphragm beams and barriers, are components of the bridges contributing to the structural behavior of the RC bridges. In slab and T-beam bridges, the AASHTO code requires that a barrier be provided with main reinforcement parallel to the traffic. The edge beam can be either part of the slab section additionally reinforced, a beam integral with the slab, or a reinforced section of the slab integral with the curb. Moreover, the structural features of a typical T-beam bridge include rigid diaphragm beams at span ends. These components change regional stiffness and hence the distribution of the forces over the deck. The effect of these elements on bridge demand is elaborated in the following subsections.

3.3.1.1 Railing Effect

To evaluate the effect of edge-stiffening elements on bridge demand, railings were added to the reference slab and T-beam models. Railings were modeled as fully coupled with the bridge deck using solid elements, allowing for full composite action between the two components. This assumption is valid for reinforced concrete railings and parapets properly anchored to the superstructure deck with adequate vertical reinforcement penetrating from edge element into the deck. Railing geometries were determined using representative cross-sectional dimensions of guardrails found in Indiana bridges. According to standard drawings provided by INDOT, E706-BRSF and E706-BRPP guardrails are commonly used in slab and T-beam reinforced concrete bridges, respectively. A maximum design height of 45 in. in the BRSF and 42 in. in the BRPP is common. Since the variation in parapet width is not as large as it is in heights, the width was considered constant, measuring 12 in. and 10 in. for slab and T-beam models, respectively (see sketches provided in Table 3-4 and Table 3-5). Therefore, six discrete values were considered for railing heights ranging from 0 in. to 50 in. for slab models, while in T-beam models, this variable was increased from 0 in. to 45 in. every 15 in. as specified in Table 3-4 and Table 3-5.

Results obtained from FE analysis of 3D models indicated that inclusion of the edges changed stress/strain patterns across the bridge superstructure. In Figure 3-11, the distribution and magnitude of normal strains are shown for two slab models, one with no edge-element and the other with a 40 in. height railing. The plots were captured at the time-step associated with peak response. The plot illustrates the change of normal strain distribution across the bridge width; when the railing component was included in the model, strain concentration shifted towards the edges. This pattern was observed for shear strain as well.

The presence of railings resulted in increased stiffness of the edge strip and girders compared to interior ones. The increased stiffness changed load distribution patterns across the bridge width by increasing the share of loading allocated to the exterior strip/girder. This also resulted in a decreased portion of load allocated to typical interior strips/girders.

To examine the effect of variations in railing height, moment and shear demands were compared for models with and without (reference) railing. Figure 3-12 to Figure 3-14 show slab and T-beam models results as the railing height changes while other variables, skew angle and diaphragm width, were kept constant. Maximum shear and moment values of individual strips/girders are reported in graphs when the HL-93 truck was located in position 1-1 (refer to Figure 3-8 for truck positions). This position specifically illustrated the effect of railing height since the load was closest to the edge.

The edge-stiffening effect can be observed in Figure 3-12 and Figure 3-13, where the maximum responses of internal/external portions of the deck are shown across the bridge width. It is important to note that the increase in the share of the load in exterior strips of slab bridges was higher than in T-beam ones. This could be attributed to geometrical differences between the two edge cross-sections. In T-beam bridges, increases in railing height has a lower impact on the flexural stiffness of the combined railing-girder stiffness girder, compared to slab bridges where the railing height (max. 50 in.) is relatively larger than slab thickness (18 in.), resulting in a larger stiffness difference between the exterior strip compared to interior ones.

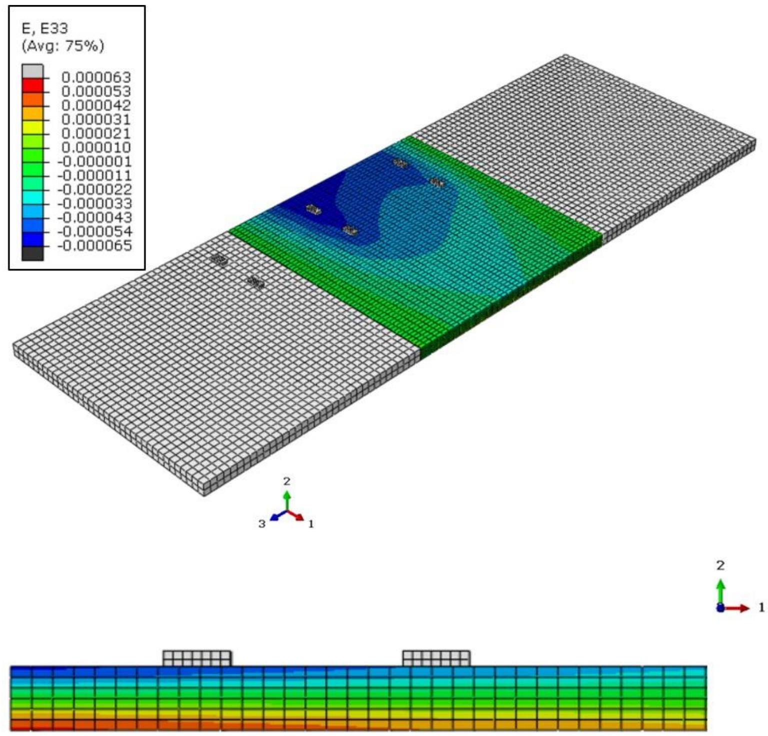

a.

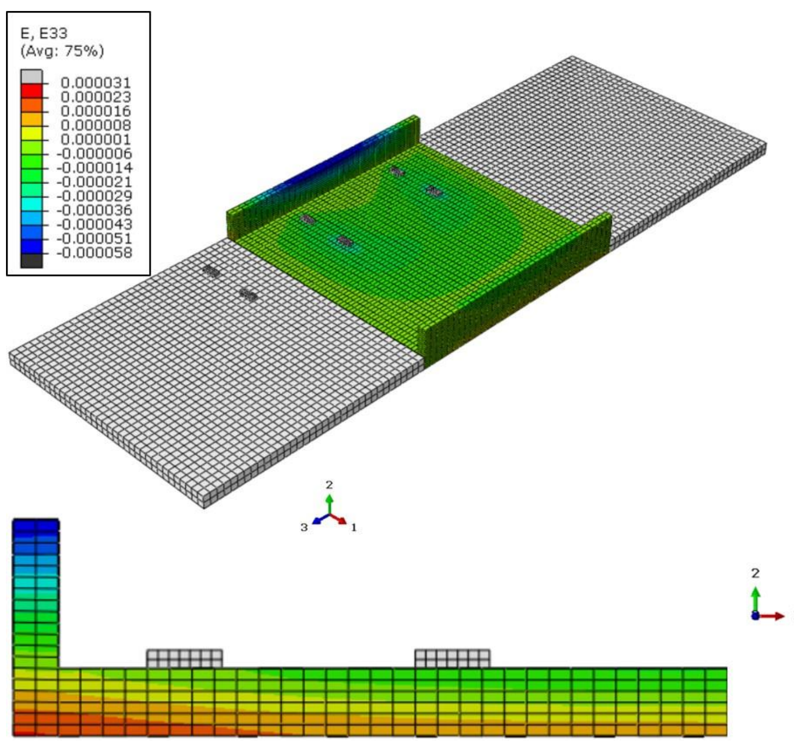

b.

Figure 3-11 Railing Effect on Strain Distribution; a. 0 in. Rail, b. 40 in. Rail

Changes in moment and shear demands for different railing height values are shown in Figure 3-14, where the ratio represents a normalized demand value. This normalized value is calculated by dividing the demand obtained for different railing heights by the demand in the reference bridge without a railing (Equation 3-1). Thus, the demand ratio for the reference models is always 1, and the trend with increasing variable amounts can be more easily observed. In these graphs, the 2D rating factor is represented as a constant value of 1 (black dashed line) since the edge effect is not considered when developing distribution factor formulations of studied bridges in AASHTO specifications.

In both bridge types, railing height increases resulted in a decrease in shear and moment in interior sections. However, this parameter had a higher impact on moments compared to shear values. In slab models, the increase in railing height led to a significant decrease in moments for interior strips while it increased in exterior strips. The reduction was almost 50% in the interior strips, while in exterior strips, it increased 6.8 times compared to the reference model. In terms of shears, exterior strips showed an increase of 4.3 times compared to the reference model, while the decrease in that of interior strips was about 22%. In the case of T-beam models, the larger increases were 28.8% in the moment and 13.9% in shear in exterior girders. In interior girders, maximum reductions of 18% in moments and 3% in shears were observed.

3.3.1.2 End-Diaphragm Effect

In T-beam bridges, girders were monolithically bounded by diaphragm beams at abutment locations. No intermediate diaphragms were provided to these bridges. Four distinct diaphragm width values were implemented in the 3D models, while the diaphragm depth was kept constant and equal to girder depth (30 in.). A diaphragm width of 0 in. represents no diaphragm, i.e., the reference model.

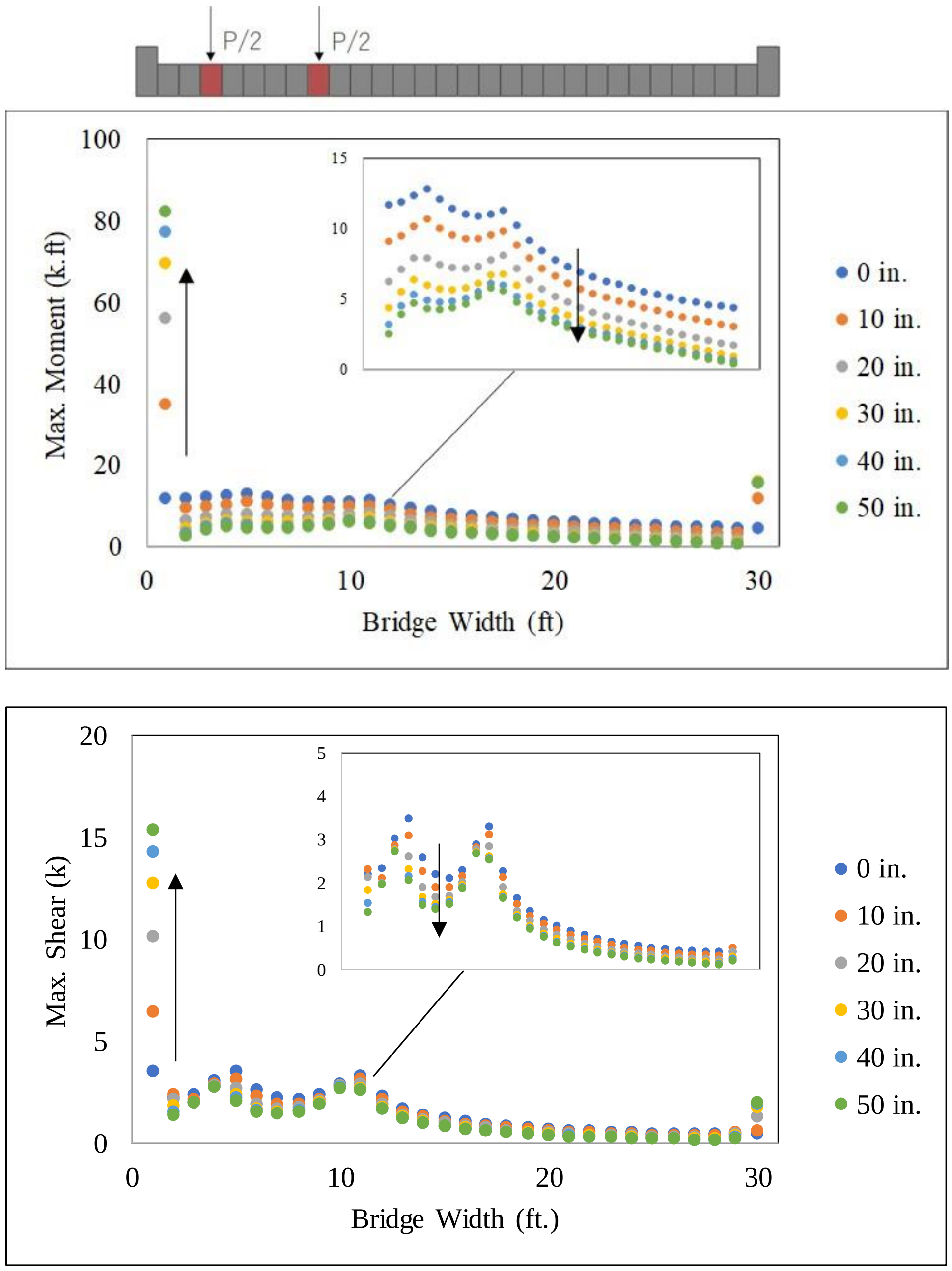

Figure 3-12 Railing Effect on Demand Distribution across Slab Bridge Width

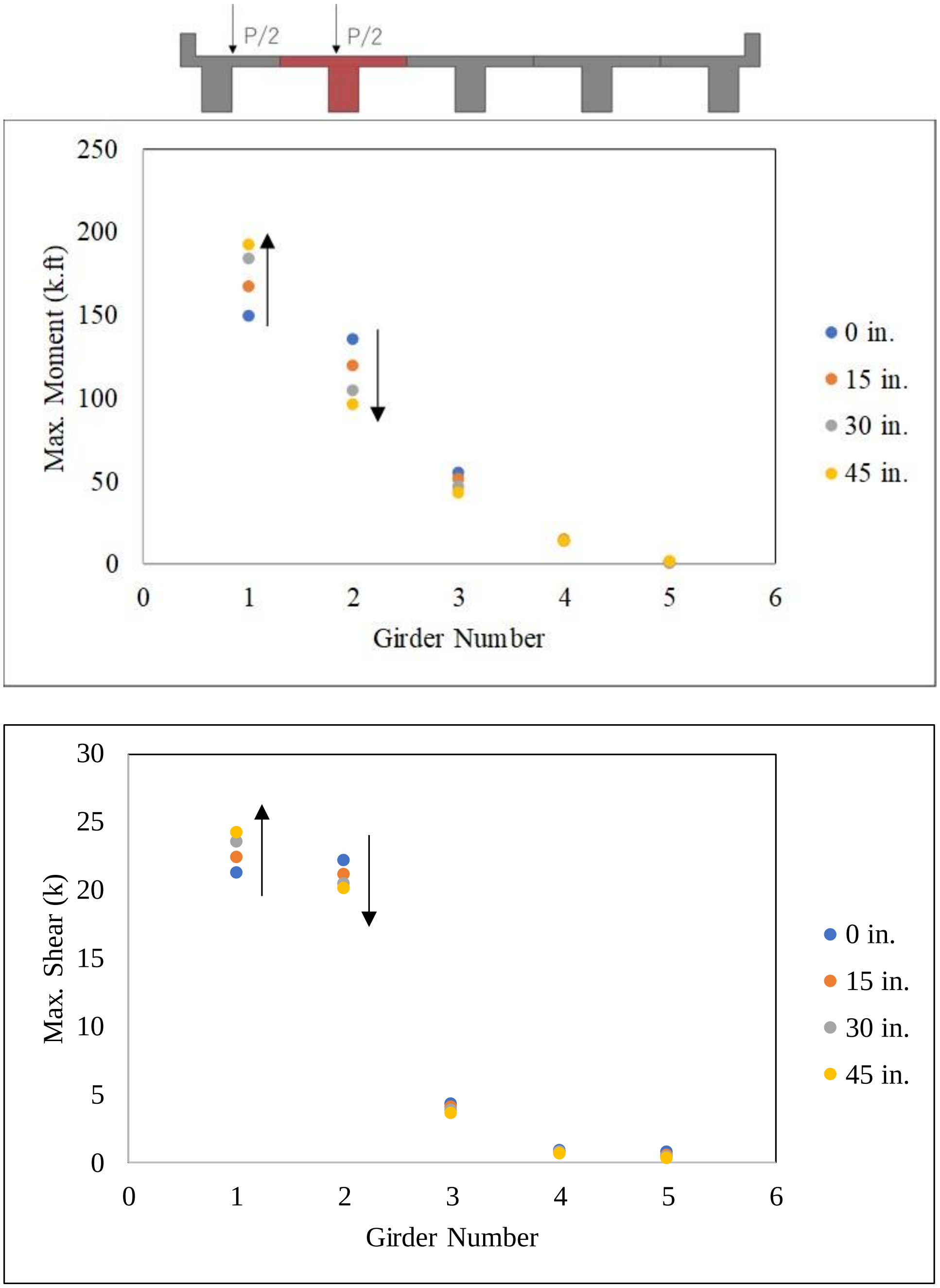

Figure 3-13 Railing Effect on Demand Distribution across T-beam Bridge Width

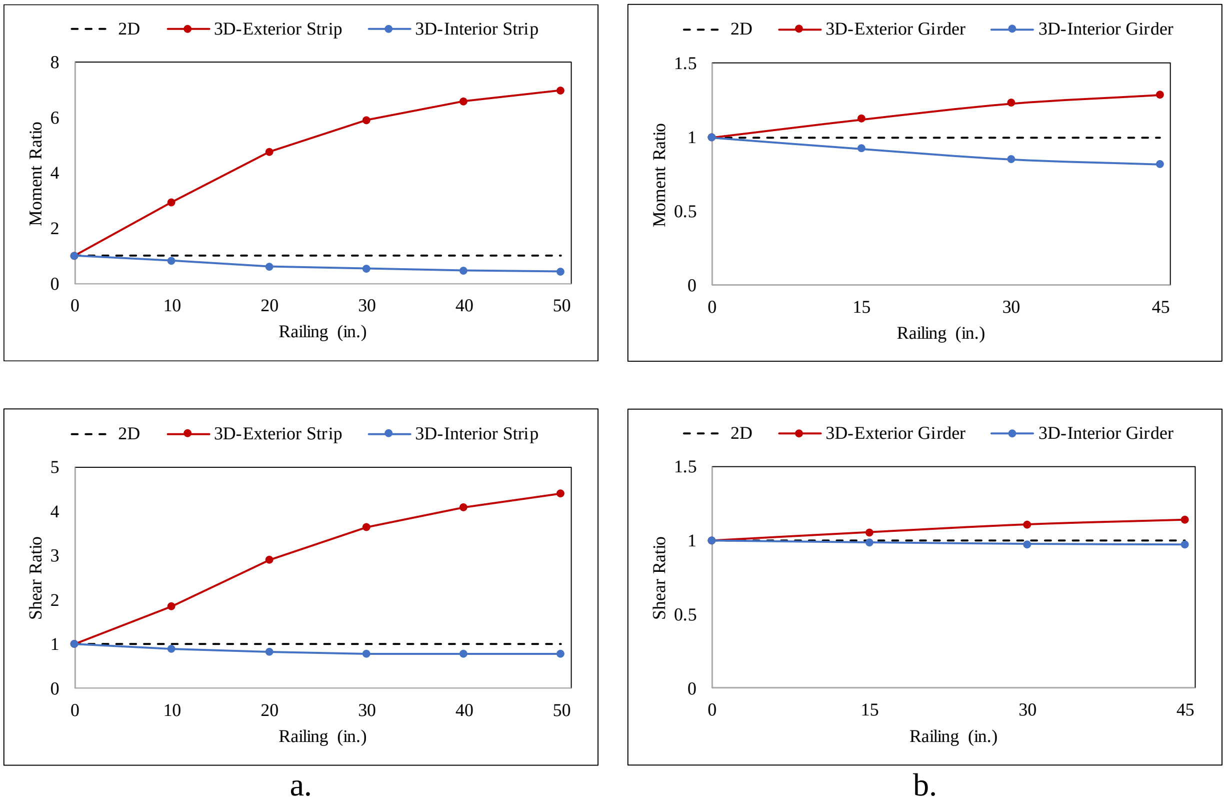

Figure 3-14 Railing Height Effect on Maximum Moment and Shear; a. Slab, b. T-beam

Figure 3-15 shows the demand variation as the diaphragm width was increased from 0 in. to 15 in. ($h_r = 0\ in.\ ,\ \theta = 0°$). Results shown in the graphs suggest that under any loading configuration, shear demand dropped by up to 15% for critical interior girders (those under applied load). However, increased shear was observed for the adjacent girders (pointed out by arrows on graphs). This could be attributed to the presence of diaphragms enabling redistribution of forces by connecting the girders at the supports where maximum shear force occurs. In Figure 3-16, demand ratios of T-beam models with end-diaphragms were compared to the constant value of 1 for 2D diaphragm factor since this effect is not included in the demand estimate in LRFD specifications. The presence of diaphragms at span ends resulted in a negligible moment reduction (up to 6%) since stiffened edges are located far away from mid-span where maximum moment occurs. With a diaphragm width of 15 in., the shear force in interior girders was reduced by 16%. However, the shear results for exterior girders were relatively unchanged (less than 1% difference).

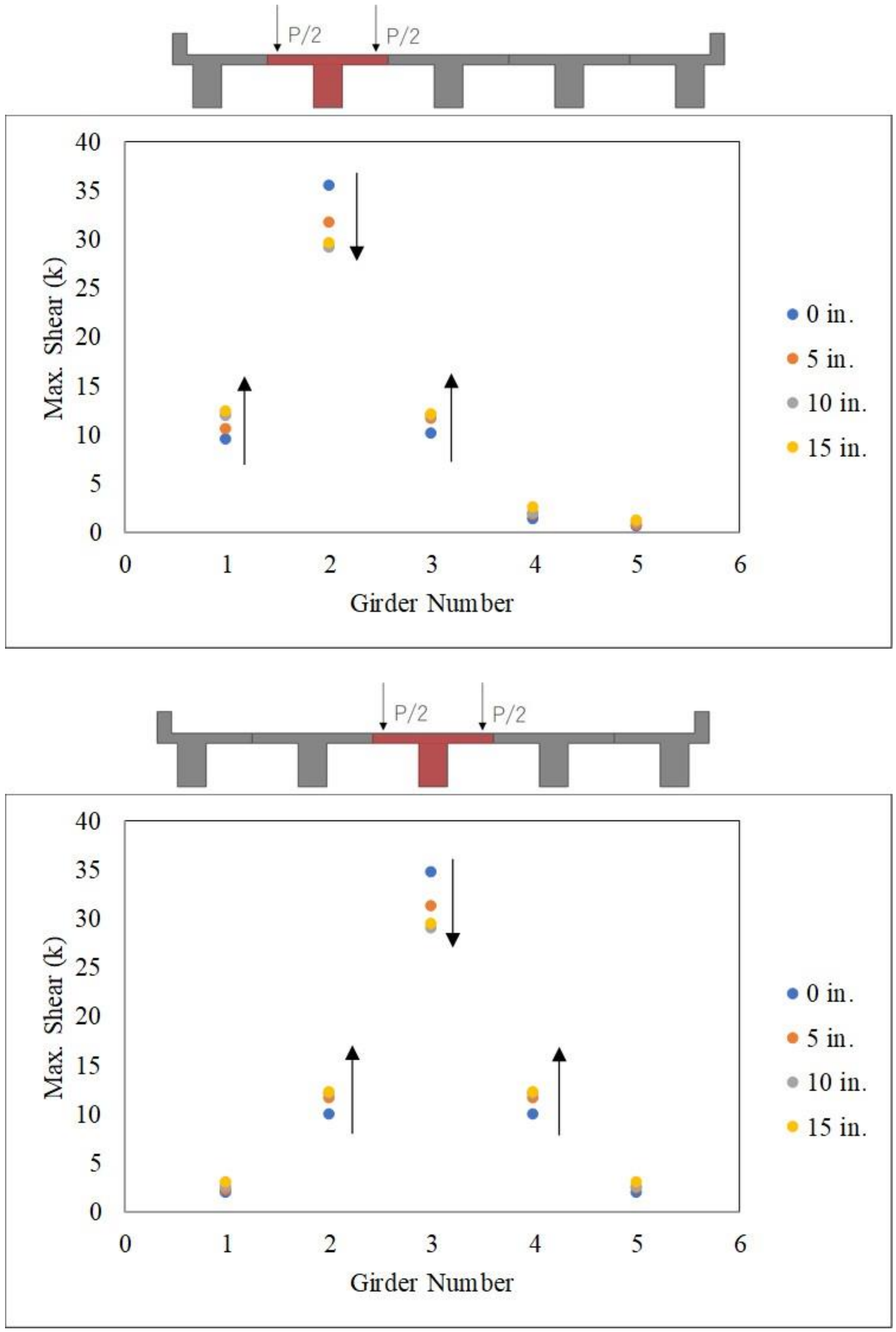

Figure 3-15 Diaphragm Effect on Demand Distribution across T-beam Bridge Width

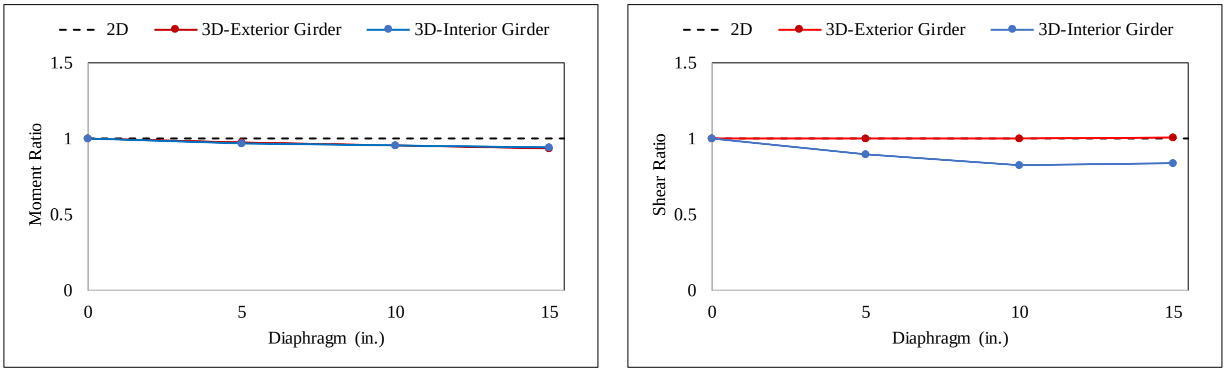

Figure 3-16 Diaphragm Width Effect on Maximum Moment and Shear; T-beam

3.3.2 Skew Effect

Skewed bridges are often encountered in highway design when the geometry cannot accommodate straight bridges. According to AASHTO, the skew angle is defined as the angle between a normal/perpendicular to the alignment of the bridge and the centerline of the supports. Based on this definition, the reference model is a right-angle bridge with 0-degree skew. To evaluate the effect of this factor on the moments and shears in a slab bridge, the angles were increased from 0 to 40 degree within 10-degree intervals. For T-beam models, four discrete values ranging from 0 to 45 degree were considered for the skew parameter.

A comparison of FE results obtained from models with different skew angle values indicated that it changed the distribution of stress/strain across the bridge superstructure. Figure 3-17 shows the distribution and magnitude of normal and shear strains for two slab models, one with zero skew angle and the other with a 40-degree skew angle. These results correspond to the truck position associated with peak response. A reduction of almost 29% can be observed from Figure 3-17.a for the maximum normal strain of the skewed bridge model compared to the one with zero skew angle. In the case of shear strain, peak magnitude was increased by a factor of 2.2 for the 40-degree skewed bridge. As illustrated in Figure 3-17.b, maximum shear occurred under load application for the non-skewed bridge, while shear strain concentration can be observed at the obtuse corner of the skewed deck. This resulted in an increase in shear forces at exterior strips. This pattern can be observed in Figure 3-18, where maximum responses are shown across the bridge deck for different skew values.

Results plotted in Figure 3-18 indicated a reduction in the longitudinal moment in interior and exterior strips/girders of slab and T-beam bridges with an increasing skew angle. In slab bridges, moment reduction up to about 30% was observed in interior and exterior strips for a deck skew of 45 degree. For interior/exterior girders, the maximum moment dropped by almost 40% when the skew angle of 45 degree was considered for T-beam models. Shear forces increased in exterior strips/girders when the skew angle was greater than 0 degrees. However, shear changes observed in interior ones were insignificant with respect to the skew angle (average of less than 3%).

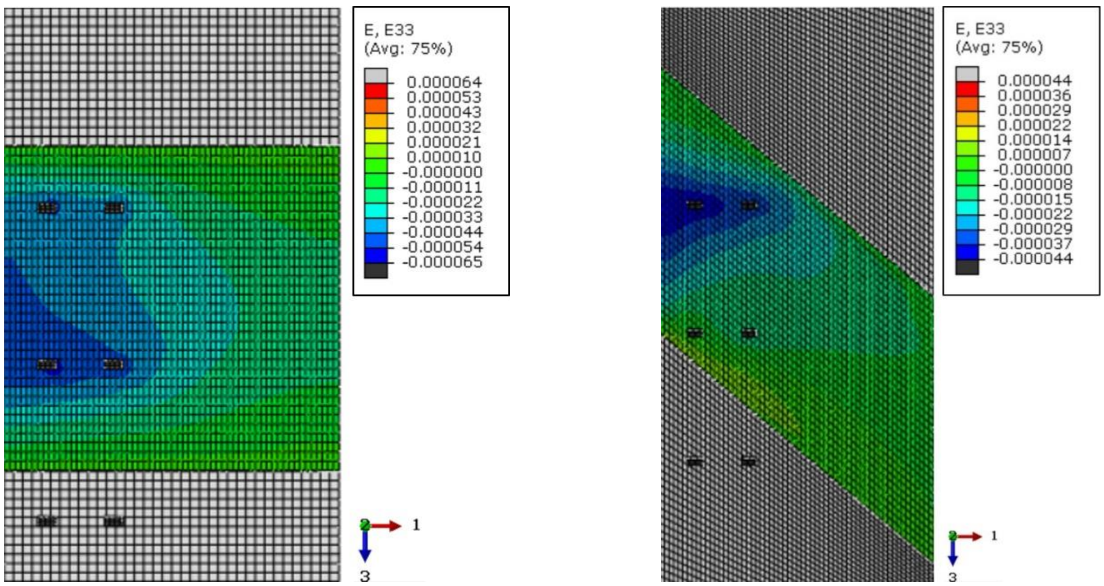

a.

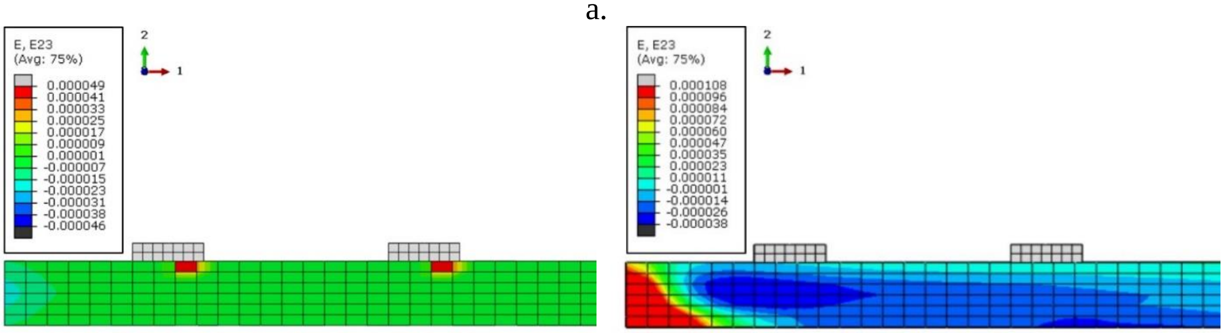

b.

Figure 3-17 Skew Effect on Strain Distribution; a. Normal, b. Shear

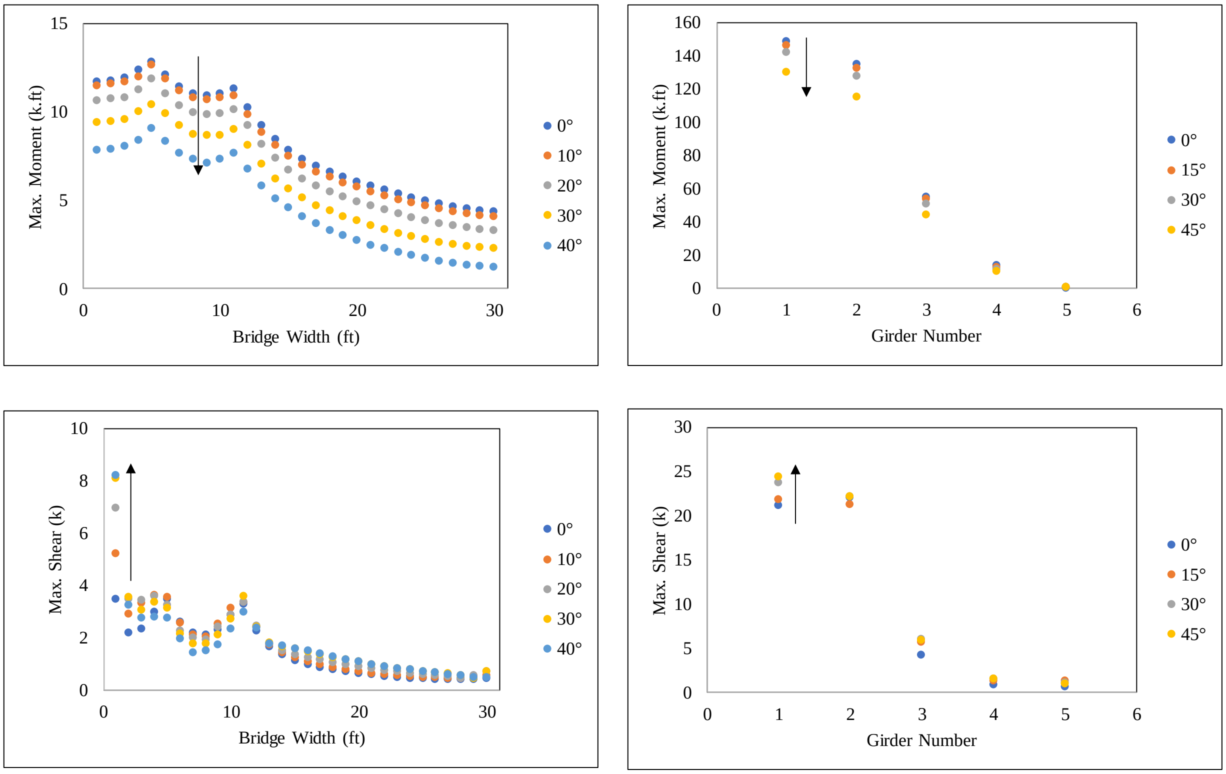

a. b.

Figure 3-18 Skew Effect on Demand Distribution across Bridge Width; a. Slab, b. T-beam

In Figure 3-19, the maximum moment and shear demands for different skew values were normalized with respect to the response in the reference bridge ($\theta = 0°$). In these graphs, ratios obtained from the finite element analysis were compared to corresponding skew correction factors specified in AASHTO (black dashed line). In the AASHTO LRFD specifications, the correction factor is given in Article 4.6.2.3, Equation 4.6.2.3-3, to adjust moment/shear demand in skewed slab bridges. The skew correction factor formulation is shown in Equation 3-2, where θ stands for the skew angle. In T-beam bridges, the skew correction factor is specified in accordance with Tables 4.6.2.2.2e-1 and 4.6.2.2.3c-1 for moment and shear, respectively. The application of these factors reduces the bending moment (Equation 3-3) and increases the shear forces (Equation 3-4) for skewed T-beam bridges. In Equation 3-3 and Equation 3-4, S, L, $K_g = n(I + Ae^2)$, t_s, and θ are respectively girder spacing, span length, longitudinal stiffness, slab thickness, and skew angle. In K_g formula, n is the modular ratio between beam and slab materials, I is girder stiffness, A is girder area, and e is the eccentricity between centroids of girder and slab.

$$1.05 - 0.25\tan(\theta) \leq 1 \tag{3-2}$$

$$1 - \left(0.25\left(\frac{k_g}{12Lt_s^{\,3}}\right)^{0.25}\left(\frac{S}{L}\right)^{0.5}\right)(tan\theta)^{1.5} \quad 30° \leq \theta \leq 60° \tag{3-3}$$

$$1 + 0.2\left(\frac{12Lt_s^{\,3}}{k_g}\right)^{0.3} tan\theta \quad 0° \leq \theta \leq 60° \tag{3-4}$$

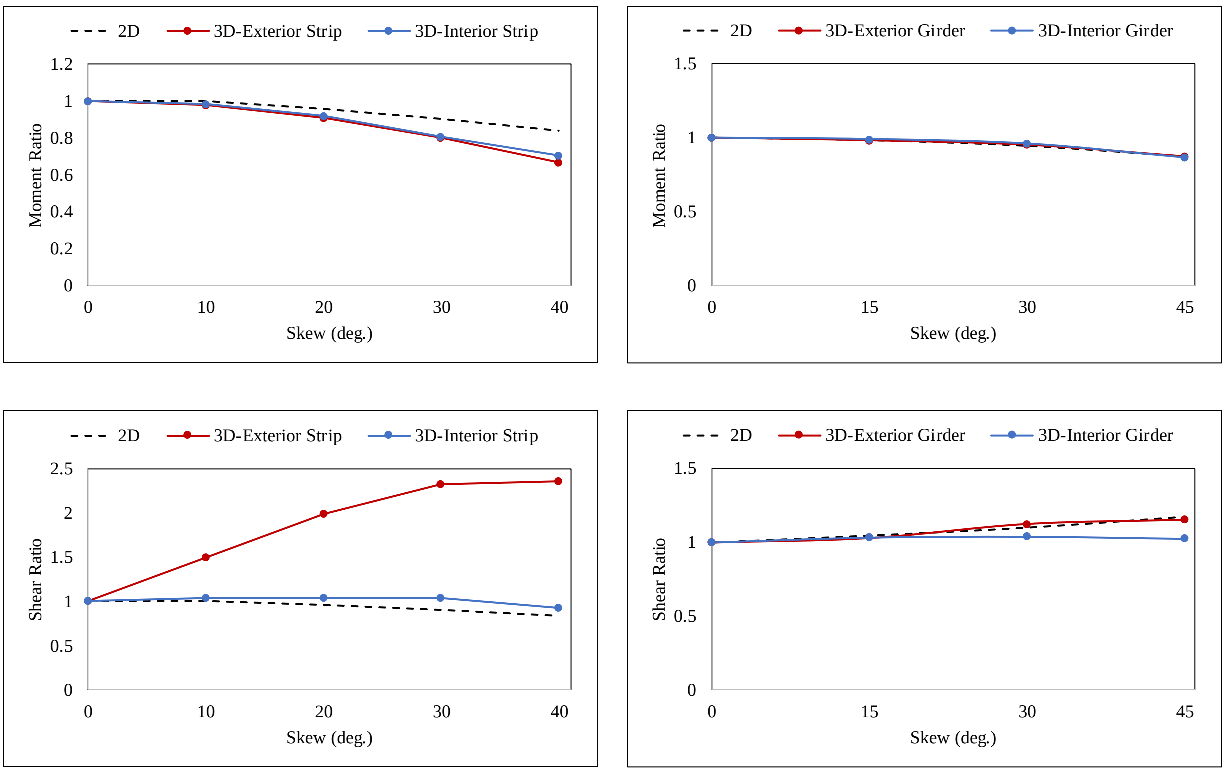

a. b.

Figure 3-19 Skew Angle Effect on Maximum Moment and Shear; a. Slab, b. T-beam

As shown in Figure 3-19.b, skew ratios obtained from 3D T-beam models were in good agreement with values obtained using the code-specified skew correction factor. For moment response, the average difference between 2D and 3D values was less than 1%. In terms of shear, this difference was about 5% and less than 1% for interior and exterior girders, respectively. Considering interior strips of slab models, 2D and 3D results varied with an average of about 7% for both moment and shear. However, the ascending pattern observed in Figure 3-19.a indicated that the AASHTO skew factor formulation provided for interior strips of slab differs with 3D analysis results of shear forces in exterior strips. FE results suggested that a skew angle of 40 degree could result in an increase of 2.4 times the shear demand in exterior strips.

3.3.3 Continuity Effect

Slab and T-beam three-span bridges were modeled to examine the impact of continuity on the significance of the studied parameters. In slab bridges, the middle span was typically 29 ft, which corresponds to the span length of single-span bridges. The length of adjacent spans was taken as 23 ft to enforce a ratio of spans length equal to 1.25 that matches the proportion observed in three-span bridges of the NBI dataset. For T-beam bridges, this value was 1.4, and therefore, span lengths were selected as 29-35-29 ft Bridge cross-sections were modeled identical to that of the single-span bridge in both bridge types.

Similar to single-span cases, three-span reference models were non-skewed bridges without secondary elements. The key parameters were changed one at a time, and bridge responses were calculated under the loading discussed in Section 3.2. Figure 3-20 to Figure 3-23 show the ratio of maximum shear and positive/negative moment to that in the reference model for each parameter considered. The parameters' range of variation is similar to that used in single-span models for each bridge type (see Table 3-4 and Table 3-5).

According to results presented in Figure 3-20, live-load responses decreased in interior strips/girders when railing was included in slab and T-beam three-span models. As expected, the opposite effect was observed in the exterior ones. It can be seen that the reduction in positive moment was slightly more than in the case of negative moment (about 2% on average for both bridge types). Similar to single-span bridges, shear demand was impacted less than moment. For slab bridges, increasing the railing height from 0 in. to 50 in. reduced shear, negative and positive moments by up to 12%, 40%, and 43%, respectively. Corresponding values (22% for shear and 55% for moment) obtained for single-slab models confirmed the observation that the effectiveness of edge-stiffening decreased for continuous bridges. In average, reduction in moment and shear response of interior strips of three-span slab bridge was 0.8 and 0.5 times of those in a single-span bridge, respectively (see Figure 3-21). The same pattern was observed in T-beam models with maximums of 1%, 7%, and 12% reduction in shear, negative moment, and positive moment, respectively. The corresponding values of shear and positive moment in the single-span T-beam models were 3% and 18%, respectively.

As illustrated in Figure 3-22, results in skewed three-span slab bridges showed that interior and exterior strips experienced up to 20% less bending moment on average. Shear forces for exterior strip increased by a factor of 2, while for interior strips, it decreased up to 7% for the skew angle of 40 degrees. These values were 12% (moment) and 7% (shear) in T-beam bridges.

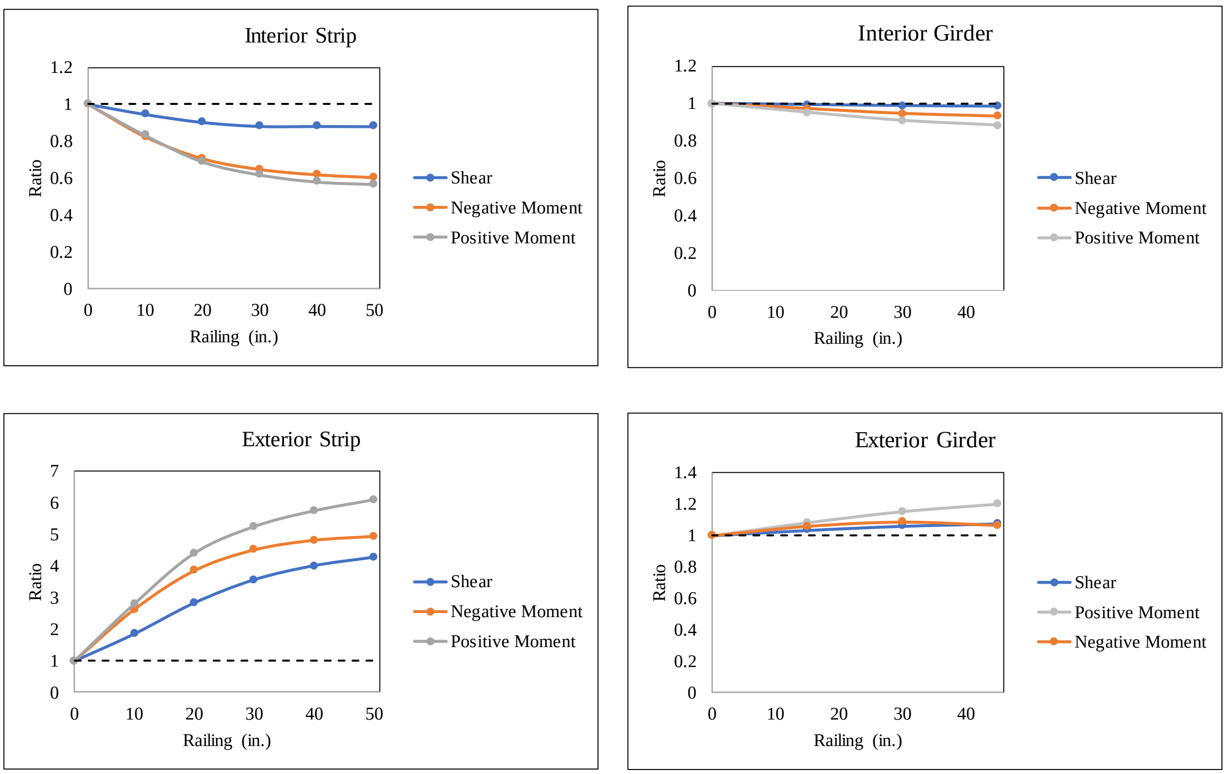

a. b.

Figure 3-20 Railing Height Effect in Three-Span Bridges; a. Slab, b. T-beam

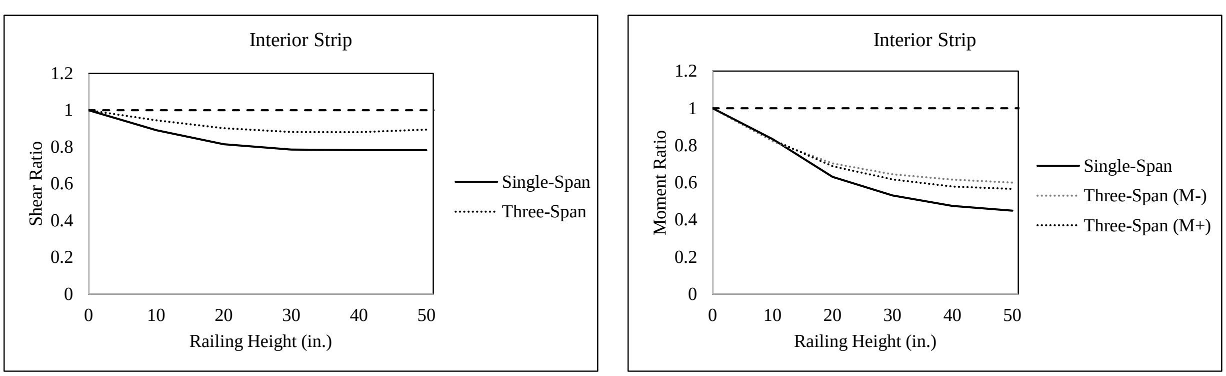

Figure 3-21 Rail Effect in Single-Span vs. Three-Span Slab Bridge

In three-span T-beam bridges with end-diaphragms, moments and shears remained almost unchanged with respect to values in bridges with no diaphragm, less than 1% difference (Figure 3-23). The edge-stiffening effect of end-diaphragms decreased significantly due to the longer length of the bridge (almost tripled compared to the single-span bridge). Maximum shear and negative moment occurred at interior supports. This location was far enough from end-diaphragms to be influenced by their presence. Based on these results, it was concluded that the effect on the negative moment and shear of the key parameters, i.e., railing height and end-diaphragms in three-span T-beam bridges was negligible when compared with those of the reference model. Therefore, this group sample was eliminated from the parametric study.

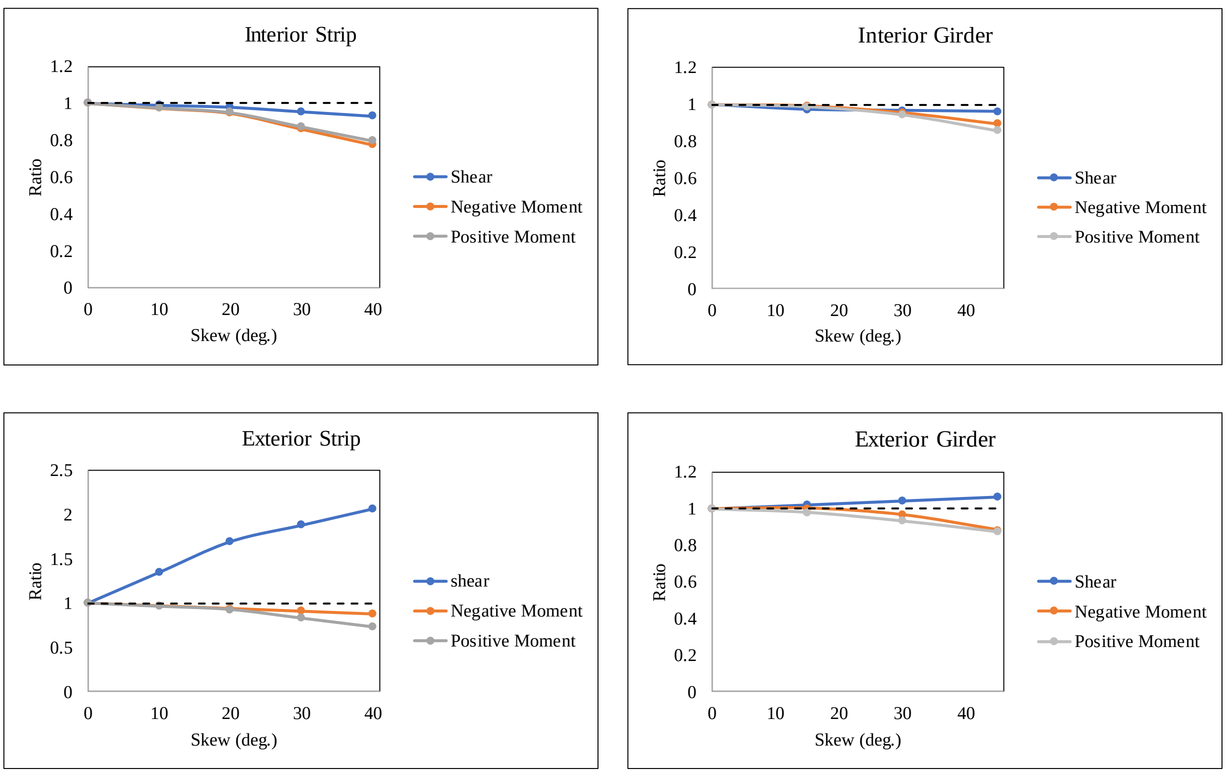

a. b.

Figure 3-22 Skew Angle Effect in Three-Span Bridges; a. Slab, b. T-beam

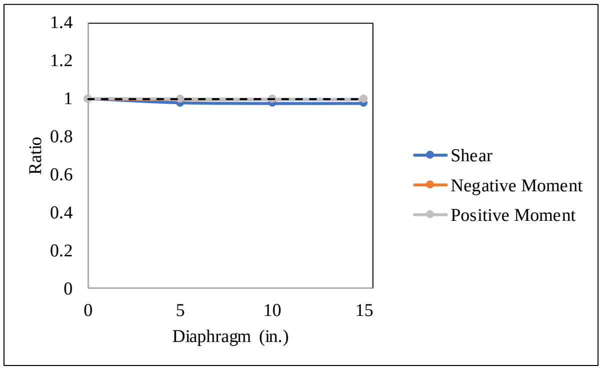

Figure 3-23 Diaphragm Width Effect in Three-Span T-beam Bridges

3.4 Summary of Findings

In the present chapter, a parametric study was conducted to assess the impact of geometrical parameters, including railing height, skew angle, and diaphragm width on moment and shear demand in slab and T-beam RC bridges. Bending moment and shear forces were obtained from 3D modeling of bridges with the abovementioned geometrical features and compared with corresponding benchmark bridges' results.

Railing height was confirmed as a parameter that produced the most drastic change in moment and shear demands in bridges with respect to the reference models. When railing height was increased in slab models, moment and shear demands increased respectively by a factor of 7 and 4 in exterior strips. This resulted in a reduction of about 50% moment and 20% shear in interior ones. In the case of T-beam models, increases of about 29% in moment and 14% in shear were observed in exterior girders. In interior girders, maximum reductions of 18% in moments and 3% in shears were observed. The same pattern was observed for three-span bridges. However, it was observed that edge-stiffening efficacy decreased for continuous bridges.

Increases in the skew angle were found to result in a reduction in longitudinal moment in interior and exterior strips/girders for both single and three-span bridges. This observation was consistent with the AASHTO reduction factor specified for moment adjustment of skewed bridges. In exterior strips/girders, shear forces were increased for skew angles larger than 0 degree. In T-beam bridges, this observation was consistent with AASHTO recommendations for skew correction factor, and therefore, modifications will not be proposed for this factor. However, in slab bridges, the AASHTO skew factor provided for interior strips did not agree with 3D analysis results of shear forces in exterior strips.

The addition of diaphragms in single-span T-beam bridges at span ends resulted in reduced moment and shear responses in interior girders. However, this effect was negligible (about 1% difference) in three-span T-beam models. Since the effect of studied parameters on the negative moment and shear of continuous T-beam cases was negligible, this group was eliminated from the parametric study.

The parametric study results were used in the statistical study performed to formulize the effect of secondary elements in form of modification factors applicable to available distribution factor provisions. More details are presented in the following chapter.

4. IDENTIFICATION & VERIFICATION OF MODIFICATION FACTORS USING STATISTICAL ANALYSIS

4.1 Introduction

Statistical methods include methodologies to collect, organize, and analyze a sample set of data. The goal of the statistical study is to utilize quantified models and representations to characterize a given set of data and draw conclusions that are applicable to the whole data population. For this purpose, the appropriate choice of the methods, sample selection, and statistical tests are of great importance. In Chapter 3, a parametric study was carried out on a sample of bridges to explore the effect of parameters such as railing height, skew angle, and diaphragm width on shear and moment demand estimates. The parametric study results were used as a sample data set in a statistical study designed to obtain trends that apply to slab and T-beam bridge population in Indiana. In particular, demand ratios discussed in Section 3.3 were categorized as dependent variables, and studied parameters were categorized as independent ones. Statistical analysis was used to estimate the relationship between the variables and summarize the inferences into a mathematical form. This mathematical solution was formulated as modification factors that could be applied to current live load distribution factors to incorporate the effect of secondary elements in bridge demand evaluations.

4.2 Data Collection

The first step in statistical analysis was the determination of variables. The main objective of this research was to investigate the effect of secondary elements on bridge response. 3D models were used to produce data (bridge responses) for the parameters considered in the study (bridge non-structural elements). As expressed in Equation 4-1, the demand ratio was defined as the maximum response of a bridge with variable parameters to the response of the reference model. Therefore, demand ratios of sample bridges obtained from FE analysis were considered as dependent variables. The height of railings, angle of skew, and the width of end-diaphragms were considered independent variables. The demand ratio for reference models, a constant value of 1, served as a benchmark to decide if a variable had a decreasing or increasing effect. Demand ratios could reach values greater or smaller than 1 depending on the effect of the independent variables. The ratios were calculated separately for shear/moment responses of interior/exterior strips or girders subjected to single/multiple-lane loading applications.

Based on this classification, dependent variables were represented as $Y(y_1 \dots y_i)$ and independent variables were represented as $X(x_1 \dots x_i)$ throughout this study. i ranges from 1 $to\ n$ with n standing for sample size. According to variables and their corresponding values presented in Table 3-4 and Table 3-5, sample size was 30 and 64 for slab and T-beam sample bridges, respectively.

$$demand\ ratio = \frac{max.response\ in\ models}{reference\ model\ response} \tag{4-1}$$

4.3 Descriptive Statistics

All statistical definitions presented herein were adopted from "The Cambridge Dictionary of Statistics" (Everitt 2002) and "A Dictionary of Statistics" (Upton and Cook 2014), unless otherwise noted.

Descriptive statistics are generally used to describe the basic features of the data in a study. Mean, variance, and standard deviation are three main descriptive statistics describing the central tendency of a data set. Mean is arithmetic average, and variance is a measurement of the span of numbers in a dataset. Standard deviation, defined to be the square root of the variance, is used to indicate how far dataset values place from the mean. The mean and standard deviation were calculated to approximate the central tendency of variables in the sample data set. Moreover, these parameters were necessary for the calculation of other statistics used in statistical analysis. Mean and standard deviation, and range of variables are reported in Table 4-1 and Table 4-2 for slab and T-beam bridge models variables, respectively.

The correlation coefficient is a measure to estimate the statistical relationship between two sets of variables. This coefficient is defined as the covariance of the variables divided by the product of their standard deviations, as expressed in Equation 4-2. In Equation 4-2, r is the correlation coefficient, x, y, and n are independent variable, dependent variable, and sample size, respectively. r ranges between ± 1. The magnitude of this coefficient indicates the relationship strength, and the sign shows the direction of the relationship. A coefficient value of 1 shows the strongest correlation, while a value of 0 indicates the lack of any linear relationship between the two variables.

The values of the correlation coefficient are summarized in Table 4-3. The positive correlation coefficients obtained for the variable of railing height in exterior sections indicated trend similarity between the variable and moment/shear responses in both bridge types. It confirmed that by increasing the railing height, responses in exterior sections of the bridge increases. The negative coefficients obtained for interior sections indicated the opposite trend. In general, the relationship was stronger in moment responses than for shear. Also, larger coefficients for demand in slab bridges compared to those in T-beams, indicated that the effect of the railing parameter was more significant in slab type bridges.

Coefficient values obtained for the variable of diaphragm width in T-beam bridges showed no correlation between the variable and moment and shear responses in exterior girders. However, a negative correlation was observed for response in interior girders indicating that by increasing the width of the end-diaphragms, demand decreases in critical interior girders.

$$r(x,y) = \frac{n\sum xy - (\sum x)(\sum y)}{\sqrt{[n\sum x^2 - (\sum x)^2][n\sum x^2 - (\sum x)^2]}} \tag{4-2}$$

Table 4-1 Descriptive Statistics of Variables; Slab Bridges

<table>
<tr><th colspan="5">Variable</th><th>Mean</th><th>Standard Deviation</th><th>Range</th></tr>
<tr><td rowspan="2">Independent Variable</td><td colspan="4">Railing Height</td><td>25.00</td><td>17.37</td><td>0-50</td></tr>
<tr><td colspan="4">Skew Angle</td><td>20.00</td><td>14.38</td><td>0-40</td></tr>
<tr><td rowspan="8">Dependent Variable</td><td rowspan="8">Demand Ratio</td><td rowspan="4">Single-Lane</td><td rowspan="2">Moment</td><td>Interior Strip</td><td>0.60</td><td>0.18</td><td>0.4-1</td></tr>
<tr><td>Exterior Strip</td><td>4.28</td><td>2.10</td><td>0.7-7.0</td></tr>
<tr><td rowspan="2">Shear</td><td>Interior Strip</td><td>0.87</td><td>0.09</td><td>0.8-1.0</td></tr>
<tr><td>Exterior Strip</td><td>3.44</td><td>1.07</td><td>1.0-4.8</td></tr>
<tr><td rowspan="4">Multiple-Lane</td><td rowspan="2">Moment</td><td>Interior Strip</td><td>0.61</td><td>0.16</td><td>0.4-1.0</td></tr>
<tr><td>Exterior Strip</td><td>3.96</td><td>1.97</td><td>0.6-6.8</td></tr>
<tr><td rowspan="2">Shear</td><td>Interior Strip</td><td>0.89</td><td>0.09</td><td>0.7-1.0</td></tr>
<tr><td>Exterior Strip</td><td>4.12</td><td>1.37</td><td>1.0-5.9</td></tr>
</table>

Table 4-2 Descriptive Statistics of Variables; T-beam Bridges

Variable					Mean	Standard Deviation	Range
Independent Variable	Railing Height				22.50	5.63	0-45
	Skew Angle				22.50	16.90	0-45
	Diaphragm Width				7.50	16.90	0-15
Dependent Variable	Demand Ratio	Single-Lane	Moment	Interior Girder	0.82	0.09	0.7-1.0
				Exterior Girder	1.09	0.13	0.8-1.3
			Shear	Interior Girder	0.91	0.08	0.8-1.1
				Exterior Girder	1.10	0.05	1.0-1.2
		Multiple-Lane	Moment	Interior Girder	0.85	0.08	0.7-1.0
				Exterior Girder	1.11	0.14	0.8-1.4
			Shear	Interior Girder	0.88	0.12	0.6-1.0
				Exterior Girder	1.04	0.06	0.9-1.2

Table 4-3 Correlation Coefficients

Bridge Type	Loading Configuration		Single-Lane Loading				Multiple-Lane Loading			
	Demand Ratio		Shear		Moment		Shear		Moment	
	Section		Int.*	Ext.**	Int.	Ext.	Int.	Ext.	Int.	Ext.
Slab	Variable	Railing Height	-0.86	0.94	-0.90	0.95	-0.65	0.94	-0.72	0.91
		Skew Angle	0.02	0.18	-0.28	-0.21	-0.49	0.14	-0.58	-0.32
T-beam		Railing Height	-0.01	0.51	-0.79	0.92	0.00	0.69	-0.27	0.87
		Skew Angle	-0.13	0.72	-0.49	-0.34	-0.94	-0.38	-0.92	-0.41
		Diaphragm Width	-0.73	-0.06	-0.27	-0.10	-0.19	0.08	-0.26	-0.07

*Interior strip/girder

** Exterior strip/girder

4.4 Regression Model

Regression is a statistical process to determine the numerical relationship between variables that are correlated (Weisberg 2005). A regression model is presented as a mathematical formulation that relates the dependent variable (Y) to the independent variable (X). The former is referred to as the explained variable and the latter as the explanatory (regressor/predictor) variable. The regression analysis is performed on available data (observed pairs of (y_i, x_i)) to estimate the dependency function ($f(x_i)$) between the variables. The regression function $f(x_i)$ relates available data points (y_i, x_i) and, more importantly could be used for prediction purposes for data not included in the selected sample. The basic regression model is expressed in Equation 4-3 for $i = 1{:}\,n$ where n is the sample size. ε_i is an estimate of the individual errors.

$$y_i = f(x_i) + \varepsilon_i \tag{4-3}$$

Classical regression theory considers the case of linear dependence; however, this assumption might be too restrictive for some problems (Spokoiny and Dickhaus 2014). Equation 4-4 shows regression function in a multivariate linear form known as multilinear regression. Multilinear regression allows the inclusion of more than one independent variable in the model. Additional variables explain the part of Y that has not been explained by the existing variable. Consequently, they improve the prediction performance of the regression model. In Equation 4-4, a and b are regression coefficients known as intercept and slope, respectively. k is the number of predictors (X) included in the regression model. The sign of the slope indicates the direction of the relationship between the regressor and the dependent variable.

$$f(x) = a + b_1X_1 + b_2X_2 + \cdots + b_kX_k \tag{4-4}$$

Linear regression functions can be extended to nonlinear ones using different forms of mathematical functions instead of straight lines (Weisberg 2005). More sophisticated functions such as polynomial, logarithmic, and power trendlines could improve the smoothness of the regression model and consequently increase the approximation accuracy. Moreover, a combination of predictors could be used in nonlinear regression models to reflect the joint effects of two or more variables. Products of predictors are called interactions. The use of interactions in a regression model with k predictors may expand/shrink the model to more/fewer than k terms.

In some problems with predictors within a different range of numbers, variables need to be scaled through a procedure known as the transformation of predictors (Washington et al. 2010). This process scales variables so that the regression model can capture the effect of all predictors in the same level to produce a reasonable approximation. Transformation (expressed in Equation 4-5) scales all variables within the range of 0 and 1. After finalizing the regression model, regression coefficients (intercept and slopes) should be transformed through a re-scaling process so that they apply to the original variables. In Equation 4-5, $\bar{x}_i$, x_i, min, and max represent scaled variable, original variable, minimum, and maximum values of variable set, respectively.

$$\bar{x}_i = \frac{x_i - min}{max - min} \tag{4-5}$$

4.5 Statistical Tests

There are different approaches to test the reliability of a statistical model, such as regression in statistics. The results of the tests indicate whether the model was sufficient to describe the studied data. Different numerical and graphical methods are used in the verification process which some examine the included variables while others investigate the performance of the statistical model. These include analysis of goodness of fit, regression residuals, and model validation. Statistical tests applied in the present study are summarized in the following subsequent sections.

4.5.1 Student T-test

As explained previously, the first step in the regression procedure was to determine potential predictors. In multivariate regression models, where there is more than one variable to describe the outcome, it is critical to include crucial explanatories and disregard those that do not impact the results. The t-test is one of the statistical tools widely used to determine the significance of predictors included in a regression model. The t-test compares the statistical difference between two or more sets of data. If two sets of variables are statistically equal, then one set is not statistically significant and, therefore, should be eliminated from the list of regressors.

In the regression procedure, the t-statistic of each predictor should be compared to the t-value. The t-value is obtained using predefined t-tables shown in Figure 4-1. To use this table, the degree of freedom (df) and Confidence Level (CL) are needed. The degree of freedom is defined as $df = n - 1$ where n is the sample size. Confidence Level is a measure for the certainty of statistical results. CL of 95% is commonly used for statistical studies indicating that one can be 95% certain that the true value lies within the range denoted by the confidence interval (Winters et al. 2010). The confidence interval is usually assumed as twice the standard deviation. When the t-statistics for a given predictor is smaller than the t-value, that variable is identified as statistically insignificant and should not to be included in the regression model.

Moreover, application of the t-test on the regressors reduces the probability of having an over-parametrized regression function. This function might result in overfitting problem, which happens when a regression model is developed using too many numbers of parameters. Over-parametrized regression function might fit the sample data perfectly, but the performance decreases significantly when applied to another set of data. Moreover, the function seems more complicated and, therefore, not considered a user-friendly model.

t Table

cum. prob	$t_{.50}$	$t_{.75}$	$t_{.80}$	$t_{.85}$	$t_{.90}$	$t_{.95}$	$t_{.975}$	$t_{.99}$	$t_{.995}$	$t_{.999}$	$t_{.9995}$
one-tail	0.50	0.25	0.20	0.15	0.10	0.05	0.025	0.01	0.005	0.001	0.0005
two-tails	1.00	0.50	0.40	0.30	0.20	0.10	0.05	0.02	0.01	0.002	0.001
df											
1	0.000	1.000	1.376	1.963	3.078	6.314	12.71	31.82	63.66	318.31	636.62
2	0.000	0.816	1.061	1.386	1.886	2.920	4.303	6.965	9.925	22.327	31.599
3	0.000	0.765	0.978	1.250	1.638	2.353	3.182	4.541	5.841	10.215	12.924
4	0.000	0.741	0.941	1.190	1.533	2.132	2.776	3.747	4.604	7.173	8.610
5	0.000	0.727	0.920	1.156	1.476	2.015	2.571	3.365	4.032	5.893	6.869
6	0.000	0.718	0.906	1.134	1.440	1.943	2.447	3.143	3.707	5.208	5.959
7	0.000	0.711	0.896	1.119	1.415	1.895	2.365	2.998	3.499	4.785	5.408
8	0.000	0.706	0.889	1.108	1.397	1.860	2.306	2.896	3.355	4.501	5.041
9	0.000	0.703	0.883	1.100	1.383	1.833	2.262	2.821	3.250	4.297	4.781
10	0.000	0.700	0.879	1.093	1.372	1.812	2.228	2.764	3.169	4.144	4.587
11	0.000	0.697	0.876	1.088	1.363	1.796	2.201	2.718	3.106	4.025	4.437
12	0.000	0.695	0.873	1.083	1.356	1.782	2.179	2.681	3.055	3.930	4.318
13	0.000	0.694	0.870	1.079	1.350	1.771	2.160	2.650	3.012	3.852	4.221
14	0.000	0.692	0.868	1.076	1.345	1.761	2.145	2.624	2.977	3.787	4.140
15	0.000	0.691	0.866	1.074	1.341	1.753	2.131	2.602	2.947	3.733	4.073
16	0.000	0.690	0.865	1.071	1.337	1.746	2.120	2.583	2.921	3.686	4.015
17	0.000	0.689	0.863	1.069	1.333	1.740	2.110	2.567	2.898	3.646	3.965
18	0.000	0.688	0.862	1.067	1.330	1.734	2.101	2.552	2.878	3.610	3.922
19	0.000	0.688	0.861	1.066	1.328	1.729	2.093	2.539	2.861	3.579	3.883
20	0.000	0.687	0.860	1.064	1.325	1.725	2.086	2.528	2.845	3.552	3.850
21	0.000	0.686	0.859	1.063	1.323	1.721	2.080	2.518	2.831	3.527	3.819
22	0.000	0.686	0.858	1.061	1.321	1.717	2.074	2.508	2.819	3.505	3.792
23	0.000	0.685	0.858	1.060	1.319	1.714	2.069	2.500	2.807	3.485	3.768
24	0.000	0.685	0.857	1.059	1.318	1.711	2.064	2.492	2.797	3.467	3.745
25	0.000	0.684	0.856	1.058	1.316	1.708	2.060	2.485	2.787	3.450	3.725
26	0.000	0.684	0.856	1.058	1.315	1.706	2.056	2.479	2.779	3.435	3.707
27	0.000	0.684	0.855	1.057	1.314	1.703	2.052	2.473	2.771	3.421	3.690
28	0.000	0.683	0.855	1.056	1.313	1.701	2.048	2.467	2.763	3.408	3.674
29	0.000	0.683	0.854	1.055	1.311	1.699	2.045	2.462	2.756	3.396	3.659
30	0.000	0.683	0.854	1.055	1.310	1.697	2.042	2.457	2.750	3.385	3.646
40	0.000	0.681	0.851	1.050	1.303	1.684	2.021	2.423	2.704	3.307	3.551
60	0.000	0.679	0.848	1.045	1.296	1.671	2.000	2.390	2.660	3.232	3.460
80	0.000	0.678	0.846	1.043	1.292	1.664	1.990	2.374	2.639	3.195	3.416
100	0.000	0.677	0.845	1.042	1.290	1.660	1.984	2.364	2.626	3.174	3.390
1000	0.000	0.675	0.842	1.037	1.282	1.646	1.962	2.330	2.581	3.098	3.300
z	0.000	0.674	0.842	1.036	1.282	1.645	1.960	2.326	2.576	3.090	3.291
	0%	50%	60%	70%	80%	90%	95%	98%	99%	99.8%	99.9%
	Confidence Level										

Figure 4-1 Student T-test Distribution (Everitt 2002)

4.5.2 Analysis of the Residuals

In the regression procedure, the goal was to define a regression function that best fitted the data; however, assumption on the errors was inevitable. The residuals are estimates of the individual errors (ε_i) defined in Equation 4-3. Residuals are the differences between observed data (actual) and those predicted using the regression function. In statistics, the Residual Sum of Squares (RSS) is a measure of the efficiency of a regression model in explaining the data (Weisberg 2005). This statistic estimates the amount of variance in a data set that is not captured by the model. Equation 4-6 expresses the formulation to calculate RSS where y_i and $f(x_i)$ are actual and predicted values, respectively. In an efficient regression model, RSS is minimized as much as possible.

$$RSS = \sum_{i=1}^{n} (y_i - f(x_i))^2 \tag{4-6}$$

4.5.3 Goodness of fit

The goodness of fit of a statistical model describes the discrepancy between actual data and the predicted values obtained from a regression model. The coefficient of determination, also known as R-squared (R^2) is a measure of fitness that indicates how much the independent variable explains variation of a dependent variable. As expressed in Equation 4-7, R^2 ranges from 0 to 1.

The coefficient of determination of 0 means the model cannot replicate the observed data, while the value of 1 for R^2 indicates that all predicted values perfectly matched with observed ones. When there are more than one regressors included in the model, the adjusted R-squared ($\bar{R}^2$) should be used to examine the goodness of fit of the model in question (see Equation 4-8).

$$0 \leq R^2 = 1 - \frac{LL(\beta)}{LL(0)} \leq 1 \tag{4-7}$$

$$\bar{R}^2 = 1 - \frac{LL(\beta) - k}{LL(0)} \tag{4-8}$$

where $LL(\beta)$ and $LL(0)$ are log-likelihood at convergence and initial log-likelihood, respectively. k is the number of predictors. In this study, since there were more than one variable under investigation, the adjusted R-squared was used as an indicator of overall models fit.

4.6 Results and Discussion

4.6.1 Model Estimation Results

As discussed previously, the effect of edge-elements was not included in the development of current distribution factor formulations. In this study, these parameters were included in 3D modeling of the bridges, and moment and shear responses were compared to a reference case without secondary elements. The difference was calculated as demand ratios in terms of moment and shear for interior and exterior sections of the superstructure. For each case, the value obtained for demand ratio was considered as a Modification Factor (MF) applicable to the live load distribution factor to incorporate the impact of parameters not included in the DF formulations as expressed in Equation 4-9.

In this study, Nlogit-4 software was used to conduct statistical analysis and estimate regression model parameters to formulize modification factors as a function of non-structural parameters (see Equation 4-9). Values of railing height (h_r), skew angle (θ), and diaphragm width (d_w) were inserted as independent variables in the multivariate regression model. Moreover, interactions (product of variables) were introduced to the model to capture the joint effect of the studied parameters. Different forms of mathematical functions (linear, polynomial, logarithmic, etc.) were defined for each variable to perform nonlinear regression analysis. Afterward, the student t-test method corresponding to a confidence interval of 95% was used to examine the significance of each variable in the model. To do so, t-ratios for each set of variables were calculated and then were compared to the t-value obtained from the standard t-table shown in Figure 4-1. The values of 2.045 and 2.000 were obtained for slab and T-beam datasets, respectively. Any set of variables with t-statistics less than reported t-values were considered statistically insignificant and therefore, disregarded from the regression procedure.

Since values of the dependent variable (MFs) and independent variables fell within different ranges, data transformation was applied using the scaling process explained in Section 4-4. In Nlogit-4, regression analysis was performed using the likelihood method. For each regression run, t-ratio, residual sum of square, and adjusted R-squared values were calculated as indicators of the performance of the model. Models with minimized RSS (closer to 0) and maximized $\bar{R}^2$ (closer to 1) were selected as finalized formulations to approximate the modification factors.

$$\begin{aligned} &DF_{Modified} = DF_{code} * MF \\ &where \\ &MF = a + b_1 f(h_r) + b_2 f(\theta) + b_3 f(d_w) + b_4 f(h_r, \theta, d_w) \end{aligned} \tag{4-9}$$

4.6.2 Proposed Modification Factors for Slab Bridges

In 3D models of slab bridges, the railing height was varied within the range of 0 in. to 50 in. and the skew angle was changed from 0 degree to 40 degree. Obtained modification factor formulations for slab bridges are a function of these two parameters however, correlation coefficients reported in Table 4-3 indicated that the railing parameter affected the results more significantly than the parameter of skew. Model estimation results are provided in Table 4-4 for transformed variables. Using the re-scaling procedure, regression coefficients were calculated for the original set of variables. Finalized modification factor formulations and the corresponding residual sum of square and adjusted R-squared values are summarized in Table 4-5. In the MF formulations, h_r is measured from the slab top surface in inches and the skew angle is measured in degrees. In non-skewed bridges with no railing on the edges, the value of 1 should be considered for MF in all cases.

MF results are plotted using regression models in Figure 4-2 and are compared to actual values obtained from the FE analysis for single-lane and multiple-lane loadings. A good agreement was observed between the results obtained from the two approaches. As shown in the graphs, MF formulations could capture the expected trend observed in actual data sets. Adjusted R-squared was 89.8% on average, indicating strong overall goodness of fit for the regression models.

As represented in Figure 4-2, MF values for interior strips were less than the value of 1, indicating a decreasing effect of the studied parameters on the moment and shear responses in internal sections. The factors are greater than 1 in the case of exterior strips showing that railing presence increased the demand in edge components of the superstructure. In general, the effects of railing and skew parameters were expressed by linear/quadratic and tangential trendlines in regression models, respectively. For all cases except shear in interior strips, the joint effect between railing and skew parameters was observed as expressed in the corresponding MF formulations by interaction variable of $h_r.tg\theta$ (refer to Table 4-5)

It should be noted that in slab bridges, studied parameters affected moment demand more compared to shear demand resulting in larger regression coefficients in moment MF formulations. Moreover, higher residuals were observed in shear regression models since shear FE results had fewer specific trends than moment ones.

4.6.3 Proposed Modification Factors for T-beam Bridges

In 3D models of T-beam bridges, the railing height was varied within the range of 0 in. to 45 in., the end-diaphragm width within 0 in. to 15 in., and the skew angle from 0 degree to 40 degree. Therefore, the proposed modification factor formulations for T-beam bridges contain a combination of these three parameters. Finalized modification factor formulations are summarized in Table 4-6 along with the corresponding residual sum of square and adjusted R-squared values.

Model estimation results are reported in Table 4-7 for transformed variables used in the re-scaling procedure to obtain regression coefficients for the original set of variables. In the MF formulations, h_r and d_w are measured in inches and skew angle is measured in degrees. Similar to slab bridges, in non-skewed T-beam bridges without edge-elements, the value of 1 should be considered for MF in all cases.

MF regression results are compared with actual values obtained from the 3D FE analysis for single-lane and multiple-lane loading applications in Figure 4-3. A good agreement was observed between the results obtained using the two procedures with R-squared values ranging from 0.72 to 0.98. MF formulations were able to capture expected increasing/decreasing trends that were observed in actual data. As shown in the graphs, MF values for interior girders ranged less than 1, indicating a decreasing effect of the studied parameters on the moment and shear responses of internal sections. However, the factors were greater than 1 in the case of exterior girders, showing that railing increased the demand on the edge parts of the superstructure.

Table 4-4 Model Estimation Results; Slab Bridges

Loading	Section	Effect	Variable*	Parameter Estimate	Standard Error	t-Statistic
Single-Lane	Interior Strip	Moment (1)	constant	1.035	0.024	43.7
			$\overline{h_r}$	-1.700	0.082	-20.8
			$\overline{h_r}^2$	0.732	0.073	10.0
			$\overline{tg\theta}$	-0.456	0.037	-12.3
			$\overline{h_r tg\theta}$	0.430	0.061	7.0
		Shear (2)	constant	0.758	0.072	10.6
			$\overline{h_r}$	-0.820	0.095	-8.7
	Exterior Strip	Moment (3)	constant	0.079	0.014	5.5
			$\overline{h_r}$	1.658	0.056	29.8
			$\overline{h_r}^2$	-0.690	0.050	-13.8
			$\overline{tg\theta}$	-0.136	0.024	-5.7
			$\overline{h_r tg\theta}$	-0.138	0.040	-3.4
		Shear (4)	constant	0.057	0.034	1.7
			$\overline{h_r}$	1.341	0.116	11.6
			$\overline{h_r}^2$	-0.422	0.104	-4.0
			$\overline{tg\theta}$	0.312	0.052	5.9
			$\overline{h_r tg\theta}$	-0.361	0.087	-4.2
Multiple-Lane	Interior Strip	Moment (5)	constant	1.038	0.023	44.3
			$\overline{h_r}$	-1.352	0.081	-16.8
			$\overline{tg\theta}$	0.521	0.073	7.2
			$\overline{h_r tg\theta}$	-0.737	0.037	-20.2
		Shear (6)	constant	0.988	0.056	17.5
			$\overline{h_r}$	-0.459	0.075	-6.2
			$\overline{tg\theta}$	-0.362	0.072	-5.0
	Exterior Strip	Moment (7)	constant	0.107	0.015	7.1
			$\overline{h_r}$	1.635	0.058	28.1
			$\overline{h_r}^2$	-0.697	0.053	-13.3
			$tg\theta$	-0.168	0.025	-6.7
			$\overline{h_r tg\theta}$	-0.240	0.042	-5.7
		Shear (8)	constant	0.130	0.042	3.1
			$\overline{h_r}$	0.913	0.070	13.1
			$\overline{tg\theta}$	0.267	0.072	3.7
			$\overline{h_r tg\theta}$	-0.339	0.119	-2.8

* Transformed variables

Table 4-5 Proposed Modification Factor Formulations; Slab Bridges

Loading	Section	Effect	MF* Formulation		RSS	$\bar{R}^2$
Single-Lane	Interior Strip	Moment	$1 - 0.02h_r + 0.0002h_r^2 - 0.3tg\theta + 0.006h_r tg\theta$	(1)	0.04	0.98
		Shear	$1 - 0.004h_r$	(2)	0.85	0.72
	Exterior Strip	Moment**	$1.2 + 0.2h_r - 0.002h_r^2 - 1.1tg\theta^{1.5} - 0.02h_r tg\theta$	(3)	0.02	0.99
		Shear	$1.4 + 0.07h_r + 1.4tg\theta - 0.03h_r tg\theta$	(4)	0.08	0.96
Multiple-Lane	Interior Strip	Moment	$1 - 0.01h_r - 0.5tg\theta + 0.008h_r tg\theta$	(5)	0.12	0.94
		Shear	$1 - 0.003h_r - 0.2tg\theta$	(6)	0.53	0.68
	Exterior Strip	Moment**	$1.2 + 0.2h_r - 0.002h_r^2 - 1.4tg\theta^{1.5} - 0.04h_r tg\theta$	(7)	0.02	0.99
		Shear	$1.6 + 0.09h_r + 1.6tg\theta - 0.04h_r tg\theta$	(8)	0.16	0.92

* MF is 1 for all cases when h_r and θ are equal to 0.
** Range of application $0° \leq \theta \leq 45°$.

Table 4-6 Proposed Modification Factor Formulations; T-beam Bridges

Loading	Section	Effect	MF* Formulation		RSS	$\bar{R}^2$
Single-Lane	Interior Girder	Moment	$1 - 0.004h_r - 0.114tg\theta^{1.5} - 0.004w_d$	(9)	0.14	0.96
		Shear	$1 - 0.03w_d + 0.001{w_d}^2 - 0.006w_d tg\theta$	(10)	1.49	0.72
	Exterior Girder	Moment	$1 + 0.007h_r - 0.125tg\theta^{1.5} - 0.002w_d$	(11)	0.10	0.98
		Shear	$1 + 0.003h_r + 0.166tg\theta - 0.003h_r tg\theta$	(12)	0.35	0.91
Multiple-Lane	Interior Girder	Moment	$1 - 0.001h_r - 0.193tg\theta^{1.5} - 0.003w_d$	(13)	0.17	0.96
		Shear	$1 - 0.227tg\theta - 0.009w_d tg\theta$	(14)	0.22	0.97
	Exterior Girder	Moment	$1 + 0.008h_r - 0.181tg\theta^{1.5}$	(15)	0.08	0.98
		Shear	$1 + 0.004h_r + 0.04tg\theta - 0.004h_r tg\theta$	(16)	0.54	0.83

* MF is 1 for all cases when h_r, w_d, and θ are equal to 0.

Table 4-7 Model Estimation Results; T-beam Bridges

Loading	Section	Effect	Variable*	Parameter Estimate	Standard Error	t-Statistic
Single-Lane	Interior Girder	Moment (9)	constant	0.954	0.015	65.5
			$\overline{h_r}$	-0.533	0.016	-32.4
			$\overline{tg\theta^{1.5}}$	-0.339	0.016	-21.2
			$\overline{w_d}$	-0.185	0.016	-11.3
		Shear (10)	constant	0.892	0.038	23.2
			$\overline{w_d}$	-1.400	0.189	-7.4
			$\overline{w_d}^2$	0.972	0.177	5.5
			$\overline{w_d tg\theta}$	-0.326	0.085	-3.8
	Exterior Girder	Moment (11)	constant	0.379	0.012	30.7
			$\overline{h_r}$	0.697	0.014	50.1
			$\overline{tg\theta^{1.5}}$	-0.267	0.014	-19.7
			$\overline{w_d}$	-0.073	0.014	-5.3
		Shear (12)	constant	0.095	0.026	3.7
			$\overline{h_r}$	0.653	0.041	15.9
			$\overline{tg\theta}$	0.830	0.043	19.2
			$\overline{h_r tg\theta}$	-0.658	0.069	-9.5
Multiple-Lane	Interior Girder	Moment (13)	constant	0.936	0.016	58.6
			$\overline{h_r}$	-0.200	0.018	-11.1
			$\overline{tg\theta^{1.5}}$	-0.658	0.018	-36.8
			$\overline{w_d}$	-0.171	0.018	-9.3
		Shear (14)	constant	1.029	0.012	85.6
			$\overline{tg\theta}$	-0.646	0.028	-23.1
			$\overline{w_d tg\theta}$	-0.365	0.036	-10.2
	Exterior Girder	Moment (15)	constant	0.354	0.009	38.7
			$\overline{h_r}$	0.620	0.013	48.8
			$\overline{tg\theta^{1.5}}$	-0.326	0.013	-25.8
		Shear (16)	constant	0.175	0.032	5.4
			$\overline{h_r}$	0.777	0.052	15.0
			$\overline{tg\theta}$	0.171	0.058	2.9
			$\overline{h_r tg\theta}$	-0.781	0.090	-8.7

* Transformed variables

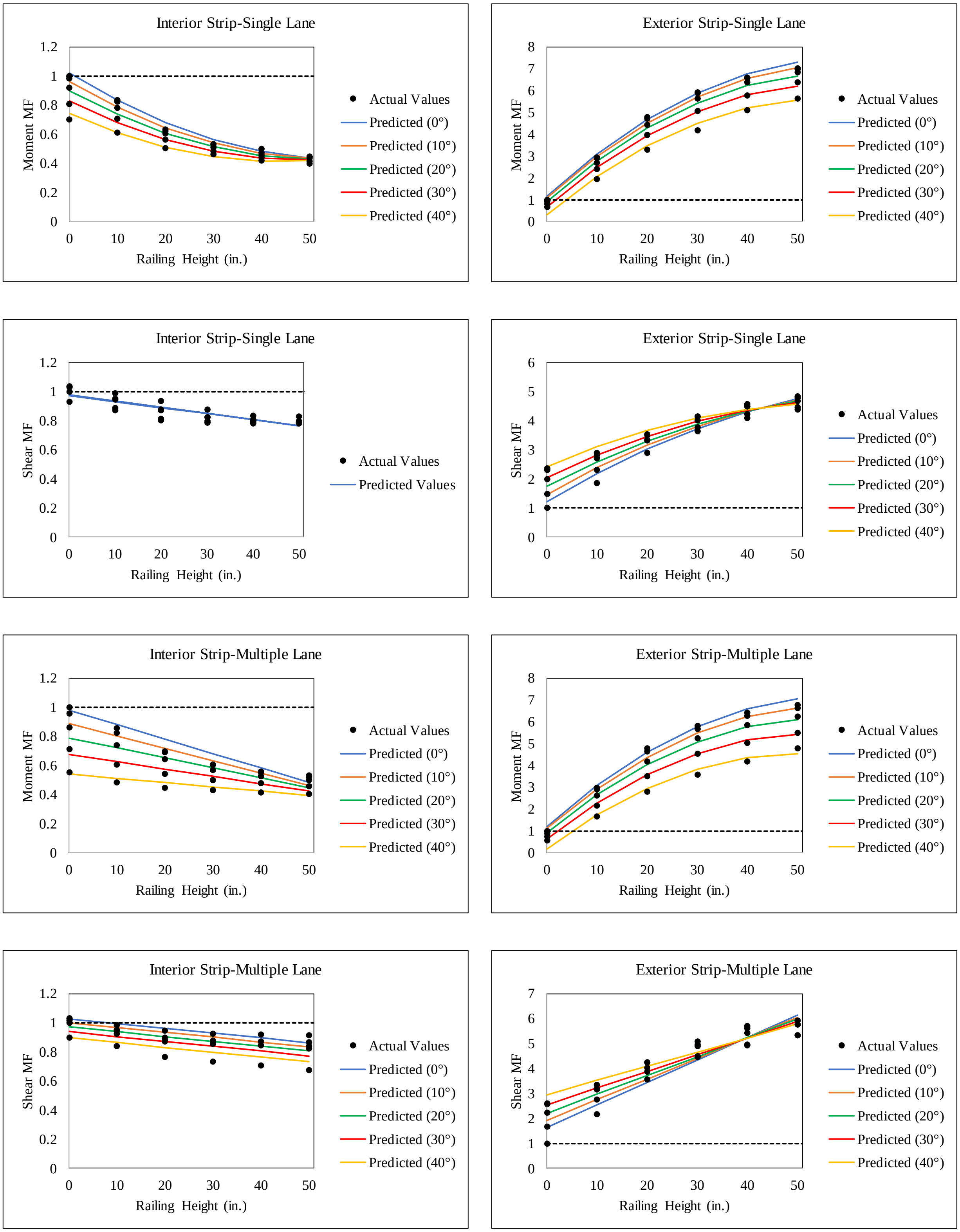

Figure 4-2 Proposed Modification Factors Compared to Actual Data (FE Analysis); Slabs

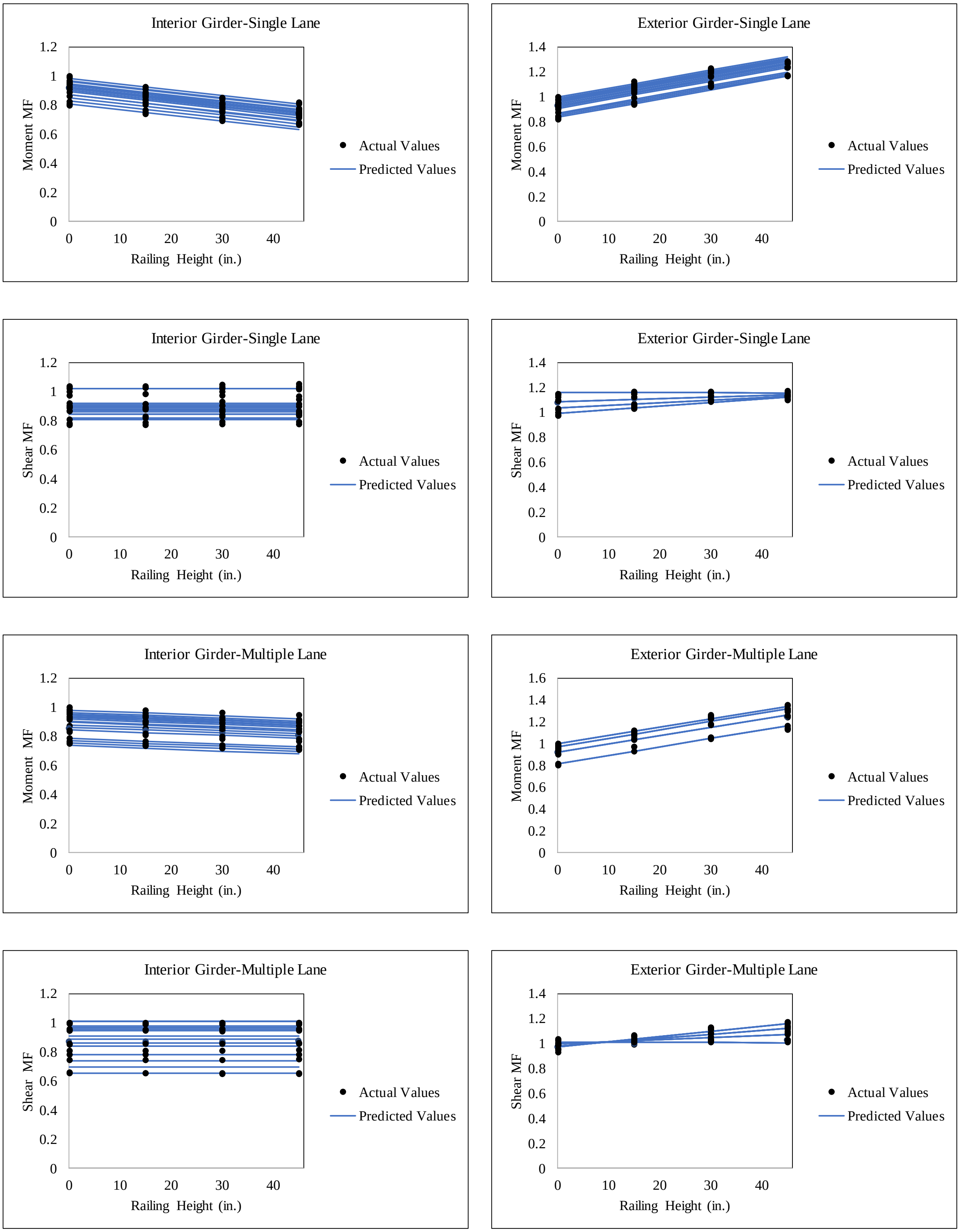

Figure 4-3 Proposed Modification Factors Compared to Actual Data (FE Analysis); T-beams

As shown in Figure 4-3, MF values showed a decreasing trend in moment responses of interior girders when railing height increased; however, the effect was negligible on shear results. The opposite trend was observed in exterior girder results. As reported in Table 4-6, MF formulations specified a decreasing trend with an increase in diaphragm width in demand for interior girders. This effect was negligible in exterior beams. In general, the effect of railing and diaphragm parameters was described using linear trendlines in regression models. The impact of skew parameter on moment and shear responses was expressed by tangential forms with different power values.

4.7 Proposed Modification Factor Verification

Regression models are mainly used to define a proper mathematical function that relates the dependent variable to independent ones. When a regression function is finalized based on available data, its reliability to predict the future (unobserved) data should be examined. In this study, the effect of variables was studied on reference bridges (slab and T-beam), and modification factors were proposed using regression models. Therefore, the performance of the MF formulations was assessed for bridges with geometrical features (span length, deck width, slab thickness, girder dimensions, etc.) different from those of reference slab and T-beam bridges. This verification indicated how well the regression model could predict the effect of studied parameters in bridges not included in the regression procedure.

Moreover, the results of proposed MF formulations were compared to those obtained from available skew modification factors in the LRFD specifications for slab and T-beam bridges. In this comparison, the value of 0 was considered for the edge-element parameters ($h_r = w_d = 0\ in.$) in proposed MF formulations consistent with LRFD assumptions.

4.7.1 Comparison of Proposed and LRFD Skew Modification Factors

In this research's parametric study, skewed superstructures combined with secondary elements were modeled to investigate the possible interaction between these parameters and assess the reliability of available skew correction factors. In the AASHTO LRFD specifications, correction factors are specified to adjust moment/shear demand in skewed bridges as expressed in Equation 3-2 to Equation 3-4.

In slab bridges, the AASHTO formulation is specified for moment responses in the interior section of slab bridges for all loading configurations. This factor was compared with the proposed MF for moment response in interior strips when $h_r = 0\ in.$ (see Table 4-8). As shown in Figure 4-4, the proposed formula could capture the decreasing trend specified in the LRFD skew factor when the skew angle increased. However, code-specified provisions seemed slightly conservative compared to corresponding FE results. The discrepancy between the results increased for larger skew values by up to 11% and 31% for the skew of 40 degree in single and multiple-lane loading, respectively.

In T-beam bridges, moment (in all girders) and shear (in exterior girder) responses should be adjusted in skewed girder bridges using skew modification factor provisions in AASHTO specifications. The skew factors are a function of bridge length, deck thickness, girder spacing/dimensions, and skew angle. The formulations are identical for single and multiple-lane loading configurations. The geometrical dimensions of average T-beam bridge were replaced in AASHTO skew factor formulations and were compared to corresponding ones obtained from regression models with $h_r = d_w = 0\ in$, as reported in Table 4-8.

As shown in Figure 4-5, the proposed formulations could capture decreasing and increasing trends expressed in LRFD skew factors for moment and shear demands, respectively, when the skew angle increased. The results obtained from the two approaches matched perfectly for single-lane loading applications with a difference of less than 1% on average. However, current formulation values seemed slightly conservative compared to FE results for multiple-lane loading cases with a difference of less than 9% on average.

Table 4-8 LRFD and Proposed Skew Modification Factors Comparison

Bridge	Effect	Girder	LRFD Skew MF	Proposed Skew MF	
				Single-Lane	Multiple-Lane
Slab	Moment	Interior	$1.05 - 0.25tg\theta$	$1.02 - 0.33tg\theta$	$1.02 - 0.53tg\theta$
T-beam	Moment	Interior	$1 - 0.128tg\theta^{1.5}$	$1 - 0.114tg\theta^{1.5}$	$1 - 0.193tg\theta^{1.5}$
		Exterior		$1 - 0.125tg\theta^{1.5}$	$1 - 0.181tg\theta^{1.5}$
	Shear	Exterior	$1 + 0.169tg\theta$	$1 + 0.166tg\theta$	$1 + 0.042tg\theta$

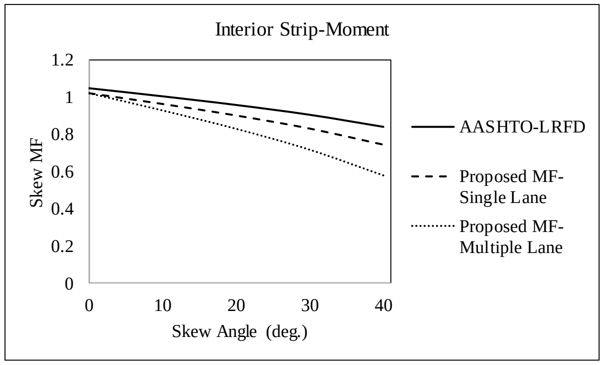

Figure 4-4 LRFD and Proposed Skew Factor Comparison in Slab Bridges

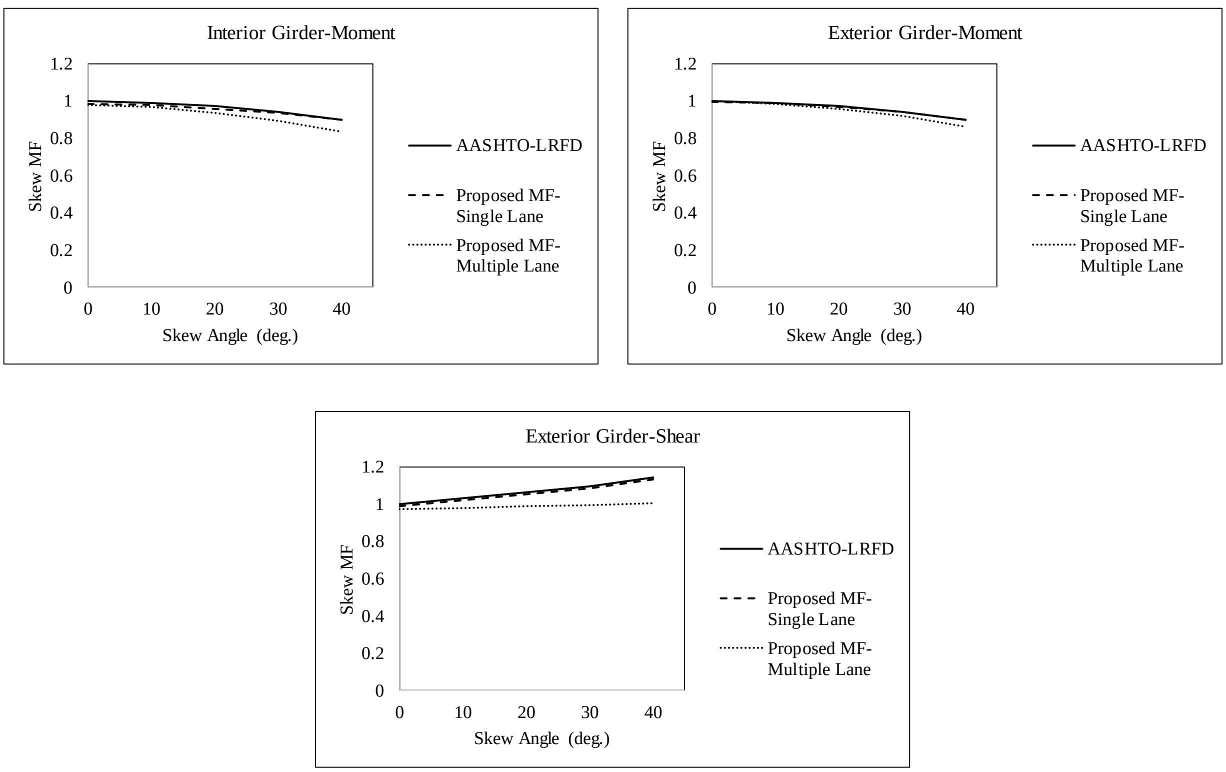

Figure 4-5 LRFD and Proposed Skew Factor Comparison in T-beam Bridges

In both bridge types, the skew factor formulations approximated using the regression method shared a similar mathematical form to the code-specified provisions with slightly different coefficients in multiple-lane loading cases. Considering that the LRFD formulations were developed using a comprehensive study (Zokaie et al. 1991) on a large sample of girder (365) and slab (130) actual bridges, the consistency between the results verified the reliability of the method adopted in this study for railing and end-diaphragm MF propositions.

Due to consistency observed between the FE analysis results and AASHTO recommendations for skew correction, modifications were not proposed for this parameter, and MF formulations were finalized for railing and diaphragm effects as reported in Table 4-9. The values in the table are applicable to the shear and bending moments from the 2D procedure using current distribution factors. When more than one factor applies, these are to be applied simultaneously to the shear force and bending moment DFs. The modifications are given for interior and exterior strips in slab bridges, and exterior and interior beams in T-beam bridges for cases of single and multi-lane loading configurations. In the cases where a parameter was shown not to influence the demand, the term NA (Not Applicable) is shown in the table. It should be noted that according to discussion presented in Section 3.3.3, the interior MFs obtained from Table 4-9 should be increased by factor of 1.1 (shear) and 1.2 (moment) for cases of continuous slab bridges (see Figure 3-21). Also, proposed MFs for T-beam bridges are only applicable to single-span cases since edge-effect was found to be negligible for these cases (refer to Section 3.3.3).

4.7.2 Verification of Proposed MFs in Random Bridges

To evaluate the performance of the proposed MF formulations, sample bridges were randomly selected from the Indiana bridges dataset. In this process, box-plots were used as a standard tool to visualize the data variability for each geometrical parameter. The main characteristics of a box-plot are shown in Figure 4-6. Box-plots were graphed for slab and T-beam datasets, for parameters such as span length, deck width, slab thickness, skew angle, and girder spacing/dimension shown in Figure 4-7 and Figure 4-8, respectively. These graphs displayed the distribution of data and indicated outlier cases. Using these plots, selected bridges with characteristics within the outlier range (shown with dots in the graphs) were disregarded and replaced with another bridge.

A total of twenty single-span slab and T-beam bridge samples (ten of each type) were randomly selected and modeled in 3D. Sample bridge characteristics are summarized in Table 4-10 (slab) and Table 4-11 (T-beam). The distribution of the selected bridge samples within each category is represented in Figure 4-7 and Figure 4-8 (e.g., S1 represents Sample 1). Each bridge superstructure was firstly modeled and analyzed as a non-skewed bridge without edge-elements. Then, secondary components were added to the model, moment, and shear responses were obtained, and demand ratios (MFs) were calculated using Equation 4-1.

In 3D modeling of slab sample superstructures, representative cross-section dimensions of edge-elements found in Indiana bridges were considered with a height of 12 in. and 33 in. representing standard curb and E706-BRSF railing, respectively. For T-beam cases, a railing height of 24 in. consistent with E706-BRPP configuration was included in bridge 3D models. Skew angle and diaphragm width values are reported in Table 4-10 and Table 4-11 for each bridge sample.

Table 4-9 Proposed Railing and Diaphragm Modification Factors

Bridge	Loading	Section	Effect	Railing MF	Diaphragm MF
Slab	Single-Lane	Interior Strip	Moment	$1 - h_r(0.02 + 0.006tg\theta) + 0.0002h_r^2$	NA
			Shear	$1 - 0.004h_r$	
		Exterior Strip	Moment	$1.2 + h_r(0.2 - 0.02tg\theta) - 0.002h_r^2$	
			Shear	$1.4 + h_r(0.07 - 0.03tg\theta)$	
	Multiple-Lane	Interior Strip	Moment	$1 - h_r(0.01 + 0.008tg\theta)$	
			Shear	$1 - 0.003h_r$	
		Exterior Strip	Moment	$1.2 + h_r(0.2 - 0.04tg\theta) - 0.002h_r^2$	
			Shear	$1.6 + h_r(0.09 - 0.04tg\theta)$	
T-beam	Single-Lane	Interior Girder	Moment	$1 - 0.004h_r$	$1 - 0.004w_d$
			Shear	NA	$1 - w_d(0.03 - 0.006tg\theta) + 0.001{w_d}^2$
		Exterior Girder	Moment	$1 + 0.007h_r$	$1 - 0.002w_d$
			Shear	$1 + h_r(0.003 - 0.003tg\theta)$	NA
	Multiple-Lane	Interior Girder	Moment	$1 - 0.001h_r$	$1 - 0.003w_d$
			Shear	NA	$1 - 0.009w_d tg\theta$
		Exterior Girder	Moment	$1 + 0.008h_r$	NA
			Shear	$1 + h_r(0.004 - 0.004tg\theta)$	NA

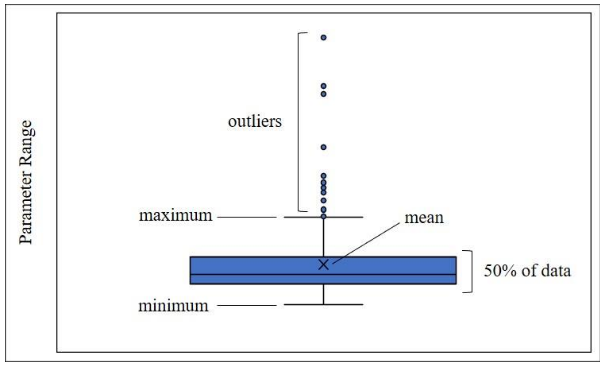

Figure 4-6 Typical Box-Plot Characteristics

MFs obtained from FE analysis were compared to those calculated using the proposed formulations for each bridge sample. Figure 4-9 and Figure 4-10 illustrate a comparison between the results obtained from the two approaches for slab and T-beam samples, respectively. In the graphs, modification factors obtained using proposed formulations and FE analysis are represented as “predicted” and “actual” MF, respectively, and black dashed line represents the 1:1 line. Moreover, Root Mean Square Error (RMSE), as a measure of the differences between predicted and observed value were calculated and is reported in the graphs for each case.

A comparison of the results is shown in Figure 4-9 and Figure 4-10 and indicated that regression models could predict MFs in samples that were not included in the original modeling process. Results obtained from MF formulations (prediction) and 3D models (actual) were scattered closely around the 1:1 line. The discrepancy between the results was inevitable, considering that samples considered for the verification process were different in geometrical features than those of reference bridges used in the regression procedure.

In slab samples, the average RMSE of 0.07 was obtained for predictions of interior strip modification factors. This value was 0.42 for those of exterior strips. Since root mean square error shares the same unit as data under investigation, a range of data should be considered when interpreting the size of this error. In this case, RMSE values could be considered relatively small, bearing in mind that range of MF values for interior strips between 0 to 1 and for exterior strips between 1 to 6. In T-beam samples, the average RMSE of 0.07 is relatively small, considering the variation range of 0 to 1.4 for MFs in interior and exterior girders.

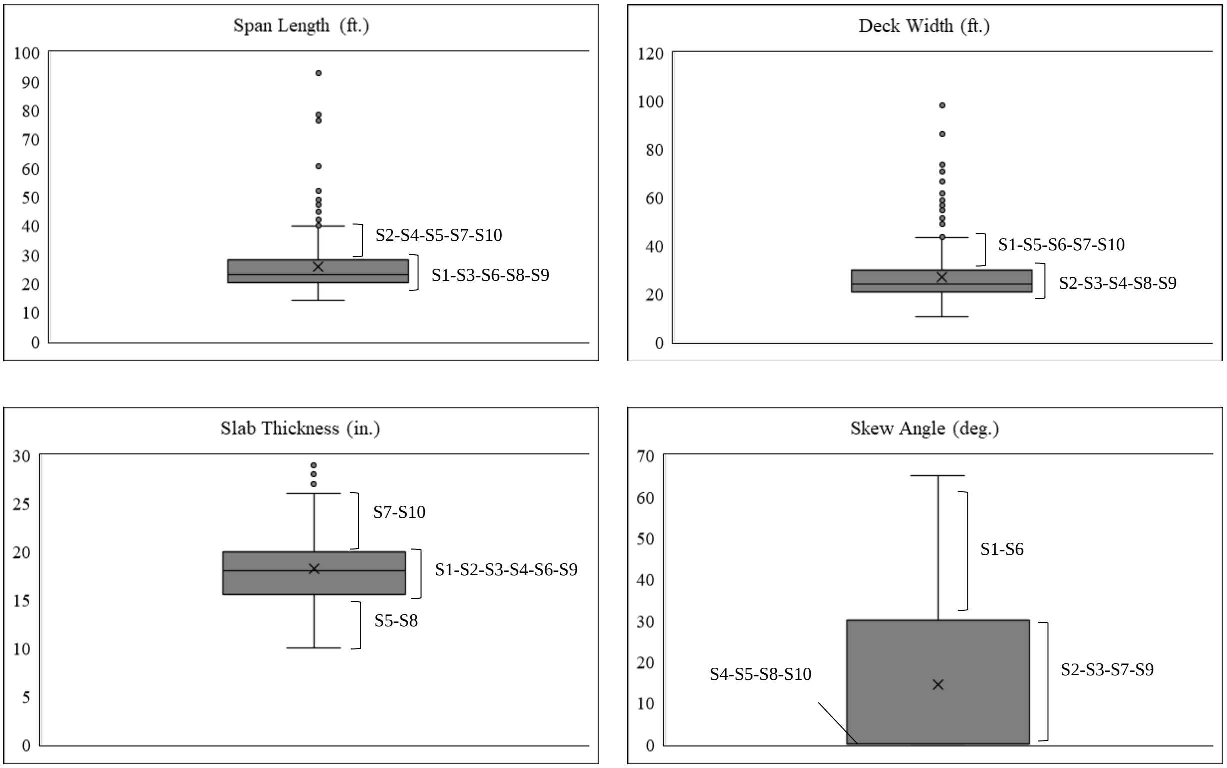

Figure 4-7 Box-Plots for Slab Samples

Table 4-10 Slab Bridge Samples Information

Sample No.	Span Length (ft)	Deck Width (ft)	Slab Thickness (in.)	Skew Angle (deg.)
1	27.5	32.4	15.5	44°
2	33.0	23.9	18.0	15°
3	28.2	30.0	18.0	30°
4	35.6	25.6	19.0	0°
5	21.4	26.5	13.0	0°
6	26.0	32.0	18.0	45°
7	37.2	36.0	25.0	25°
8	21.8	24.5	15.0	0°
9	25.9	24.0	18.0	5°
10	38.7	31.8	25.0	0°

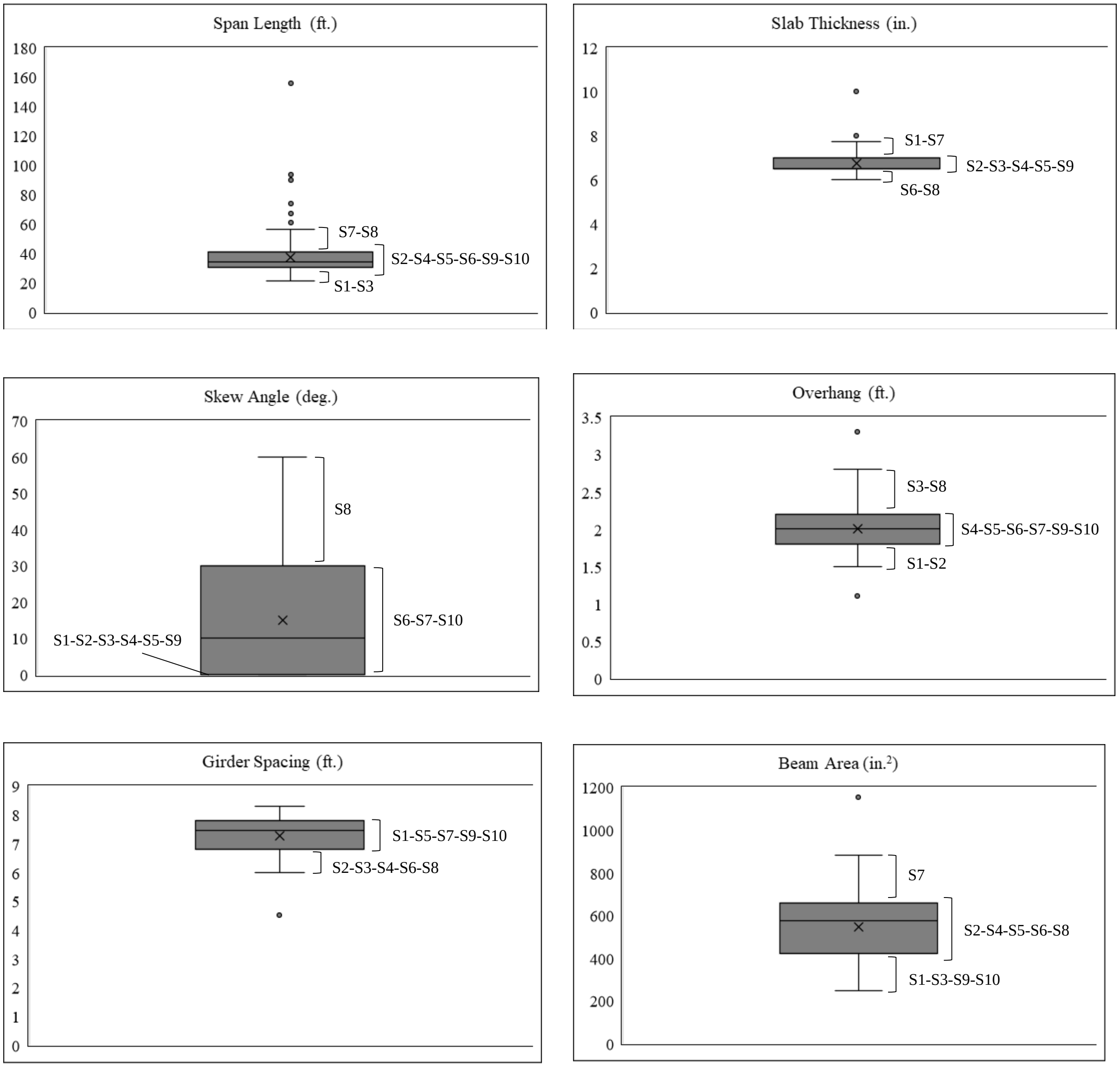

Figure 4-8 Box-Plots for T-beam Samples

To compare the size of the errors for different cases in slab and T-beam samples with different range of data, RMSEs were normalized according to the range of data in each category. To do so, Normalized Root Mean Square Error (NRMSE) values were calculated by dividing RMSEs by the average of actual data in each data set. NRMSEs reported in Figure 4-9 and Figure 4-10ranged between 7%-13% and 4%-10% in slab and T-beam samples, respectively indicating that all MF models resulted in comparable levels of prediction of performance.

Table 4-11 T-beam Bridge Samples Information

Sample No.	Span Length (ft)	Deck Width (ft)	Slab Thickness (in.)	Girder Width/Height (in.)	Girder Spacing (in.)	Overhang Length (ft)	Skew Angle (deg.)	diaphragm Width (in.)
1	28.0	34.0	7.25	19.0 / 20.0	92.4	1.6	0°	15
2	36.0	29.4	6.50	16.5 / 26.0	78.0	1.7	0°	18
3	24.0	38.3	6.50	16.5 / 18.0	80.4	2.4	0°	15
4	36.0	28.8	6.50	16.5 / 35.0	75.6	1.8	0°	12
5	40.0	33.4	6.50	24.0 / 25.5	87.6	2.1	0°	12
6	36.5	29.2	6.25	16.5 / 25.5	75.6	2.0	10°	10
7	45.0	32.2	7.50	22.0 / 33.0	81.6	2.0	15°	18
8	44.0	43.0	6.00	24.0 / 24.0	75.0	2.8	35°	18
9	30.0	42.6	6.50	16.5 / 20.5	93.6	1.8	0°	12
10	32.0	31.4	6.50	16.5 / 24.0	82.8	1.9	25°	0

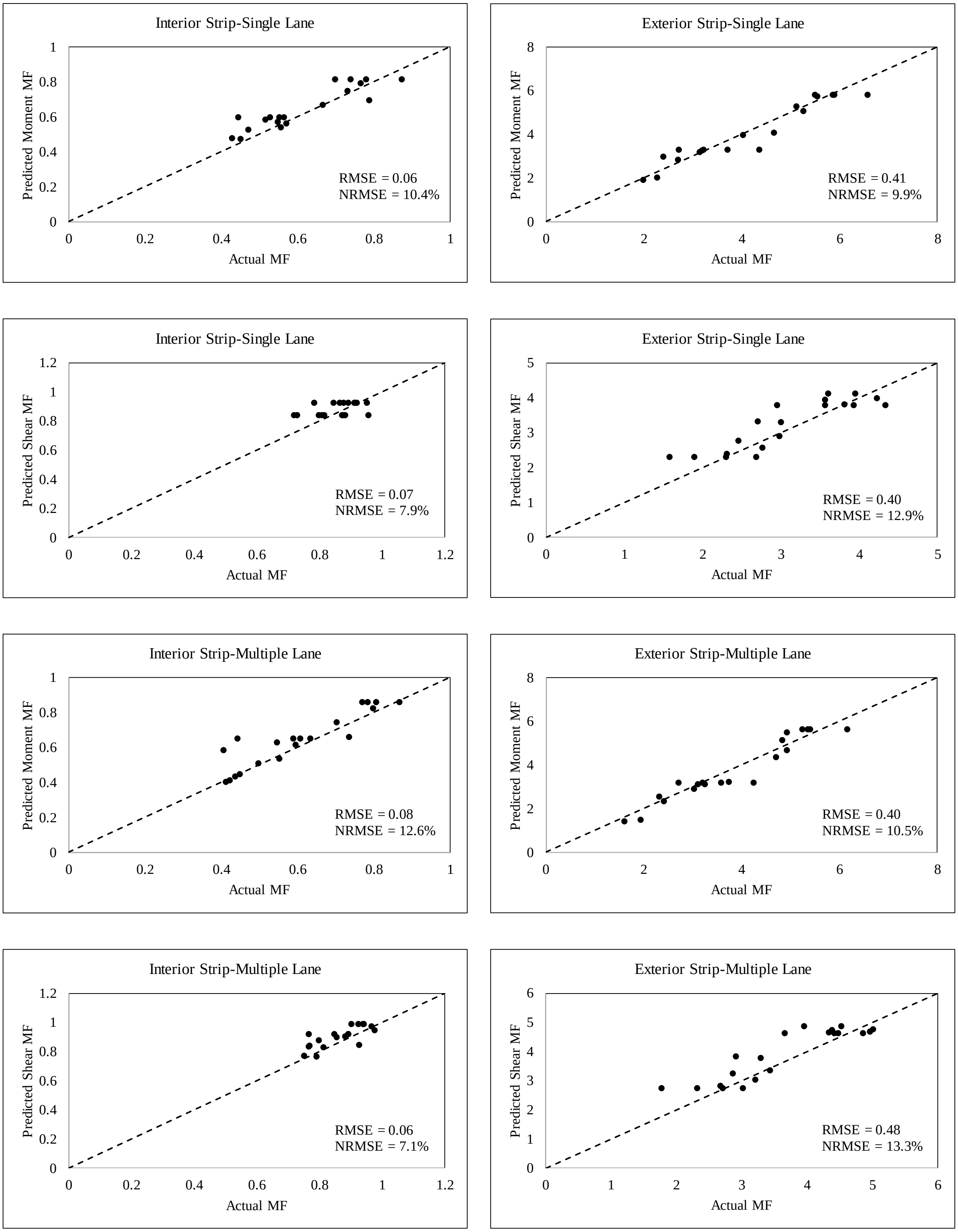

Figure 4-9 Comparison of Predicted and Actual (from FE Analysis) MFs; Slab Samples

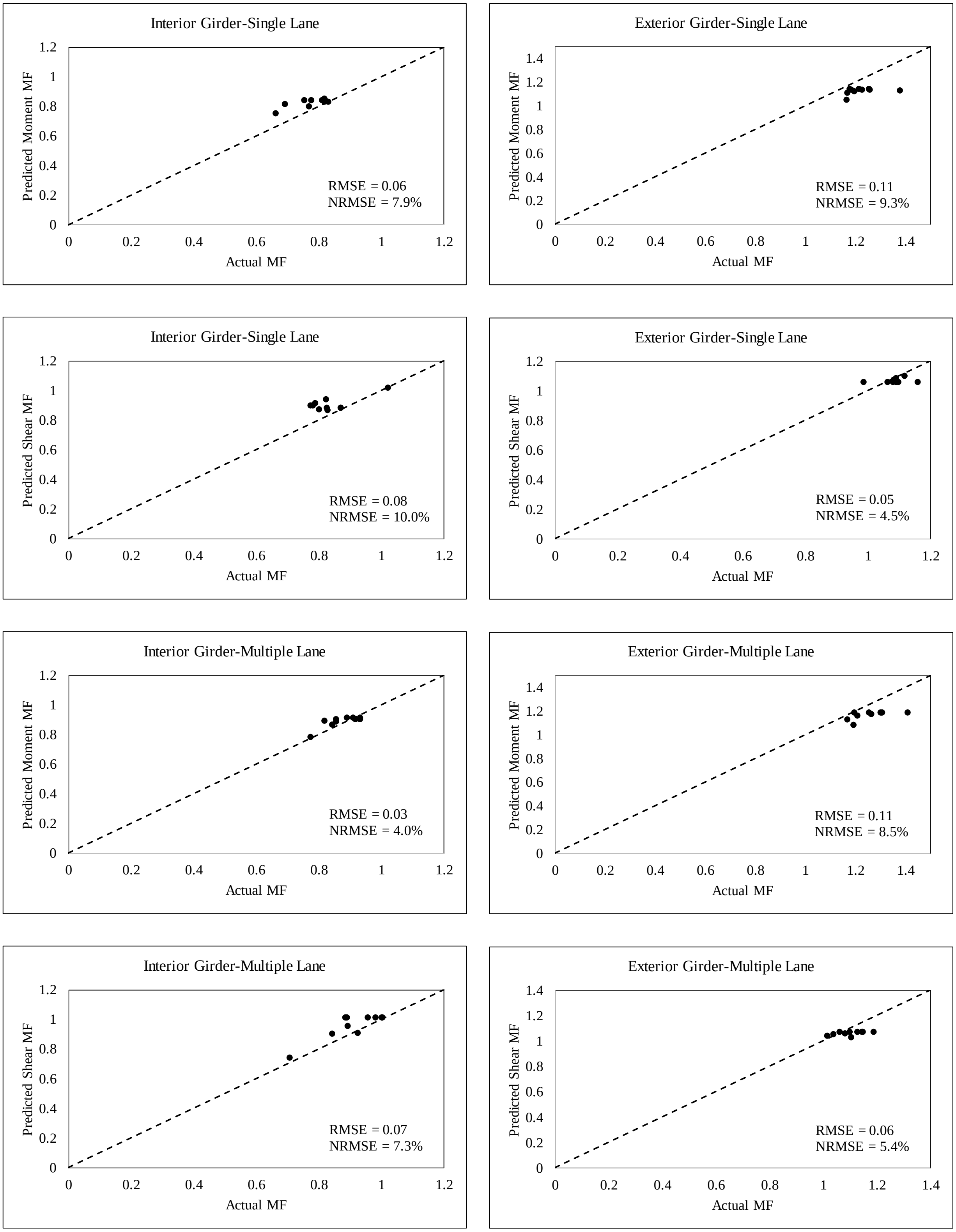

Figure 4-10 Comparison of Predicted and Actual (from FE Analysis) MFs; T-beam Samples

4.8 Summary of Findings

Regression analysis was performed to fit the observed data into mathematical formulations. Results of regression analysis were provided in forms of modification factors as a function of edge-element dimensions, i.e., railing height and diaphragm width. The modification factor formulations were proposed for moment and shear demand in interior and exterior sections in a bridge superstructure. Residuals, adjusted R-squared, and t-ratio statistics were used to evaluate the performance of regression models. A good agreement was observed between the predicted (regression) and observed (3D models) values with adjusted R-squared of 89.8% and 91.4% on average for slab and T-beam models, respectively. The average residuals were 0.228 in slab and 0.386 in T-beam bridges.

The prediction power of proposed MF formulations was assessed for twenty randomly selected bridges with geometrical properties different from those of reference slab and T-beam bridges. This verification indicated how well the regression model could predict the effect of studied parameters in bridges not included in the regression procedure. The superstructure of selected bridge samples was modeled in 3D (including non-structural components), and live load demand was estimated. An acceptable discrepancy was observed between the results obtained from MF formulations (prediction) and 3D models (actual) with normalized root mean square error of 10% and 7% on average in slab and T-beam samples, respectively.

Moreover, the results of proposed skew MF formulations were compared to those in the LRFD specifications for slab and T-beam bridges. The results obtained from the two approaches agreed well for single-lane loading cases, however, LRFD results were slightly conservative in multiple-lane loading cases. Therefore, modifications were not proposed for skew parameter, and MF formulations were finalized for railing and diaphragm effects. Moreover, the consistency observed in this comparison verified the reliability of the method adopted in this study for railing and end-diaphragm MF propositions.

5. SUMMARY OF FINDINGS, CONCLUSION & FUTURE WORK

5.1 Summary of Findings

This thesis investigates procedures for load rating evaluation in reinforced concrete bridges. The main contribution of this work is an improved methodology for the live load estimation in slab and T-beam reinforced concrete bridges in Indiana using the tools of Finite Element (FE) analysis.

A focused review of available literature on the live load distribution factor formulation was conducted to identify gaps and limitations in current demand estimate provisions in the American Association of State Highway and Transportation Officials (AASHTO) manual. The impact of identified limitations was explored in the strength assessment of bridge evaluation procedures for a case study of selected Indiana bridges.

National Bridge Inventory (NBI) and Indiana Department of Transportation (INDOT) records were surveyed to select a small sample of bridges located in Indiana, including five slab and five T-beam Reinforced Concrete (RC) bridges. Sample bridge superstructures were analyzed using FE methods, and load rating results were compared to those obtained following AASHTO Load and Resistance Factor Design (LRFD) standard specifications. This study's findings indicated that the AASHTO LRFD might underestimate Rating Factor (RF) mainly due to the overestimate of the live load Distribution Factors (DF) compared to 3D analysis.

AASHTO recommends using a simple and practical method for demand estimate using DF formulations provided for slab and girder bridges. DF provisions include key bridge parameters such as slab and beams properties; however, they neglect non-structural elements' effect. FE results of studied sample bridges revealed that the contribution from secondary members such as curbs, railings, and sidewalks added to system stiffness, which favorably affected both demand distribution and structural capacity. Consideration of this beneficial effect is crucial in load rating of older concrete bridges. These were designed using smaller truck loads and that rate structurally deficient under current truck loads. To further explore the effect of structural elements on bridge demand such as railing height, diaphragm width, and skew angle parameters 3D FE models were analyzed, and live load shears and moments were obtained. The inclusion of the secondary elements changed both the magnitude and distribution of bending moment and shear throughout the bridge superstructure. The main findings were:

- Railing height was confirmed as a parameter that produced the most drastic change in bridge demand. The edge-stiffening effect increased moments and shears in exterior beams and one-way strips in solid concrete slab bridges, and demand reduction in interior parts.
- The same effect was observed with the addition of diaphragms in T-beam bridges, resulting in reduced moment and shear responses in interior girders. Their effect was found to be negligible on the response of exterior girders.
- Proposed modification factors are given for single-span bridges. In the case of continuous T-beam bridges, edge-effect was found to be negligible. In the case of slab bridges, the factors should be used in multiple-span bridges considering discussion presented in Section 3.3.3 and Section 4.7.1 on decreased edge-stiffening efficacy for continuous bridges.

Regression analysis of the results obtained from the parametric study was used to develop Modification Factors (MF) applicable to current DFs. The main findings were:

- Proposed MFs are a function of edge-element dimensions of railing height and diaphragm width.
- The proposed modifications are applicable to the load distribution factors in the AASHTO LRFD used in the 2D load rating procedure and are given for interior and exterior sections of the bridges for cases of single and multi-lane loading configurations.

5.2 Conclusions

Based on the research findings, the following conclusions were arrived at:

1. Conventional Load Rating (CLR) methodology currently in practice results in conservative estimates of rating factor in older RC slab and T-beam bridges. Rating factors obtained from 3D FE analysis were greater than those obtained using the 2D-based LRFD approach, and the live load distribution factor was shown to be the main parameter affecting the results.

2. Detailed modeling of bridge superstructures with the inclusion of non-structural components, particularly edge-elements, had a substantial influence on stress distribution over the bridge deck, causing higher stress concentrations in the edges and lower stresses in interior sections. Distribution factors currently used in the rating of these bridges must be updated to include the edge effect of secondary concrete elements to estimate demand.
3. On the capacity side, an important consideration is the inclusion of the reinforced concrete railings, parapets, curbs, and sidewalks, properly anchored with adequate vertical steel reinforcement into the bridge superstructure, in determining exterior sections' capacity. The increased capacity due to edge-elements' participation compensates the increase in share load of exterior sections (increased DFs) keeping the RF in satisfactory range.
4. To simplify incorporating these geometric features in load rating calculations by structural engineers using current 2D rating methods, a modified live load distribution factor formula, where secondary members' effect could be taken into account, would improve the rating evaluation of existing bridges.
5. Modification factors proposed in this study are intended to better represent in the bridge rating the favorable effect of non-structural elements on demand calculations in interior sections and improve the accuracy of demand estimates in exterior sections, particularly in slab bridges where no DF formulation is provided in current specifications.
6. The use of proposed railing modification factors to current DF formulations applies to any edge reinforced concrete components such as railing, parapet, and curb properly anchored to the deck. Additionally, diaphragm factors were proposed to incorporate the beneficial effect of end-diaphragms in demand estimates of T-beam bridges.
7. The study showed almost similar results for the effect of skew on moment and shear forces compared to LRFD skew correction factors, and therefore, no modification is proposed for this parameter. However, in some cases, the skew parameter is presented in railing/diaphragm modification factor formulations to reflect the joint effect observed between the parameters.
8. The proposed modification factors were obtained for reference bridges with average geometrical properties. Therefore, it is necessary to exercise caution when applying the factors to bridges with geometries greatly different from the bridges used in this study.

9. Current DFs can be used with proposed modification factors in conventional load rating methods to incorporate 3D effects while maintaining the simplicity of load rating procedures. The proposed modification would benefit an important population of Indiana bridges that with current procedures might be unnecessarily identified as structurally deficient or functionally obsolete. It would also prevent unnecessary posting and rerouting of vehicles in some circumstances.

5.3 Future Work

Railing configurations considered in this study were adopted from commonly used barriers used in Indiana, E706-BRSF in slab and E706-BRPP in T-beam bridges. The range considered for railing height variable in the parametric study covered the maximum design height of 45 in. in the BRSF and 42 in. in the BRPP. Since the variation in parapet width is not as large as it is in heights, the width was considered constant, measuring 12 in. and 10 in. However, the results indicate that the edge beam response is influenced by the moment of inertia of exterior sections. The edge beam geometry affects the flexural and shear stiffness, and consequently, the share of stresses and loads attracted to these regions. As possible future work, the width of the parapet could be considered in a parametric study on the distribution of loads. This consideration is beneficial for the evaluation of bridges with wide barriers, thick curbs, and sidewalks. Moreover, railings were modeled as solid sections in 3D modeling of the superstructures and cross-sectional discontinuity was not considered. However, voided parapets are commonly used in girder RC bridges and modeling them in 3D could enlighten its impact on extend of the edge-stiffening effect observed in this research.

In this study, it was assumed that the edge-element on each side of the roadway was cast monolithically with the slab, and the tie bars extended from the slab to the edge member. Therefore, full railing participation was considered in load-bearing and capacity calculations. To further investigate the reliability of this assumption, one can design a series of experiments on the proper anchorage of these elements in bridge retrofitting.

Findings of this study suggest that the addition of edge components such as curbs, railings, and sidewalk could be considered as a potential retrofitting technique for bridges that exhibit border-line load rating results in the interior sections of the bridge superstructure provided that the non-structural elements are properly designed, reinforced, and anchored to the deck.

Supplementary investigation is required to assess this rehabilitation suggestion. Also, caution should be exercised in construction practices associated with these retrofits since they attract a great amount of stress. The presence of partial vertical joints or improper reinforcement detailing might create cracking due to stress concentrations. Thus, in order to consider the damage analysis, further investigation is required to fully explore this effect using nonlinear finite element analysis.

This research aimed to explore potential improvement to load rating evaluation in slab and T-beam bridges using proposed modifications to the load estimate procedure. This can also be extended to similar structural systems such as cast-in-place multicell box, precast solid, voided, or cellular concrete box slab bridges, and I-beam, double-T, and other concrete girder bridge sections with monolithic concrete deck. Performing detailed 3D modeling of such superstructures with railings and parapets integrated with slab could provide insights into the effectivity of secondary elements and the applicability of present study findings. With the lessons learned from such a study, one can extend the use of proposed modifications in similar bridge systems with proper adjustments.

Finally, all the conducted analyses presented in this thesis assume linear-elastic behavior. This assumption was followed for the sake of comparison with the current methodology for load distribution calculation, which is based on linear-elastic refined methods. The focus of this research was to examine the impact of non-structural elements on the transverse distribution of wheel loads, and therefore, the nonlinearity effect of materials on demand computation was out of the scope of this study. Thus, to account for the combined effects of all influencing factors, it is important to include nonlinear behavior such as damage and plasticity when defining the material properties in the 3D model.

REFERENCES

AASHTO, (2017). "LRFD Bridge Design Specifications." 7th Ed., American Association of State Highway and Transportation Officials, Washington, D.C.

AASHTO, LRFR. (2011). "Manual for Bridge Evaluation." Association of State Highway and Transportation Officials, Washington DC.

AASHTO, Standard Specifications for Highway Bridges. (2002). 17th Ed., American Association of State Highway and Transportation Officials, Washington, D.C.

Amer, A., Arockiasamy, M., and Shahawy, M. (1999). "Load Distribution of Existing Solid Slab Bridges Based on Field Tests." *Journal of Bridge Engineering*, 4(3), 189-193.

Azizinamini, A., Boothby, T. E., Shekar, Y., and Barnhill, G. (1994). "Old Concrete Slab Bridges. I: Experimental Investigation." *Journal of Structural Engineering*, 120(11), 3305-3319.

Azizinamini, A., Shekar, Y., Boothby, T. E., and Barnhill, G. (1994). "Old Concrete Slab Bridges. II: Analysis." *Journal of Structural Engineering*, 120(11), 3284-3304.

Bakht, B., and Moses, F. (1988). "Lateral Distribution Factor for Highway Bridges." *Journal of Structural Engineering*, 114(8), 1785-1803.

Barker M. G. (2001). "Quantifying Field-Test Behavior for Rating Steel Girder Bridges." *Journal of Bridge Engineering*, 6(4), 254-261.

Barr, P. J., Eberhard, M. O., and Stanton, J. F. (2001). "Live-Load Distribution Factors in Prestressed Concrete Girder Bridges." *Journal of Bridge Engineering*, 6(5), 298-306.

Bell, E. S., Lefebvre, P. J., Sanayei, M., Brenner, B., Sipple, J. D., and Peddle, J. (2013). "Objective Load Rating of a Steel-Girder Bridge Using Structural Modeling and Health Monitoring." *Journal of Structural Engineering*, 139(10), 1771-1779.

Bishara, A. G., Chuan Liu, M., and El-Ali N. D. (1993). "Wheel Load Distribution on Simply Supported Skew I-Beam Composite Bridges." *Journal of structural Engineering*, 119(2), 399-419.

Cai, C. S., and Shahawy, M. (2004). "Predicted and Measured Performance of Prestressed Concrete Bridges." *Journal of Bridge Engineering*, 9(1), 4-13.

Cai, C. S., Araujo, M., Chandolu, A., Avent, R., and Alaywan, W. (2007). "Diaphragm Effects of Prestressed Concrete Girder Bridges: Review and Discussion." *Practice Periodical on Structural Design and Construction*, 12(3), 161-167.

Cai, C. S., Shahawy, M., and Peterman, R. J. (2002). "Effect of Diaphragms on Load Distribution of Prestressed Concrete Bridges." *Transportation Research Record*, 1814, 47-54.

Chen, T. Y., Siess, C. P., and Newmark, N. M. (1957). “Studies of slab and beam highway bridges, Part IV: Moments in simply supported skew I-beam bridges.” *Engineering Experiment Station Bulletin, No. 439,* University of Illinois.

Chen, Y. (1999). “Distribution of Vehicular Loads on Bridge Girders by the FEA Using ADINA: Modeling, Simulation, and Comparison.” *Journal of Computers & Structures*, 72(1-3), 127-139.

Conner, S., and Huo, X. S., (2006). “Influence of Parapets and Aspect Ratio on Live-Load Distribution.” *Journal of Bridge Engineering*, 11(2), 188-196.

Decastro E. S. (1979). “Live Load Distribution in Skewed Prestressed Concrete I-Beam and Spread Box-Beam Bridges.” Fritz Engineering Laboratory, *Report No. 387.3,* Lehigh University, Bethlehem, Pa.

Eamon, C. D., and Nowak, A. S., (2002). “Effects of Edge-Stiffening Elements and Diaphragms on Bridge Resistance and Load Distribution.” *Journal of Bridge Engineering*, 7(5), 258-266.

Eamon, C. D., and Nowak, A. S., (2004). “Effects of Secondary Elements on Bridge Structural System Reliability Considering Moment Capacity.” *Journal of Structural Safety*, 26, 29-47.

Eom J. and Nowak A. S. (2001). “Live Load Distribution for Steel Girder Bridges.” *Journal of Bridge Engineering*, 6(6), 489-497.

Everitt, B. S. (2002). “The Cambridge Dictionary of Statistics.” 2nd Edition, *Cambridge University Press,* Cambridge, England.

Frederick, G. R., and Tarhini, K. M. (2000). “Wheel Load Distribution in Concrete Slab Bridges.” *Computing in Civil and Building Engineering*, 1236-1239.

Green, T., Yazdani, N., Spainhour, L., and Cai, C. S. (2002). “Intermediate Diaphragm and Temperature Effects on Concrete Bridge Performance.” *Transportation Research Record*, 1814, Paper No. 02-3627, 83-90.

Hasancebi, O., and Dumlupinar, T. (2013). “Detailed Load Rating Analyses of Bridge Populations Using Nonlinear Finite Element Models and Artificial Neural Networks.” *Journal of Computer and Structures*, 128, 48-63.

Hays, C. O., Larry, J., Sessions, M., and Berry, A. J. (1986). “Further Studies on Lateral Load Distribution Using a Finite Element Method.” *Transportation Research Record*, 1072, 6-14.

Huo, X. S., Wasserman, E. P., and Zhu, P. (2004). “Simplified Method of Lateral Distribution of Live Load Moment.” *Journal of Structural Engineering*, 9(4), 382-390.

Jauregui, D. V. and Barr, P. J. (2004). "Nondestructive Evaluation of the I-40 Bridge over the Rio Grande River." *Journal of Performance of Constructed Facilities*, 18(4), 195-204.

Jensen, V. P. (1938). "A Distribution Procedure for the Analysis of Slabs Continuous over Flexible Beams." *Bulletin No. 304,* University of Illinois Publication, Ill.

Jensen, V. P. (1939). "Moments in Simple Span Bridge Slabs with Stiffened Edges." *Bulletin No. 97,* University of Illinois Publication, Ill.

Jorgensen, J. L. and Larson, W. (1976). "Field Testing of a Reinforced Concrete Highway Bridge to Collapse." *Transportation Research Record 607,* Transportation Research Board, Washington, D.C., 66-80.

Khaleel, M. A., and Itani, R. Y. (1990). "Live-Load Moments for Continuous Skew Bridges." *Journal of Structural Engineering*, 116(9), 2361-2373.

Khaloo, A. R., Mirzabozorg, H. (2003). "Load Distribution Factors in Simply Supported Skew Bridges." *Journal of Bridge Engineering*, 8(4), 241-244.

Kuzmanovic, B. O., and Sanchez, M. R. (1986). "Lateral Distribution of Live Loads on Highway Bridges." *Journal of Structural Engineering*, 112 (8), 1847-1862.

Mabsout, M. E., Tarhini K. M., Frederick, G. R., and Kobrosly, M. (1997). "Influence of Sidewalk and Railing on Wheel Load Distribution in Steel Girder Bridges." *Journal of Bridge Engineering,* 2(3), 88-96.

Mabsout, M. E., Tarhini K. M., Frederick, G. R., and Tayar, C. (1997). "Finite-Element Analysis of Steel Girder Highway Bridges." *Journal of Bridge Engineering*, 2(3), 83-87.

Mabsout, M. E., Tarhini, K. M., Frederick, G. R., and Kesserwan, A. (1998). "Effect of Continuity on Wheel Load Distribution in Steel Girder Bridges." *Journal of Bridge Engineering,* 3(3), 103-110.

Mabsout, M., Menassa, C., and Tarhini, K. (2002). "Effect of Skewness in Concrete Slab Bridges." *9th Int. Conference on Computing in Civil and Building Engineering,* Taipei, Taiwan, 663-668.

Mabsout, M., Tarhini, K., Jabakhanji, R., and Awwad, E. (2004). "Wheel Load Distribution in Simply Supported Concrete Slab Bridges." *Journal of Bridge Engineering*, 9(2), 147-155.

Marx, H. J., Kachaturion, N., and Gamble, W. L. (1986). "Development of Design Criteria for Simply Supported Skew Slab-And-Girder Bridges." Civil Engineering Studies, *Structural Research Series No. 522,* University of Illinois.

Menassa, C., Mabsout, M., Tarhini, K., and Frederick, G. (2007). "Influence of Skew Angle on Reinforced Concrete Slab Bridges." *Journal of Bridge Engineering,* 12(2), 205-214.

Newmark, N. M. (1938). "A Distribution Procedure for The Analysis of Slabs Continuous over Flexible Beams." *Bulletin No. 84*, University of Illinois Publication, Ill.

Newmark, N. M. (1948). "Design of I-beam Bridges." *Journal of Structural Division, ASCE*, 74(2), 141-161.

Sanayei, M., Reiff, A. J., Brenner, B. R., and Imbaro, G. R. (2016). "Load Rating of a Fully Instrumented Bridge: Comparison of LRFR Approaches." *Journal of Performance in Construction Facility*, 30(2), 04015019.

Seok, S., Ravazdezh, F., Haikal, G., and Ramirez, J. A. (2019). "Strength Assessment of Older Continuous Slab and T-beam Reinforced Concrete Bridges." *Joint Transportation Research Program Publication*, Purdue University, IN.

Shahawy, M. and Huang, D. (2001). "Analytical and Field Investigation of Lateral Load Distribution in Concrete Slab-On-Girder Bridges." *ACI Structural Journal*, 98(4), 590-599.

Spokoiny, V. and Dickhaus, T. (2014), "Basics of Modern Mathematical Statistics." *Springer Publications*, New York.

Tarhini, K. M., and Frederick, G. R. (1992). "Wheel Load Distribution In I-Girder Highway Bridges." *Journal of Structural Engineering*, 118(5), 1285-1294.

United States Department of Transportation (2019), Federal Highway Administration Database, Retrieved from https://www.fhwa.dot.gov/resources/pubstats/, Washington, DC.

Upton, G. and Cook, I (2014). "A Dictionary of Statistics." 3rd Edition, *Oxford University Press*, Oxford, United Kingdom.

Washington S. P., Karlafits M. G., and Mannering F. (2010). "Statistical and Econometric Methods for Transportation Data Analysis." ISBN-13:978-1420082852.

Weisberg, S. (2005). "Applied Linear Regression.", *Wiley Interscience Publications*, Hoboken, New Jersey.

Westergaard, H. M. (1930). "Computation of Stresses in Bridge Slabs due to Wheel Loads." *Public Roads*, 11(1), 1-23.

Winters, R., Winters, A., and Amedee, R. G. (2010). "Statistics: A Brief Overview." *The Ochsner Journal*, 10(3), 213-216.

Yousif, Z., and Hindi, R. (2007). "AASHTO-LRFD Live Load Distribution for Beam-and-Slab Bridges: Limitations and Applicability." *Journal of Bridge Engineering*, 12(6), 765-773.

Zokaie, T. (2000). "AASHTO-LRFD Live Load Distribution Specifications." *Journal of Bridge Engineering*, 5(2), 131-138.

Zokaie, T., Osterkamp, T. A., and Imbsen, R. A. (1991). ‘‘Distribution of Wheel Loads on Highway Bridges.’’ *NCHRP 12-26/1 Final Report*, National Cooperative Highway Research Program, Washington, DC.

VITA

B.Sc. Iran University of Science and Technology, Iran - School of Civil Engineering (2013)

M.Sc. University of Bologna, Italy - Lyles School of Civil Engineering (2016)

Ph.D. Purdue University, United States of America - Lyles School of Civil Engineering (2021)